

to appear in the *Astronomical Journal*

UBVRI Light Curves of 44 Type Ia Supernovae

Saurabh Jha¹, Robert P. Kirshner, Peter Challis, Peter M. Garnavich, Thomas Matheson, Alicia M. Soderberg, Genevieve J. M. Graves, Malcolm Hicken, João F. Alves, Héctor G. Arce, Zoltan Balog, Pauline Barmby, Elizabeth J. Barton, Perry Berlind, Ann E. Bragg, César Briceño, Warren R. Brown, James H. Buckley, Nelson Caldwell, Michael L. Calkins, Barbara J. Carter, Kristi Dendy Concannon, R. Hank Donnelly, Kristoffer A. Eriksen, Daniel G. Fabricant, Emilio E. Falco, Fabrizio Fiore, Michael R. Garcia, Mercedes Gómez, Norman A. Grogin, Ted Groner, Paul J. Groot, Karl E. Haisch, Jr., Lee Hartmann, Carl W. Hergenrother, Matthew J. Holman, John P. Huchra, Ray Jayawardhana, Diab Jerius, Sheila J. Kannappan, Dong-Woo Kim, Jan T. Kleyna, Christopher S. Kochanek, Daniel M. Koranyi, Martin Krockenberger, Charles J. Lada, Kevin L. Luhman, Jane X. Luu, Lucas M. Macri, Jeff A. Mader, Andisheh Mahdavi, Massimo Marengo, Brian G. Marsden, Brian A. McLeod, Brian R. McNamara, S. Thomas Megeath, Dan Moraru, Amy E. Mossman, August A. Muench, Jose A. Muñoz, James Muzerolle, Orlando Naranjo, Kristin Nelson-Patel, Michael A. Pahre, Brian M. Patten, James Peters, Wayne Peters, John C. Raymond, Kenneth Rines, Rudolph E. Schild, Gregory J. Sobczak, Timothy B. Spahr, John R. Stauffer, Robert P. Stefanik, Andrew H. Szentgyorgyi, Eric V. Tollestrup, Petri Väisänen, Alexey Vikhlinin, Zhong Wang, S. P. Willner, Scott J. Wolk, Joseph M. Zajac, Ping Zhao, and Krzysztof Z. Stanek

Harvard-Smithsonian Center for Astrophysics, 60 Garden Street, Cambridge, MA 02138

saaurabh@astron.berkeley.edu

ABSTRACT

We present *UBVRI* photometry of 44 type-Ia supernovae (SN Ia) observed from 1997 to 2001 as part of a continuing monitoring campaign at the Fred Lawrence Whipple Observatory of the Harvard-Smithsonian Center for Astrophysics. The data set comprises 2190 observations and is the largest homogeneously observed and reduced sample of SN Ia to date, nearly doubling the number of well-observed, nearby SN Ia with published multicolor CCD light curves. The large sample of *U*-band photometry is a unique addition, with important connections to SN Ia observed at high redshift. The decline rate of SN Ia *U*-band light curves correlates well with the decline rate in other bands, as does the *U*–*B* color at maximum light. However, the *U*-band peak magnitudes show an increased dispersion relative to other bands even after accounting for extinction and decline rate, amounting to an additional $\sim 40\%$ intrinsic scatter compared to *B*-band.

¹present address: Department of Astronomy and Miller Institute for Basic Research, 601 Campbell Hall, University of California, Berkeley, CA 94720-3411

Subject headings: supernovae: general — techniques: photometric

1. Introduction

Over the last decade, type Ia supernovae (SN Ia) have become increasingly sharp tools for precision cosmology, with applications of these exquisite distance indicators ranging from our galactic neighbors to establish the Hubble constant, to halfway across the observable Universe to uncover cosmic deceleration and acceleration (Riess et al. 2004; Barris et al. 2004; Knop et al. 2003 and references therein). These cosmological applications of SN Ia rely on accurate, high-precision, and unscheduled measurements of their light curves in multiple passbands over a period of weeks, presenting a challenge to would-be observers.

The project of collecting a large sample of nearby SN Ia with high-quality, multicolor CCD photometry to be used in cosmological studies began in earnest in 1990, with the Calán/Tololo survey (Hamuy et al. 1993) that combined a photographic search for SN in the southern sky with a program of CCD followup photometry obtained with the help of visiting astronomers. Hamuy et al. (1996) present Johnson/Cousins *BVI* photometry of 29 SN Ia from this project (27 of which were discovered as part of the survey itself) out to redshifts $z \simeq 0.1$.

In 1993, astronomers at the Harvard-Smithsonian Center for Astrophysics (CfA) began a campaign of CCD photometric and spectroscopic monitoring of newly-discovered supernovae at the Fred L. Whipple Observatory (FLWO) on Mt. Hopkins in southern Arizona, and this program has been ongoing ever since. We employ a similar cooperative observing strategy for the follow-up photometry, whereby the SN monitoring program is allocated a small amount of time each night (~ 20 minutes), with the observations being carried out by the scheduled observer. Our SN program is also allocated approximately one dedicated night per month that is used for photometry of the fainter objects, photometric calibration of the SN fields, and template observations after the SN have faded.

Our cooperative observing strategy has been very successful so far. FLWO *BVRI* observations of 22 type Ia supernovae discovered between 1993 and 1996 have been published by Riess et al. (1999) and we have also undertaken *UBVRI* photometry and in-depth analysis of a number of individual SN Ia observed as part of this program: SN 1998bu (Jha et al. 1999), SN 1999by (Garnavich et al. 2004), SN 1998aq (Riess et al. 2005) and SN 2001V (Mandel et al. 2005, in preparation).

Here we report our *UBVRI* photometry for 44 SN Ia discovered between 1997 and 2000. The full data set presented here consists of 2190 observations on 338 nights, and is the largest set of homogeneously observed and reduced SN Ia data published to date.

2. Data and Reduction

2.1. Discovery

Our program of supernova photometry consists solely of follow-up; we search only our email, not the sky, to find new supernovae. A number of observers, both amateur and professional, are engaged in searching for supernovae. We rely on these searches, as well as prompt notification of candidates, coordinated by Dan Green and Brian Marsden of the IAU’s Central Bureau for Astronomical Telegrams (CBAT), with confirmed SN reported in the IAU Circulars. In some cases the SN discoverers provide spectroscopic classification of the new objects, but generally spectroscopy is obtained by others, and reported separately in the IAU Circulars. With our spectroscopic SN follow-up program at the F. L. Whipple Observatory 1.5m telescope and FAST spectrograph (Fabricant et al. 1998), we have classified a large fraction of the new, nearby supernovae reported over the last several years and compiled a large spectroscopic database (Matheson et al. 2005, in preparation).

Given a newly discovered and classified supernova, several factors help determine whether or not we include it in our monitoring program. Because of their importance, SN Ia are often given higher priority over other types, but factors such as ease of observability (southern targets and those discovered far to the west are less appealing), supernova phase (objects whose spectra indicate they are after maximum light are given lower priority), redshift (more nearby objects are favored), as well as the number of objects we are already monitoring are significant. Our final sample of well-observed SN Ia is not obtained from a single well-defined set of criteria, and selection effects in both the searches and follow-up may make this sample unsuitable for some applications (such as determining the intrinsic luminosity function of SN Ia, for example). A thorough discussion of the selection biases in the Calán/Tololo supernova search and follow-up campaign can be found in Hamuy & Pinto (1999).

The discovery data for the sample of SN Ia presented here are given in Table 1. All of the SN Ia listed were discovered with CCD images, except for SN 1997bp which was discovered visually, and SN 1999ef and SN 1999gh which were discovered photographically. New, systematic CCD supernova searches have provided the great majority of our sample: the Beijing Astronomical Observatory Supernova Survey (Li et al. 1996; designated as BAO in Table 1), the UK Nova/Supernova Patrol (Armstrong & Hurst 1996; UK), the Puckett Observatory Supernova Search (Puckett 1998; POSS), the Tenagra Observatories supernova patrol (Schwartz 1997; TO), and the Lick Observatory Supernova Search (Treffers et al. 1997; LOSS). In addition, we note in Table 1 supernovae whose classification as SN Ia is from our spectroscopic monitoring program described above (designated as “CfA”).

2.2. Observations

All the photometry presented here was obtained with the F. L. Whipple Observatory (FLWO) 1.2m telescope, with either the “AndyCam” CCD camera or the “4Shooter” 2x2 CCD mosaic (Szentgyorgyi et al. 2005, in preparation). Both instruments use thinned, backside illuminated, anti-reflective coated Loral

2048² CCD detectors, situated at the f/8 Cassegrain focus. The pixel scale is approximately 0''.33 per pixel, yielding a field of view of over 11' on a side for each chip. All the data were taken in a 2x2 binned mode, resulting in a sampling of 0''.66 per pixel that is well matched to the typical image quality (1''.5 to 2'' FWHM). We have ensured that all data used are within the linear regime of the detectors. Observations using the 4Shooter taken before October 1998 were made with the “chip 1” CCD detector, while those taken afterwards were made on “chip 3”, which has slightly improved quantum efficiency but slightly inferior cosmetic characteristics.

Both instruments have good near-ultraviolet and near-infrared response, and our observations have been in the Johnson *UBV* and Kron-Cousins *RI* bandpasses. The data were taken with two *UBVRI* filtersets, the “SAO” set and the newer “Harris” set. Observations before December 1998 were taken with the SAO filterset (the same described by Riess et al. 1999 and Jha et al. 1999), while those taken after May 1999 were taken with the Harris set. Between December 1998 and May 1999 only the Harris *UBVR* filters were available, and the *I* filter used was from the SAO filterset. Because of the importance of knowing precisely the bandpasses used for a given observation (particularly for supernova photometry), we discuss these in greater detail in §2.4.

Our observing approach, combining nightly requests for one or two objects with monthly dedicated nights, allows us to sample the light curves with the appropriate cadence. Generally observations are more frequent when the SN Ia are near maximum light, and less frequent (but deeper) as each SN Ia fades. During the period of these observations, the FLWO 1.2m was equipped with the 4Shooter or AndyCam usually only during dark time, with an infrared imager on the telescope when the moon was near full. This unfortunately leads to ~1 to 2 week gaps in our light curves, but in most cases the light curves are still well-defined and suitable for distance analyses.

2.3. Differential Photometry

To measure the brightness of the supernova in any image, we perform the photometry differentially with respect to stars in the field of view, allowing for useful measurements even in non-photometric conditions. In general we use as many of these comparison stars (or “field standards”) as feasible, choosing stars that are bright enough to be precisely measured but faint enough to not saturate the detector in the late-time, deeper images. In addition, we try to choose comparison stars that cover a range of color comparable to those exhibited by SN Ia over their evolution, though it is often not possible to find stars in the field that are as blue as SN Ia at or before maximum light. Figure 1 shows *R*-band finder charts for all of the supernovae and their associated comparison stars.

All of the CCD observations were reduced uniformly, with bad pixel masking, bias subtraction and flat-field correction using the NOAO Image Reduction and Analysis Facility (IRAF) CCDPROC package¹. In

¹IRAF is distributed by the National Optical Astronomy Observatories, which are operated by the Association of Universities for Research in Astronomy, Inc., under cooperative agreement with the National Science Foundation.

addition, we remove, to the extent possible, the small but non-negligible, amount of fringing for observations in the *I*-band via a fringe frame created from combined night-sky exposures of sparse fields.

A major complication in supernova photometry arises in separating light from the SN itself from light from the underlying galaxy at the SN position. Poor subtraction of the background light can have significant effects on the supernova light curve shapes and colors (cf. discussion in Riess et al. 1999; Boisseau & Wheeler 1991). For this reason, we take observations of the supernova fields the following year, after the SN has faded, to use as templates that are subtracted from all of the previous images. We have used galaxy subtraction to perform the differential photometry of all the SN Ia except for SN 2000cx, which was located very far from the nucleus of its (elliptical) host galaxy, where the galaxy background was negligible and template subtraction only added undesirable correlated noise. For SN 2000cx, we performed point-spread function (PSF) fitting photometry on the SN and comparison stars, using the DAOPHOT/ALLSTAR (Stetson 1987, 1994) package in IRAF.

For the other 43 objects, we employed template subtraction as follows. Generally a number of late-time images were taken in each passband with exposure times comparable to or slightly longer than the deepest images with the SN present, and we chose the set of images with the best seeing to serve as the templates. For each passband, all of the images were registered to the template, and the image subtraction was performed using the ISIS subtraction package (Alard & Lupton 1998) as modified by B. Schmidt (personal communication), to allow for more robust selection of regions in the two images suitable for determination of the convolution kernel (avoiding saturated stars, cosmic rays, and cosmetic defects). We subtracted the template from each SN image, and replaced a small region around the SN with the template-subtracted version. In the typical case, where the template image quality was better than the SN image, we convolved the template to the SN image, subtracted, and replaced the SN neighborhood from the subtracted image back into the original SN image. In the rare case, where the SN image quality was better than the template, we degraded the SN image to match the PSF of the template image, subtracted, and replaced the subtracted SN neighborhood back into the convolved (degraded) SN image. This procedure ensures that the PSF of the SN matches the PSF of the comparison stars. We also added artificial stars of known brightness into the SN images, mimicking the SN subtraction procedure on these stars. Finally, we performed aperture photometry as well as DoPHOT PSF-fitting photometry (Schechter, Mateo, & Saha 1993) on the SN, comparison stars and artificial stars in the galaxy-subtracted images. We have checked that the recovered magnitudes of the added stars match their input magnitudes, and that the aperture and PSF photometry gave consistent results, generally to better than 0.01 mag. We have also verified that this photometry derived via galaxy subtraction is consistent with direct PSF photometry for SN where the galaxy background is exceptionally smooth. For our final differential photometry, we have chosen to use the aperture photometry of the SN and comparison stars, with an aperture radius given by 0.75 times the FWHM of the PSF.

This general strategy is identical to that used by the High-Z Supernova Search Team (Schmidt et al. 1998) in analysis of high-redshift SN Ia; while the actual software is in a state of constant evolution, we have used one incarnation for all the light curves presented here. The result of this process is homogeneous and reliable differential *UBVRI* photometry of each supernova and its associated comparison stars on the natural system of the observations (i.e., instrumental magnitudes).

2.4. Calibration

We calibrate each of the supernova fields following the precepts of Harris, Fitzgerald & Reed (1981), using the all-sky *UBVRI* standard stars of Landolt (1992). On photometric nights, we typically observe on the order of 10 to 15 Landolt fields over a wide range of airmass (generally from 1.1 to ~ 2). We perform aperture photometry on the reduced Landolt fields using the APPHOT package in IRAF, using a 6 pixel aperture radius ($\sim 4''$) that is then corrected to a 15 pixel radius ($\sim 10''$) via a curve of growth defined by a few isolated, bright stars in each image. We then determine the zeropoints and transformation coefficients linear in airmass and color from the instrumental magnitudes *ubvri* to the standard Landolt *UBVRI* magnitudes and *U–B*, *B–V*, *V–R*, and *V–I* colors. For nights when many standard stars were observed, we check the linear solution by also fitting a quadratic term in color as well as a color times airmass term; in all cases the coefficients for the higher order terms are negligible, and so we use only the linear solutions. Because of the different detector and filterset combinations we have used, we take care to keep track of the transformation coefficients separately. As expected, for a given detector/filterset combination, the variations in the zeropoints and airmass terms are small but significant, while the color terms are always consistent within the fit uncertainties.

Once we have the standard solution for a photometric night, we apply this solution to the instrumental aperture magnitudes of the comparison stars in each SN field, measured in exactly the same way as the Landolt standard stars. This yields the standard *UBVRI* magnitudes of the comparison stars in each SN field. For most of the fields, we have several calibrations, enabling us to average the results and identify and eliminate outliers. For a handful of SN, however, we have only one night of photometric calibration, a somewhat perilous situation. Nevertheless, for every one of these objects we have checked that other SN fields taken on the same night have photometry that is consistent on other nights, bolstering our confidence that the photometry of objects with only one night of calibration is not significantly in error. In Table 2, we present the final comparison star *V* magnitudes and colors with their uncertainties (in the mean), as well as the number of photometric nights averaged to yield the results. We also give positions of the supernovae and comparison stars, referenced to the USNO-A2.0 catalogue (Monet et al. 1998), with a typical root-mean-square (RMS) uncertainty of $\pm 0''.3$. The location of the supernovae and comparison stars are shown in Figure 1.

We present the average color terms for each detector/filterset combination in Table 3, along with the internal uncertainties in the mean. We do not have data on any photometric nights when the AndyCam and the Harris filters were on the telescope, and thus we could not use observations of standard stars to determine the color terms for this detector/filterset combination. Instead we used the color terms based on the calibrated comparison stars themselves (allowing for a variable zeropoint for each frame, given the non-photometric conditions). For the other detector/filterset combinations, we successfully used this method to check the color terms for consistency.

Armed with the comparison star standard magnitudes and the color terms for each detector/filterset combination, we determined the zeropoint for each SN image by transforming the comparison star standard magnitudes to instrumental magnitudes (using the appropriate color term) and comparing to them to the

observed comparison star magnitudes. Because the SN is observed at the same time (and thus, airmass) as the comparison stars, the airmass term is consumed into the zeropoint, which is robustly determined from the flux-weighted average of the comparison stars. We then use this zeropoint to determine calibrated instrumental magnitudes for the SN, and use the linear color term transformation to arrive at the final Landolt standard magnitudes for the supernova. We keep track of and propagate the uncertainties throughout this procedure, including photon noise in the instrumental magnitudes, dispersion in the photometric solution, uncertainties in the transformation coefficients, and internal uncertainty in the zeropoint for each image. The final standard system *UBVRI* magnitudes of the supernovae, along with the uncertainties and the detector/filterset combination are given in Tables 4 to 47. The *UBVRI* light curves of the 44 SN Ia are shown in Figure 2 relative to maximum light (defined in the *B*-band) and corrected for time-dilation to the SN rest frame (cf. Table 49, §3.2).

We have used linear color transformations between the supernova instrumental magnitudes and standard magnitudes as has been conventional when presenting SN Ia light curves, but these may be inappropriate due to the strong, broad features present in SN spectra, as compared to the stars from which the color terms are derived. Fortunately, our primary concern is accurate photometry of SN Ia near and soon after maximum light, when the SN flux is still dominated by the continuum in this “photospheric” phase, where the linear transformations derived from stars would be most appropriate. Furthermore, for most of the detector/filter combinations, the color terms do not strongly suggest the effective wavelengths are far from the standard bandpasses. The ultimate test, though, is in the light curves, which also give no evidence for systematic differences between observations taken with different detector/filterset combinations. For instance, the smoothness of the light curve of SN 1998es (Table 27), observed with both instruments with multiple filtersets, is evidence of the internal consistency and homogeneity of the photometry. This is particularly important in the *U*-band, for which this sample represents the first large collection of SN Ia photometry, but which is also notoriously difficult to transform to a standard system (see, e.g., Suntzeff et al. 1999; Jha et al. 1999).

Though we have strived to ensure that the transformations to the standard system result in consistent, homogeneous photometry, the future uses of these data might nonetheless be limited by the accuracy of these transformations. It may be more convenient and useful to have the data as measured on the natural system. Given the color terms in Table 3, it is straightforward to transform the data back to the natural system (and the natural system magnitudes are available on request). This is only useful, however, in conjunction with the natural system passbands. We have synthesized these passbands by combining the primary and secondary mirror reflectivities (taken simply as two reflections off an aluminum surface), the measured filter transmissions, and the measured detector quantum efficiencies (QE).² We have assumed that the shape of the QE curves for the two 4Shooter chips is identical. The synthesized passbands are shown in Figure 3, along with the standard *UX* and *BVRI* passbands of Bessell (1990). Because the *U* passband is defined by

²We reiterate the footnote of Suntzeff et al. (1999), that the Bessell (1990) passband convention that we adopt also includes a term in the passband that is a linearly increasing function of wavelength. In this convention, then, the magnitude measured with a photon counting detector is $m = -2.5 \log \left\{ \int F_\lambda(\lambda) R(\lambda) d\lambda \right\} + \text{const}$, where $F_\lambda(\lambda)$ is the source flux density and $R(\lambda)$ is the bandpass response.

the atmospheric cutoff in the blue, we follow the Bessell convention of realizing this passband at airmass 1.0 (using the IRAF Kitt Peak atmospheric extinction curve, adjusted to match the average observed extinction coefficients), whereas the *BVRI* passbands are extra-atmospheric (i.e., airmass 0). As shown in Figure 3, the correspondence between the natural system passbands and the Bessell standard response curves is quite good, save for the *I*-band in the SAO filterset. The synthesized passbands are also tabulated in Table 48.

Through synthetic photometry, we have verified that the natural system passbands yield color terms consistent with those directly measured, cf. Table 3. We have also tried to constrain the natural system passbands directly, though observations of spectrophotometric standard stars on the photometric night of 2001 October 24 UT with the FLWO 1.2m telescope using chip 3 of the 4Shooter and the Harris filterset. We took multiple *UBVRI* observations of the following eight tertiary spectrophotometric standard stars (Massey et al 1988; Hamuy et al. 1992), over a wide airmass range throughout the night: BD +28°4211, Feige 34, Feige 110, G191B2B, Hiltner 600, LTT 9239, LTT 9491, and Wolf 1346. All of these stars also have published spectrophotometry in the red to $1\mu\text{m}$ (Massey & Gronwall 1990; Hamuy et al. 1994), allowing us to measure synthetic *BVRI* magnitudes. The ground-based spectrophotometry does not extend far enough to the blue with enough precision to synthesize *U* magnitudes (the Bessell UX passband extends down to 300 nm), and so for the *U*-band we have used the results of Bohlin, Dickinson, & Calzetti (2001), who give HST/STIS fluxes for five of the standards (BD +28°4211, Feige 34, Feige 110, G191B2B, and LTT 9491) extending below the atmospheric limit.

For each passband, we model the response curve as a cubic spline through a number of spline points spaced equally over the wavelength region where we expect a nonzero response. For each observation in the passband (~ 20 each in *BVRI* and 13 in *U*), we correct the standard star spectrum for atmospheric extinction (as above, to zero airmass for *BVRI* and 1.0 airmass for *U*), and synthesize photometry using the model passband. We find the best-fit model passband by minimizing the residuals between the synthetic and observed magnitudes, using a downhill-simplex (amoeba) method (Press et al. 1992). Our model is specified by the amplitudes (restricted to between zero and one) at the fixed spline points, with the normalization adjusted to yield a fixed zeropoint. The number of spline points in our model is somewhat arbitrary, limited by the number of individual measurements (~ 20 in *BVRI* and 13 in *U*). We have found that, in general, having fewer spline points is generally advantageous, avoiding pathological cases and overfitting the measurements at the expense of detailed information about the shape of the response curve. We have also imposed constraints that the model passband is “reasonable”; it is forced to zero at the ends and not allowed to be wildly oscillatory.

Given these constraints, the best-fit model passbands from the spectrophotometric data are shown in Figure 4, along with the 4Shooter/Harris passbands synthesized from the CCD QE curves, filter transmissions, etc. from Figure 3, and the Bessell (1990) passbands. Because of the somewhat arbitrary nature of the model, as well as uncertainties in the photometry, these best-fit response curves should be viewed as “typical” realizations of the true response, rather than exact representations. There is a range of models that fit the data reasonably well (with a dispersion of ~ 0.02 mag in *BVRI* and ~ 0.04 mag in *U*, similar to the scatter typically exhibited by the Landolt standards), and this range overlaps well with the calculated passbands. A few of the discrepancies between the solid and dashed curves seem to be robust; in particular,

the spectrophotometric data favor a B response which is narrower than the filter transmission would predict. To test this definitively, we would need a larger data set, with more spectrophotometric standards.

Though we have only tried this exercise with one detector/filterset combination, the results suggest that the match between the best-fit model passband and the calculated passbands is generally good, with the calculated passband yielding photometry always within 2σ of the best-fit. Furthermore, the constancy of the color terms for a particular detector/filterset indicates that effects such as variable detector response or mirror reflectivity (due to cleanliness, for instance) do not significantly affect the natural system bandpasses. We thus conclude that the response curves shown in Figure 3 and Table 48 are good representations of the natural system.

3. Results

3.1. Comparison with Published Photometry

A number of the supernovae presented here have published photometry from other groups. Because of the difficulties in supernova photometry (correcting for galaxy contamination, transformation to the standard system, etc.), systematic differences between SN photometry from different telescopes are common. These differences are generally small, at the level of a few hundredths of a magnitude (see, e.g., Suntzeff et al. 1999; Jha et al. 1999; Riess et al. 1999), though larger differences can occur with worse filter mismatches. In this paper, we strive to present photometry that is internally as homogeneous as possible, but it is still useful to compare these data with independent observations. When the systematic differences are small, combining these independent data sets is highly desirable, producing dramatic improvements in the light curve sampling.

3.1.1. SN 1997bp

Altavilla et al. (2004) present photometry of 18 SN Ia from ESO (La Silla) and Asiago Observatories including four objects also presented here. For SN 1997bp in NGC 4680, the two data sets are quite complementary in supernova phase, with the Altavilla et al. photometry filling in a gap in our light curve just after maximum light. Based on the few contemporaneous points, the photometry shows good agreement in $BVRI$, with offsets $\lesssim 0.05$ mag. However, the U -band photometry is more discordant; the Altavilla et al. measurements of SN 1997bp are ~ 0.15 mag fainter in U than the photometry presented here.

3.1.2. SN 1997br

Li et al. (1999) present extensive $BVRI$ photometry of SN 1997br in ESO 576-40 from observations at the Beijing Astronomical Observatory 0.6m and the Lick Observatory 0.76m Katzman Automatic Imaging

Telescope (KAIT). There is good agreement in the V and I -band photometry presented by Li et al. and that presented here (r.m.s. offsets $\lesssim 0.05$ mag), but there are larger, systematic differences in B (an r.m.s. offset of 0.08 mag, with the Li et al. photometry fainter before maximum light but brighter at later times $\gtrsim 30$ days after maximum light). The most significant discrepancy is in the R photometry, where the Li et al. photometry is fainter than the FLWO photometry by ~ 0.18 mag on average, and approaching ~ 0.25 mag even near maximum light. The field comparison stars we have in common show good agreement³. However, the color terms presented by Li et al. are relatively large in R , e.g., $(v-r)/(V-R) = 1.20$ for the KAIT observations, and the photometry differences correlate well with the SN color, implying that the transformation to the standard system is the likely culprit.

Altavilla et al. (2004) report 3 epochs of $BVRI$ photometry of SN 1997br and these show good agreement ($\lesssim 0.05$ mag) with the FLWO photometry presented here (also showing a similar offset when compared to the Li et al. R -band data). Altavilla et al. also present two U -band points, in fairly good accord ($\lesssim 0.1$ mag) with the FLWO photometry.

3.1.3. SN 1997cn

Turatto et al. (1998) present $UBVRI$ photometry of SN 1997cn in NGC 5490 from a number of telescopes at ESO, La Silla. Our photometry agrees well with theirs in B and V ; in U our photometry is generally brighter by ~ 0.15 mag, but is consistent within the photometric uncertainties for this faint object. Our R and I -band photometry is also brighter, by ~ 0.08 mag. We have one comparison star in common with Turatto et al. (their star 2 is our star 9) and our photometry for this star agree within the reported uncertainties in all bands.

3.1.4. SN 1998de

Extensive $BVRI$ observations of SN 1998de in NGC 252 are presented by Modjaz et al. (2001). The data presented there have been K -corrected to the SN rest frame, and to facilitate direct comparison with our observations, M. Modjaz has kindly supplied us with their standard magnitudes before K -correction. Our data set is relatively sparse compared to that presented by Modjaz et al.⁴ but the agreement is very good before maximum light ($\lesssim 0.05$ mag). Our I -band data taken about 45 days past maximum light show a large discrepancy (~ 0.4 mag), likely a result of the transformation to the standard system at a phase when the SN spectrum is highly non-stellar. Comparison star C of Modjaz et al. is the same as our star 8, and our

³The finder chart presented by Li et al. (1999) seems to indicate their star E corresponds to our comparison star 6, but the photometry in their Table 1 matches our photometry of comparison star 5, which is somewhat fainter and much redder than star 6. Because of its faintness, Li et al. do not assign much weight to this star, so it is unlikely to explain the discrepant R magnitudes.

⁴This is due to the fact that the SN peaked at the end of July, just as FLWO undergoes a month-long shutdown because of the southern Arizona monsoons.

calibration is consistent.

3.1.5. SN 1999aa

Krisciunas et al. (2000) present *BVRI* observations of SN 1999aa in NGC 2595 that very nicely complement the data presented here. In addition the photometric agreement is superb, with r.m.s. offsets $\lesssim 0.03$ mag near maximum light and $\lesssim 0.06$ mag at late times. Combining the data sets yields an excellent light curve for this object.

Altavilla et al. (2004) present 3 epochs of *UBVRI* photometry of SN 1999aa, with good accord in *BVR* at the level ~ 0.04 mag, with larger discrepancies in *I* (~ 0.1 mag at 30 days past maximum light and ~ 0.2 mag at 60 days past maximum light). The *U*-band agreement is also good: ~ 0.05 mag at +30 days and ~ 0.1 mag at +60 days.

3.1.6. SN 1999cl

Krisciunas et al. (2000) also present *BVRI* observations of the nearby SN 1999cl in NGC 4501 (M88). The data are not as extensive as for SN 1999aa, nor is the photometric agreement as good. The two sets agree relatively well in all bands at maximum light (~ 0.03 mag), but the photometry of Krisciunas et al. at about a month past maximum is brighter than our (single) late time point at that epoch by 0.1 to 0.3 mag in the different bands. Moreover, the discrepancy is larger in the red. This is a good indication of contamination from the host galaxy; indeed, Krisciunas et al. note that SN 1999cl might be an object where galaxy subtraction would improve their aperture photometry performed without a template. Our late-time images after the SN had faded show that the host galaxy makes a non-negligible contribution to the flux at the position of the supernova. Based on this discrepancy, Krisciunas et al. have reanalyzed their data for SN 1999cl with subtraction of host-galaxy template images, and the new results bring the photometry into much better agreement (K. Krisciunas, personal communication).

3.1.7. SN 1999ek

Extensive *BVRI* photometry of SN 1999ek in UGC 3329 is provided by Krisciunas et al. (2004), supplemented by the handful of data points presented here. Comparing the one epoch common to both data sets shows good agreement (~ 0.05 mag) in *B* and *I*, as well as excellent agreement (~ 0.01 mag) in *V* and *R*. In addition, Krisciunas et al. list *BVRI* magnitudes for two of the field comparison stars we have used, with excellent agreement (~ 0.01 mag) in all bands.

3.1.8. SN 1999gp and SN 2000ce

Krisciunas et al. (2001) present *BVRI* photometry of five SN Ia, including SN 1999gp in UGC 1993 (with galaxy subtraction) and SN 2000ce in UGC 4195. For SN 1999gp, the two sets of photometry match extremely well ($\lesssim 0.03$ mag), with only a small (~ 0.05 mag) consistent difference in the *R* band photometry. This discrepancy can be traced directly to the comparison stars, as the ones in common show an identical offset. Our comparison star photometry for the SN 1999gp field comes from 5 photometric nights, with consistent *R* photometry on all epochs. We thus recommend that the Krisciunas et al. SN 1999gp *R* photometry be adjusted 0.05 mag brighter to be consistent with the data presented here. As in the case of SN 1999aa, the data sets are nicely complementary.

The light curve of SN 2000ce also benefits from the combined data sets. In fact, the overlap is very slight (we have two epochs in common, and only one for all the bands simultaneously). Nonetheless, the agreement of the photometry at these epochs is good ($\lesssim 0.04$ mag).

3.1.9. SN 2000cx

Li et al. (2001) and Candia et al. (2003) present an immense data set in *UBVRI* for the unique SN 2000cx in NGC 524, with an additional two epochs of *UBVRI* reported in Altavilla et al. (2004). The photometry presented here is also quite extensive, except for the fact the SN was discovered in mid July, just prior to the aforementioned August shutdown of FLWO. Thus, our data set consists of only set of points near maximum light, before a large number of observations beginning a month later. The data taken together comprise the most optical photometry of any SN Ia, and generally show good photometric agreement, at the level of ~ 0.05 mag, as far as 100 days past maximum light (see Figure 3 of Candia et al.). At even later times, the agreement is still generally good, though there are some larger discrepancies, worst in *I*-band where the FLWO data and the KAIT data of Li et al. differ by ~ 0.4 mag. Candia et al. provide more detailed comparisons of subsets of this large data set.

Though we have described photometric agreement from different telescopes at the level of $\lesssim 0.05$ mag as “good”, it nonetheless remains the case that these differences are systematic and often exceed the nominal published uncertainties. The problem is almost certainly caused by variations in the photometric passbands at different sites that cannot be corrected by a simple linear transformation based on a broad-band color. Some of these discrepancies can be overcome by corrections derived from direct application of instrumental passbands to supernova spectrophotometry (e.g., Jha et al. 1999). Stritzinger et al. (2002) have formalized this idea through “S-corrections” determined in analogy to K-corrections. However, the calculated S-corrections have not always proved effective in reconciling discordant photometry. In addition, accurate S-corrections require accurate knowledge of both instrumental bandpasses and SN spectrophotometry, neither of which are always available. These issues in combining photometry from different sites are compounded in cosmological applications of SN Ia over a wide range of redshifts, and will be an important source of systematic uncertainty that must be controlled in the era of precision cosmology.

3.2. SN and Host Galaxy Properties

In Table 49 we list basic data about each SN Ia. The host-galaxy heliocentric redshifts listed are taken from the Updated Zwicky Catalog (Falco et al. 1999) if possible, and from the NASA/IPAC Extragalactic Database⁵ (NED) otherwise, where we favor optical redshifts over H I redshifts if there is a discrepancy. For three objects, host galaxy redshifts were not available, and we report them here based on spectroscopy with the FLWO 1.5m telescope plus FAST spectrograph (Fabricant et al. 1998) and cross-correlation with galaxy templates: the host of SN 1997dg, $c z_{\text{helio}} = 9238 \pm 14 \text{ km s}^{-1}$; the host of SN 1998dx (UGC 11149), $c z_{\text{helio}} = 16197 \pm 32 \text{ km s}^{-1}$; and the host of SN 2000cf (MCG +11–19–25), $c z_{\text{helio}} = 10920 \pm 20 \text{ km s}^{-1}$.

The supernovae in the sample range from heliocentric redshifts of 1968 to 16197 km s^{-1} , with median and mean redshifts of 4888 and 5274 km s^{-1} , respectively. The mean redshift is significantly less than both the original CfA sample of Riess et al. (1999; $\overline{cz} \approx 7500 \text{ km s}^{-1}$) and the Calán/Tololo sample of Hamuy et al. (1996a; $\overline{cz} \approx 13500 \text{ km s}^{-1}$). Nonetheless, most of the objects are in the Hubble flow; 39 of the 44 SN Ia have $cz \geq 2500 \text{ km s}^{-1}$ in the CMB rest frame, a slightly larger fraction than the original CfA sample (17 out of 22).

The host-galaxy morphology information shown in Table 49 is taken from NED, and the supernova offset from the nucleus is taken from the IAU CBAT list of supernovae⁶. Gallagher et al. (2005) present an analysis of correlations between these properties and SN luminosity. In Table 49 we also list the Galactic reddening towards each supernova, derived from the dust maps of Schlegel, Finkbeiner & Davis (1998).

3.3. Light Curve Properties

In Table 50 we list the times of maximum light in B for each supernova, as determined from either a direct polynomial fit to the B light curve, or from MLCS2k2 fits (Jha, Riess, & Kirshner 2005, in preparation). We also present the epoch of the first observation in our data set (measured in the SN rest frame). Over half the objects (25 out of 44) have observations before maximum light, and seventy percent (31 out of 44) have observations earlier than 5 days past maximum light.

We have also fit the BVI light curves of our supernova sample to determine maximum light magnitudes and the parameter $\Delta m_{15}(B)$, that has been shown to correlate with the supernova intrinsic luminosity (Phillips 1993). Though originally defined as the measured decline rate of the supernova in B from maximum to 15 days past maximum light, we follow Hamuy et al. (1995, 1996a) where $\Delta m_{15}(B)$ is a parameter in a multi-dimensional fit to template light curves (each with a predefined $\Delta m_{15}(B)$). We have followed the recipe of Hamuy et al. (1996a) in our fits, using a parabolic fit through the minimum reduced χ^2 in a fit of the BVI light curves to each of a set of templates (“de”-K-corrected and time-dilated to the observer’s frame,

⁵The NASA/IPAC Extragalactic Database (NED) is operated by the Jet Propulsion Laboratory, California Institute of Technology, under contract with the National Aeronautics and Space Administration.

⁶<http://cfa-www.harvard.edu/iau/lists/Supernovae.html>

for each SN). We have used the six *BVI* templates presented by Hamuy et al. (1996b), and augmented this sample with templates based on an additional four well-observed SN Ia in order to produce more robust measurements of $\Delta m_{15}(B)$: SN 1995al (Riess et al. 1999; $\Delta m_{15}(B) = 0.83$), SN 1998aq (Riess et al. 2005; $\Delta m_{15}(B) = 1.13$), SN 1998bu (Suntzeff et al. 1999; Jha et al. 1999; $\Delta m_{15}(B) = 1.01$) and SN 1999by (Garavich et al. 2004; $\Delta m_{15}(B) = 1.90$). We were able to get reliable $\Delta m_{15}(B)$ measurements for all but four of the SN Ia⁷; these values (not corrected for host-galaxy reddening) and their uncertainties (estimated from the curvature of the best-fit parabola) are listed in Table 50. We also present the *BVI* magnitudes at maximum light (in *B*) for each SN determined from the best-fit template.

To further explore the light curve properties of this sample, and in particular, to study the *U*-band light curves, we have also fit the light curves to templates, based on the timescale stretch parameterization developed by the Supernova Cosmology Project (Perlmutter et al. 1997, 1999; Goldhaber et al. 2001). The stretch template presented by Goldhaber et al. (2001) is only for the *B*-band; we would like to fit the *UBV* light curves, for which the simple stretching of the time axis does a good job of fitting the observed data. To construct *U* and *V*-band templates, one possibility is to use composite light curves, combining a large number of supernovae to produce an average template. However, because some objects are better sampled in different bands, the average templates produced this way might not consistently represent a supernova of “average” light curve shape and/or luminosity. For this reason, we have constructed *UBV* templates based on photometry of a single supernova, the well-observed SN 1998aq (Riess et al. 2005). To retain consistency with the Goldhaber et al. (2001) normalization, we have corrected our SN 1998aq *UBV* stretch templates to $s = 1$, by fitting the *B* template to the SCP1997 template presented in that paper.

In fitting our stretch templates to the data, we generally follow the methodology of Goldhaber et al. (2001) as applied in their analysis of the Calán/Tololo sample (Hamuy et al. 1996a). We restrict the light curves to between -10 and $+40$ days in the SN rest frame, and we only include objects with photometry commencing earlier than 5 days after maximum light. Because we are interested in understanding the general light-curve properties of these SN Ia, we allow the fits to be as unrestrictive as possible: we fit for the stretch individually in each of the three bands, and allow the times of maxima to vary in each band (plus or minus a few days), as well as individually fitting for the *UBV* peak magnitudes⁸. We also impose an error floor on the photometry equal to 0.007 times the peak flux, as did Goldhaber et al. (2001, see their Table 7); while this is negligible near maximum, it becomes the dominant uncertainty in the photometry at late times (for instance, corresponding to ± 0.2 mag in the *U*-band at $+40$ days). As in the $\Delta m_{15}(B)$ fits above, we fit the data in the observer’s frame (de-K-correcting and time-dilating the templates).

The limits on the epoch of first observation, and the requirement that we need ≥ 5 points between -10 and $+40$ days in each of the three bands for a meaningful fit limits the application of this method to 22 of

⁷The four objects include SN 1998D and SN 1999cw, for which the first observation was well after maximum light; SN 1998co, for which the data are quite sparse; and SN 2000cx, whose light curve is unique among all SN Ia (Li et al. 2001).

⁸We fit the data in magnitude space, rather than flux space, out of convenience. Because we are only fitting the light curves between -10 and $+40$ days, the difference between the two approaches is negligible. Determining rise-time information at very early epochs clearly benefits from fitting in flux space, where negative and zero fluxes are common.

the 44 SN Ia presented here. The results are presented in Table 51, listing the *UBV* peak magnitudes and timescale stretch factors, along with the differences in the time of maximum light in *U* and *V* relative to $t_{B\max}$, all with error estimates given by the formal uncertainties in the fit.

4. Discussion: *U*-band Light Curves

The *U*-band photometry presented here, while just a fraction of the whole dataset, is the first large sample of homogeneously observed and reduced *U* photometry of SN Ia. The *BVRI* properties of SN Ia are well-studied, and while our data provide a much expanded sample of *BVRI* light curves, here we focus on the new element, the *U*-band data. Though a number of other SN Ia individually also have published *U*-band photoelectric or CCD photometry, the difficulties of transforming this photometry (with the variety of instruments, filters, sensitivities, etc.; see, e.g., Schaefer 1995; Suntzeff et al. 1999) to a standard system leads us first to examine the *U*-band properties of SN Ia from FLWO observations alone, as we have taken care to ensure internal consistency.

Figure 5 shows the composite *U*-band light curve of the 44 SN Ia presented in this paper, along with six other SN Ia with *U* data from the FLWO 1.2m: SN 1995al and SN 1996X (for which *BVRI* light curves were presented by Riess et al. 1999), SN 1998aq (Riess et al. 2005), SN 1998bu (Jha et al. 1999), SN 1999by (Garnavich et al. 2004), and SN 2001V (Mandel et al. 2005, in preparation). Of the *UBVRI* passbands, the SN Ia light curve declines fastest in *U*, with an average SN Ia dropping ~ 1.5 mag in *U* over the first 15 days after B_{\max} , as compared to only a ~ 1.1 mag drop in *B* and ~ 0.5 mag drop in *V* over that time period. Over the first 30 days after B_{\max} , the declines in *U*, *B*, and *V* are ~ 3.2 , ~ 2.6 , and ~ 1.4 mag, respectively. At late time, $t \gtrsim 35$ days after B maximum light, the *U*-band light curves follow the typical exponential decline, decaying at 0.020 ± 0.001 mag day $^{-1}$.

In Figure 6 we plot the distribution of the epoch of *U*-band maximum light relative to *B*-band maximum light, using the stretch templates results for the 22 SN Ia listed in Table 51, along with the 6 additional SN Ia listed above. As can also be seen in Figure 5, the SN Ia clearly peak earlier in the *U*-band than in *B*, with an average time offset of -2.3 days and a dispersion of only 0.4 days. The earlier peak in *U* also implies the decline rate in *U* relative to maximum light in *U* is not so different from the decline rate in *B* relative to maximum light in *B*. A typical SN Ia that drops ~ 1.1 mag in *B* over the first 15 days after maximum light (as above), declines by ~ 1.2 mag in *U* over the first 15 days after *U* maximum. We note that our precise photometry confirms the result of Leibundgut et al. (1991), who found that maximum in light in *U* occurs ~ 2.8 days before maximum light in *B*, based on a compilation of heterogeneous photoelectric *UBV* photometry.

The decline rate in *U* is well correlated with the decline rate in *B*, as shown in Figure 7, which plots the timescale stretch factors for the 28 SN Ia described above. However, as the figure also illustrates, there is a significant scatter. The relationship between the stretch factor in *V* and the stretch factor in *B* is considerably tighter. Nonetheless, these correlations imply that *U* light curves can provide leverage in determining the intrinsic luminosities of SN Ia. The best-fit linear relations between s_U , s_B , and s_V are given in the figure.

Given the scatter, the relations are consistent with a “universal” stretch, $s = s_U = s_B = s_V$, though the data for a number of objects individually favor slightly different stretch factors in each band. The slope of the luminosity/stretch relation is ~ 1.7 (Nugent, Kim, & Perlmutter 2002), meaning that the dispersion in the s_U - s_B relation ($\sigma \simeq 0.08$) translates into an uncertainty of $\sigma \simeq 0.14$ mag in luminosity, comparable to the typical dispersion in measuring SN Ia distances (e.g., in the stretch/luminosity relation itself). Similarly, the dispersion in the s_V - s_B relation corresponds to $\sigma \simeq 0.09$ mag.

We can also examine the correlation between the timescale stretch factors and $\Delta m_{15}(B)$ for these 28 SN Ia (cf. Table 50); the results are shown in Figure 8. The correlation between $\Delta m_{15}(B)$ and s is clear, with s_V and s_B producing a tighter relationship. It also appears that much of the dispersion comes at the low $\Delta m_{15}(B)$ (large s) end of the diagram, implying that there may be larger intrinsic variation in the light curves of the most luminous SN Ia. The dispersions in $\Delta m_{15}(B)$ are 0.17, 0.12, 0.10 for the relations with s_U , s_B , and s_V , respectively. Using the luminosity- $\Delta m_{15}(B)$ relationship presented by Phillips et al. (1999), the luminosity scatter corresponding to these dispersions are 0.14, 0.10 and 0.08 mag, similar to the results above directly comparing stretch to luminosity. We note that the relations between $\Delta m_{15}(B)$ and s presented in Figure 8 match well the results of Garnavich et al. (2004; see their Figure 6).

In addition to the U -band light curve shapes, we can explore the $U-B$ color with this data set. We display 27 SN Ia⁹ in the color-color diagram shown in the top panel of Figure 9. We note that the stretch-template fits to the peak magnitudes include the effects of K-correction, which can be significant, particularly in the U -band ($K_{UU} \simeq 0.12$ mag for $z = 0.03$ at maximum light; Jha, Riess, & Kirshner 2005, in preparation). We have also corrected the colors for (the generally small) Galactic reddening (cf. Table 49), assuming the $R_V = 3.1$ extinction law of Cardelli, Clayton, & Mathis (1989). For 23 of the 27 SN Ia, we were also able to correct for the host-galaxy extinction, via measurement of the tail $B-V$ evolution and the method of Lira (1995) and Phillips et al. (1999), as described in detail in Jha, Riess, & Kirshner (2005, in preparation). The colors corrected for host-galaxy reddening are shown in the bottom panel of Figure 9. These results sharpen those of Schaefer (1995) and Branch, Nugent, & Fisher (1997), who display relations between the $U-B$ and $B-V$ maximum light colors of SN Ia based on a handful of objects with heterogeneous photometry from diverse sources.

The lower panel figure shows a tight relation between the intrinsic $B-V$ and $U-B$ color at maximum light. In this plot, normal SN Ia have $B-V \simeq -0.1$ (e.g., Phillips et al. 1999)¹⁰, and there is a strong clustering of objects at this value. Note, however, the wide span of $U-B$ colors (from about -0.2 to -0.8) for these normal SN Ia. This is not an artifact of the reddening correction, nor can it be explained by variation in the extinction law in these external galaxies. If there were strong variations in the extinction law, because of the patchiness of interstellar dust, we would expect the top panel of Figure 9 to show a swarm of points at the

⁹We show 27 SN Ia rather than 28, because we exclude the highly-reddened SN 1999cl, for which there is strong evidence from near-infrared photometry that the extinction law varies significantly from the canonical $R_V = 3.1$ law (Krisciunas et al. 2000; Jha, Riess, & Kirshner 2005, in preparation).

¹⁰Phillips et al. (1999) find the “pseudo”-color $B_{\text{Bmax}} - V_{\text{Vmax}} \simeq -0.07$ for normal SN Ia. Because $V_{\text{Vmax}} \simeq V_{\text{Bmax}} - 0.02$, their result implies $(B-V)_{\text{Bmax}} \simeq -0.09$ for normal SN Ia.

lower left (corresponding to an unreddened locus) with the remainder of the points fanning out toward the upper right (corresponding to different amounts of extinction and reddening), which is clearly not what we see. We conclude that the intrinsic variation in $U-B$ color at maximum light is significantly greater than the variation seen in $B-V$.

Do these color variations correlate with light-curve shape or luminosity? There is strong evidence that objects with intrinsically red $B-V$ colors at maximum are the fast-declining, low-luminosity SN Ia (see, e.g., Garnavich et al. 2004 and references therein). The bottom panel of Figure 9 shows that the red objects in $B-V$ are also red in $U-B$. A direct check on the relation between color and light-curve shape is shown in Figure 10, which plots the intrinsic $U-B$ and $B-V$ maximum light colors against the measured timescale stretch factor (in V). The relationship between $B-V$ and s_V shown in the lower panel is in good accord with the results presented by Phillips et al. (1999) and Garnavich et al. (2004). The $U-B$ results in the top panel show that the $U-B$ color is well-correlated with stretch (and therefore, luminosity) over the whole range of luminosity in the sample. However, the scatter is also greater in $U-B$, implying that there is a significant intrinsic dispersion U -band peak brightness even after accounting for variations in light-curve shape. A simple linear fit to the data in the top panel of Figure 10 implies that this intrinsic dispersion is $\sigma_U \simeq 0.12$ mag. It would be interesting to check whether this increased dispersion is related to other factors, such as progenitor metallicity, as some theoretical studies have indicated that these factors may have more significant effects in U than in $BVRI$ (e.g., Höflich, Wheeler, & Thielemann 1998).

It is clear that the analysis of these U -band light curves and their relation to light curves in $BVRI$ and ultimately, precise distances, is intimately tied to the luminosity and extinction of each SN. To further explore these relations, a profitable strategy would be to incorporate the U -band light curves into the general framework of the Multicolor Light Curve Shape analysis presented by Riess, Press, & Kirshner (1996). We present the methods and results of this incorporation in Jha, Riess, & Kirshner (2005, in preparation).

We thank the avid supernova searchers who scan the sky and allow us to be successful in finding supernovae in our inboxes. We are also grateful for the efforts of Dan Green at the IAU CBAT for enabling our follow-up observations. We thank Paul Green, Scott Kenyon, Jeff McClintock, and Kenny Wood for assistance with the observations, Brian Schmidt for robust software, and Adam Riess, Nick Suntzeff, Dimitar Sasselov, and Alyssa Goodman for enlightening discussions and comments. We appreciate the helpful suggestions of the referee, Mario Hamuy, in improving the paper. This work was supported in part by an NSF Graduate Research Fellowship and the Miller Institute for Basic Research in Science.

REFERENCES

- Alard, C., & Lupton, R. 1998, *ApJ*, 503, 325
- Altavilla, G., Fiorentino, G., Marconi, M., Musella, I., Cappellaro, E., Barbon, R., Benetti, S., Pastorello, A., Riello, M., Turatto, M., & Zampieri, L. 2004, *MNRAS*, 349, 1344
- Armstrong, M., & Hurst, G. M. 1996, *IAU Circ.* 6497

- Barris, B.J., et al. 2004, *ApJ*, 602, 571
- Bessell, M.S. 1990, *PASP*, 102, 1181
- Bohlin, R.C., Dickinson, M.E., & Calzetti, D. 2001, *AJ*, 122, 2118
- Boisseau, J.R., & Wheeler, J.C. 1991, *AJ*, 101, 1281
- Branch, D., Nugent, P., & Fisher, A. 1997, in *Thermonuclear Supernovae*, eds. P. Ruiz-Lapuente, R. Canal, & J. Isern, Dordrecht: Kluwer Academic Publishers, 715
- Candia, P., et al. 2003, *PASP*, 115, 277
- Cardelli, J.A., Clayton, G.C., & Mathis, J.S. 1989, *ApJ*, 345, 245
- Fabricant, D., Cheimets, P., Caldwell, N., & Geary, J. 1998, *PASP*, 110, 79
- Falco, E.E., Kurtz, M.J., Geller, M.J., Huchra, J.P., Peters, J., Berlind, P., Mink, D.J., Tokarz, S.P., & Elwell, B. 1999, *PASP*, 111, 438
- Gallagher, J., Garnavich, P.M., Berlind, P., Challis, P., Jha, S., & Kirshner, R.P. 2005, *ApJ*, in press (astro-ph/0508180)
- Garnavich, P.M., Bonanos, A.Z., Jha, S., Kirshner, R.P., Schlegel, E.M., Challis, P., Macri, L.M., Hatano, K., Branch, D., Bothun, G.D., & Freedman, W.L. 2004, *ApJ*, 613, 1120
- Goldhaber, G., et al. 2001, *ApJ*, 558, 359
- Hamuy, M., Walker, A.R., Suntzeff, N.B., Gigoux, P., Heathcote, S.R., & Phillips, M.M. 1992, *PASP*, 104, 533
- Hamuy, M., et al. 1993, *AJ*, 106, 2392
- Hamuy, M., Suntzeff, N.B., Heathcote, S.R., Walker, A.R., Gigoux, P., & Phillips, M.M. 1994, *PASP*, 106, 566
- Hamuy, M., Phillips, M.M., Maza, J., Suntzeff, N.B., Schommer, R.A., & Avilés, R. 1995, *AJ*, 109, 1
- Hamuy, M., et al. 1996a, *AJ*, 112, 2408
- Hamuy, M., Phillips, M.M., Suntzeff, N.B., Schommer, R.A., Maza, J., Smith, R.C., Lira, P., & Avilés, R. 1996b, 112, 2438
- Hamuy, M., & Pinto, P. A. 1999, *AJ*, 117, 1185
- Harris, W.E., Fitzgerald, M.P., & Reed, B.C. 1981, *PASP*, 93, 507
- Höflich, P., Wheeler, J.C., & Thielemann, F.K. 1998, *ApJ*, 495, 617
- Jha, S., et al. 1999, *ApJS*, 125, 73
- Jha, S., Riess, A.G., & Kirshner, R.P. 2005, in preparation
- Knop, R.A., et al. 2003, *ApJ*, 591, 1110
- Krisciunas, K., Hastings, N.C., Loomis, K., McMillan, R., Rest, A., Riess, A.G., & Stubbs, C. 2000, *ApJ*, 539, 658

- Krisciunas, K., Phillips, M.M., Stubs, C., Rest, A., Miknaitis, G., Riess, A.G., Suntzeff, N.B., Roth, M., Persson, S.E., & Freedman, W.L. 2001, *AJ*, 122, 1616
- Krisciunas, K., et al. 2004, *AJ*, 128, 3034
- Landolt, A.U. 1992, *AJ*, 104, 340
- Leibundgut, B., Tammann, G.A., Cadonau, R., & Cerrito, D. 1991, *A&AS*, 89, 537
- Li, W.D., Qiu, Y.L., Qiao, Q.Y., Ma, J., & Hu, J.Y. 1996, *IAU Circ.* 6379
- Li, W.D., Qiu, Y.L., Qiao, Q.Y., Zhu, X.H., Hu, J.Y., Richmond, M.W., Filippenko, A.V., Treffers, R.R., Peng, C.Y., & Leonard, D.C. 1999, *AJ*, 117, 2709
- Li, W.D., Filippenko, A.V., Gates, E., Chornock, R., Gal-Yam, A., Ofek, E.O., Leonard, D.C., Modjaz, M., Rich, R.M., Riess, A.G., & Treffers, R.R. 2001, *PASP*, 113, 1178
- Lira, P. 1995, Master's Thesis, University of Chile
- Mandel, K., et al. 2005, in preparation
- Massey, P., Strobel, K., Barnes, J.V., & Anderson, E. 1988, *ApJ*, 328, 315
- Massey, P., & Gronwall, C. 1990, *ApJ*, 358, 344
- Matheson, T., et al. 2005, in preparation
- Modjaz, M., Li, W.D., Filippenko, A.V., King, J.Y., Leonard, D.C., Matheson, T., & Treffers, R.R. 2001, *PASP*, 113, 308
- Monet, D., et al. 1998, The USNO-A2.0 Catalogue, (U.S. Naval Observatory, Washington DC)
- Nugent, P., Kim, A., & Perlmutter, S. 2002, *PASP*, 114, 803
- Perlmutter, S., et al. 1997, *ApJ*, 483, 565
- Perlmutter, S., et al. 1999, *ApJ*, 517, 565
- Phillips, M.M. 1993, *ApJ*, 413, L105
- Phillips, M.M., Lira, P., Suntzeff, N.B., Schommer, R.A., Hamuy, M., & Maza, J. 1999, *AJ*, 118, 1766
- Press, W.H., Teukolsky, S.A., Vetterling, W.T., & Flannery, B.P. 1992, *Numerical Recipes in C*, 2nd ed., New York: Cambridge University Press
- Puckett, T. 1998, *IAU Circ.* 6957
- Riess, A.G., Press, W.H., & Kirshner, R.P. 1996, *ApJ*, 473, 88
- Riess, A.G., et al. 1999, *AJ*, 117, 707
- Riess, A.G., et al. 2004, *ApJ*, 607, 665
- Riess, A.G., Li, W., Stetson, P.B., Filippenko, A.V., Jha, S., Kirshner, R.P., Challis, P.M., Garnavich, P.M., & Chornock, R. 2005, *ApJ*, 627, 579
- Schaefer, B.E. 1995, *ApJ*, 450, L5
- Schechter, P.L., Mateo, M., & Saha, A. 1993, *PASP*, 105, 1342

- Schlegel, D. J., Finkbeiner, D. P., & Davis, M. 1998, *ApJ*, 500, 525
- Schmidt, B. P., et al. 1998, *ApJ*, 507, 46
- Schwartz, M. 1997, *IAU Circ.* 6700
- Schwartz, M., Li, W.D., Filippenko, A.V., Modjaz, M., & Treffers, R.R. 2000, *IAU Circ.* 7514
- Stetson, P. 1987, *PASP*, 99, 191
- Stetson, P. 1994, *PASP*, 106, 250
- Stritzinger, M., et al. 2002, *AJ*, 124, 2100
- Suntzeff, N.B., et al. 1999, *AJ*, 117, 1175
- Szentgyorgyi, A., et al. 2005, in preparation
- Treffers, R.R., Peng, C.Y., Filippenko, A.V., & Richmond, M.W. 1997, *IAU Circ.* 6627
- Turatto, M., Piemonte, A., Benetti, S., Cappellaro, E., Mazzali, P.A., Danziger, I.J., & Patat, F. 1998, *AJ*, 116, 2431

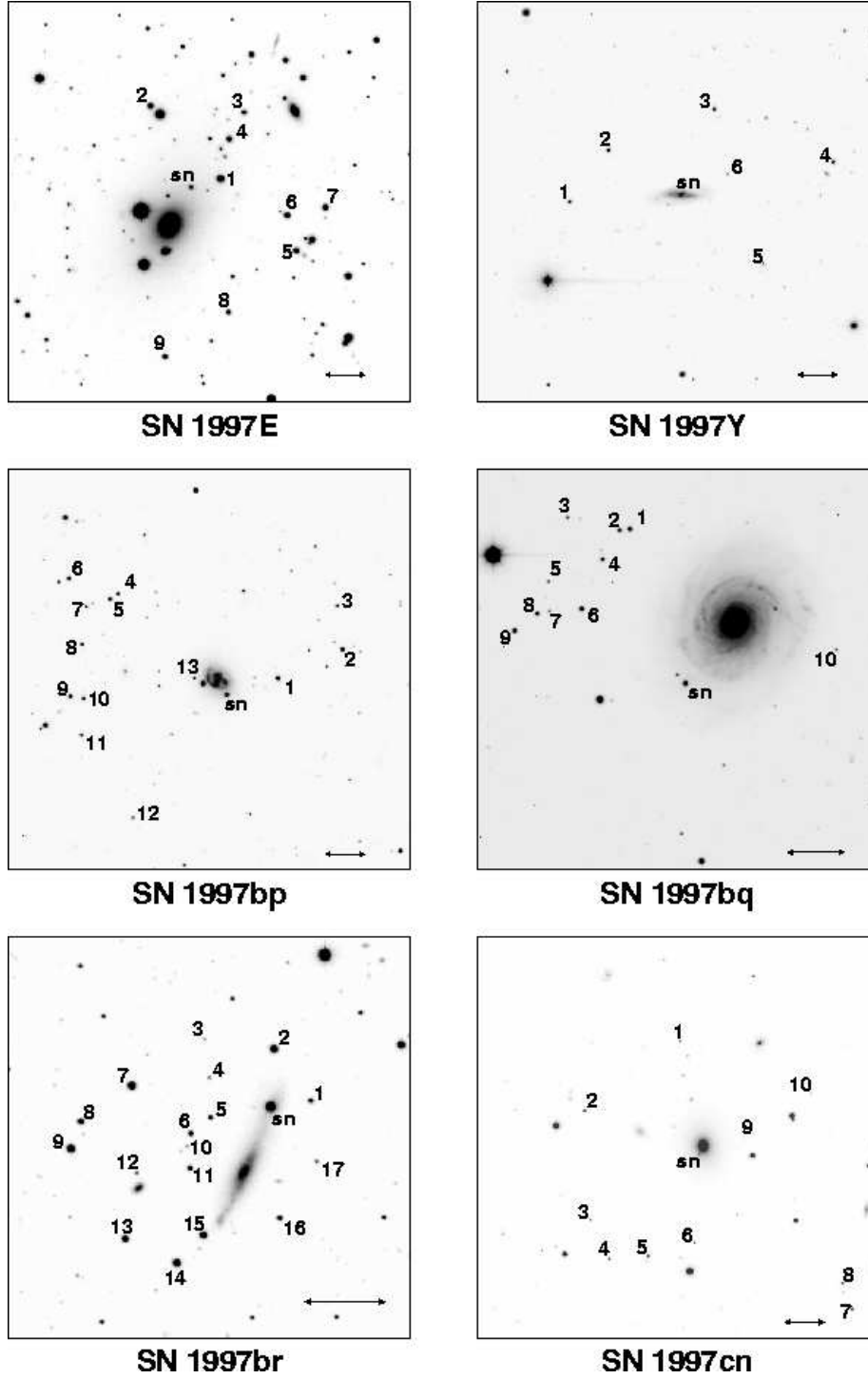


Fig. 1.— Finder charts for the 44 SN Ia presented here and associated comparison stars. The images are a combination of all the *R*-band SN images. North is up and east is to the left. The horizontal double-arrow in the lower right delineates 1'.

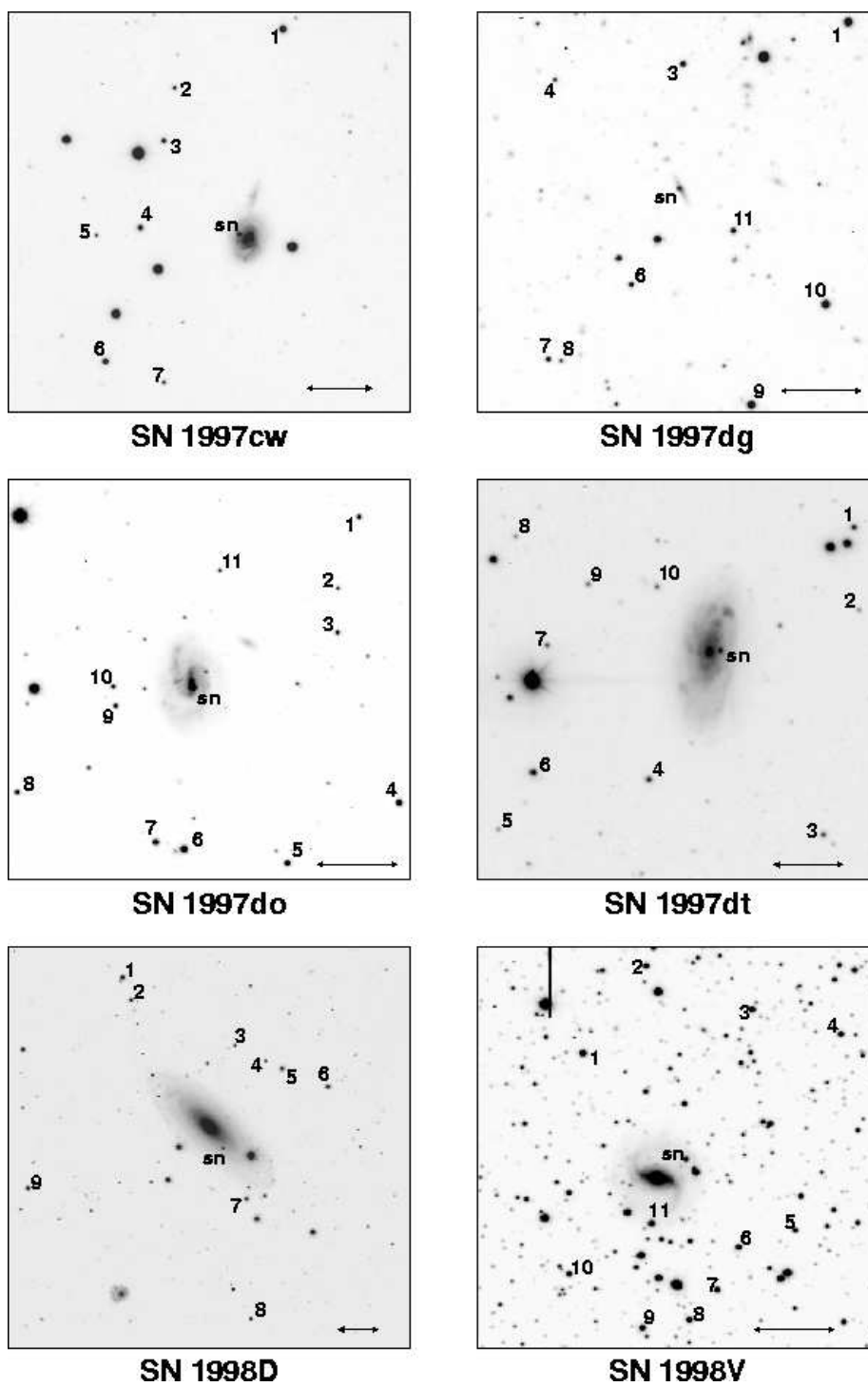


Fig. 1.— Continued

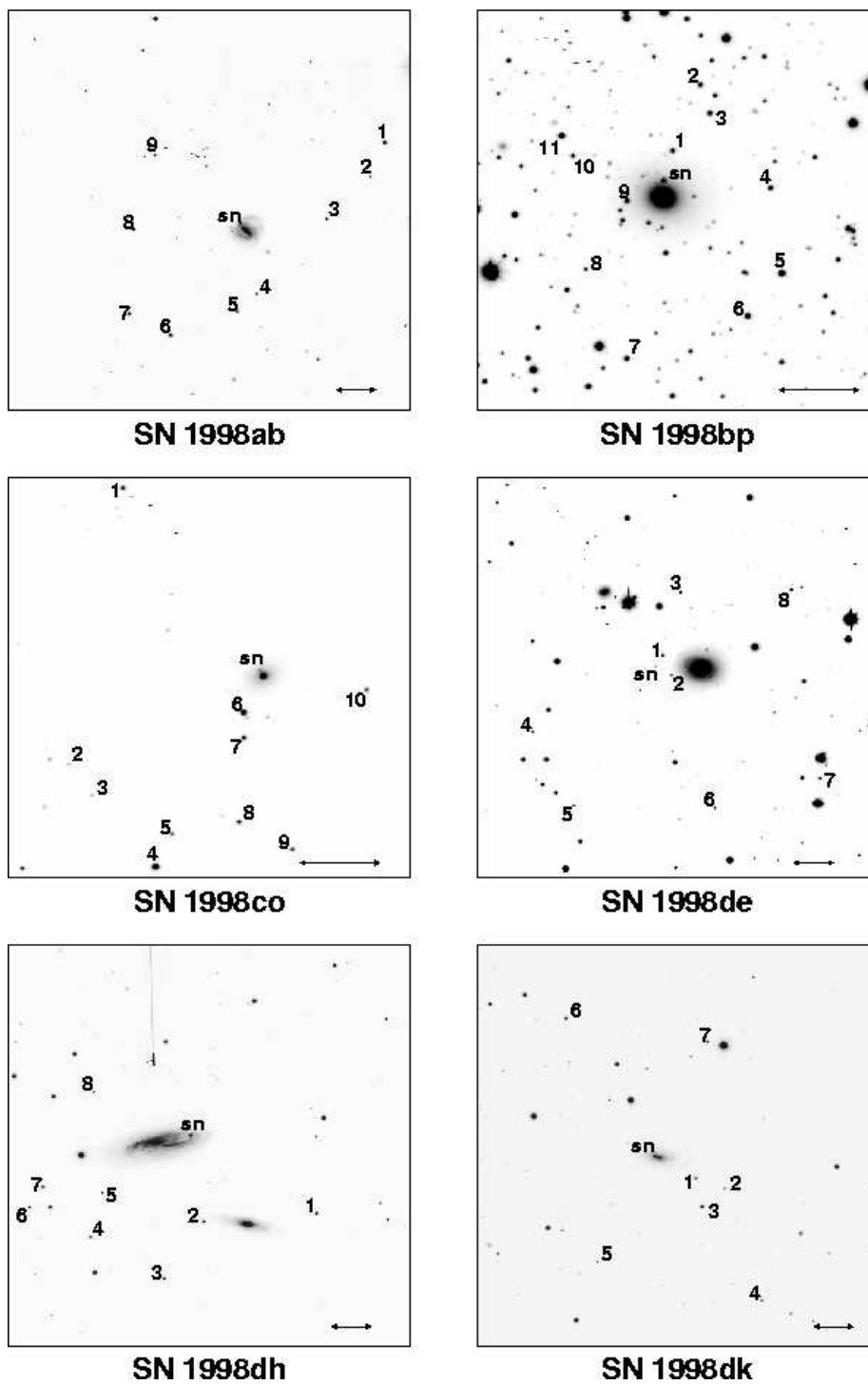


Fig. 1.— Continued

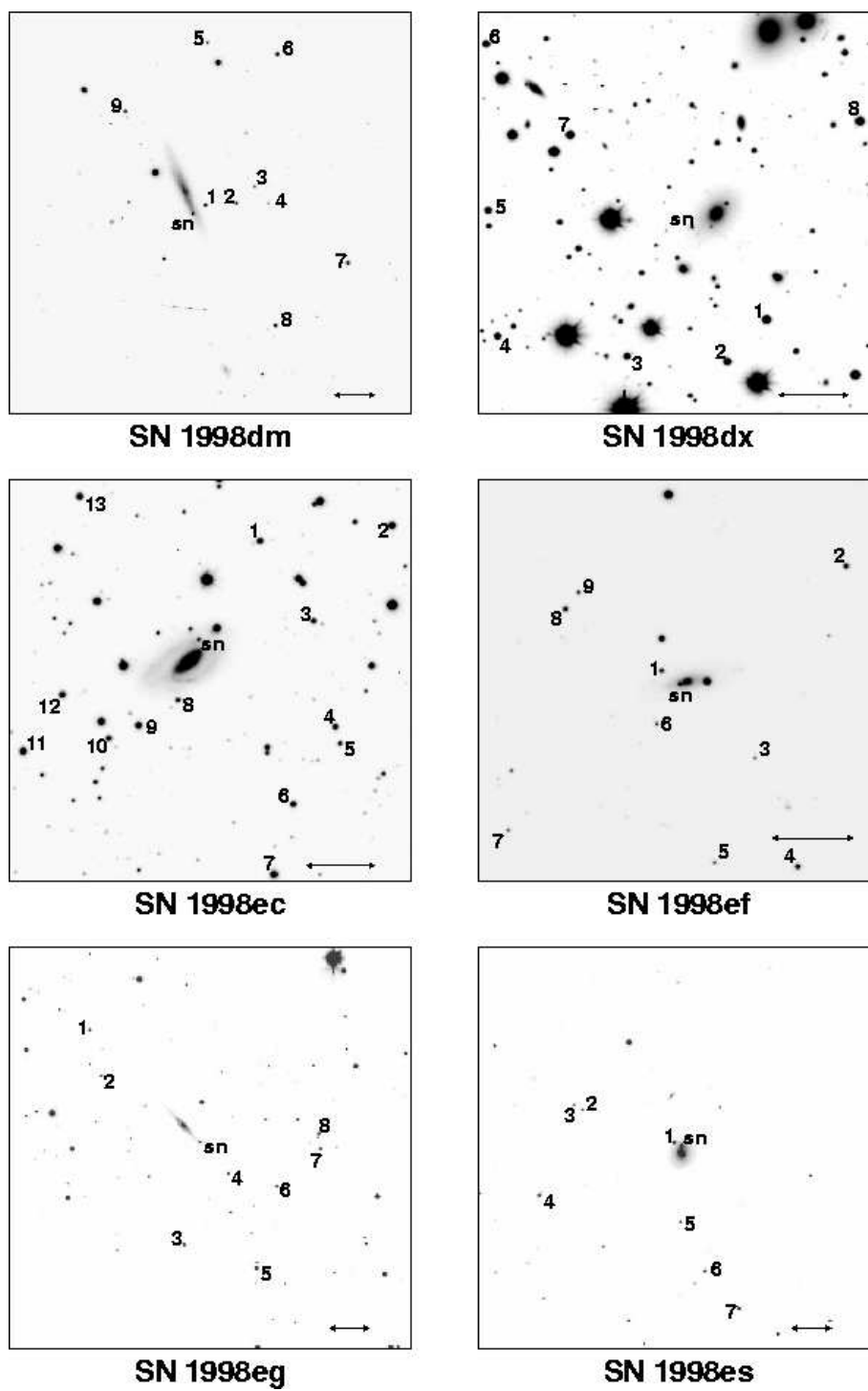


Fig. 1.— Continued

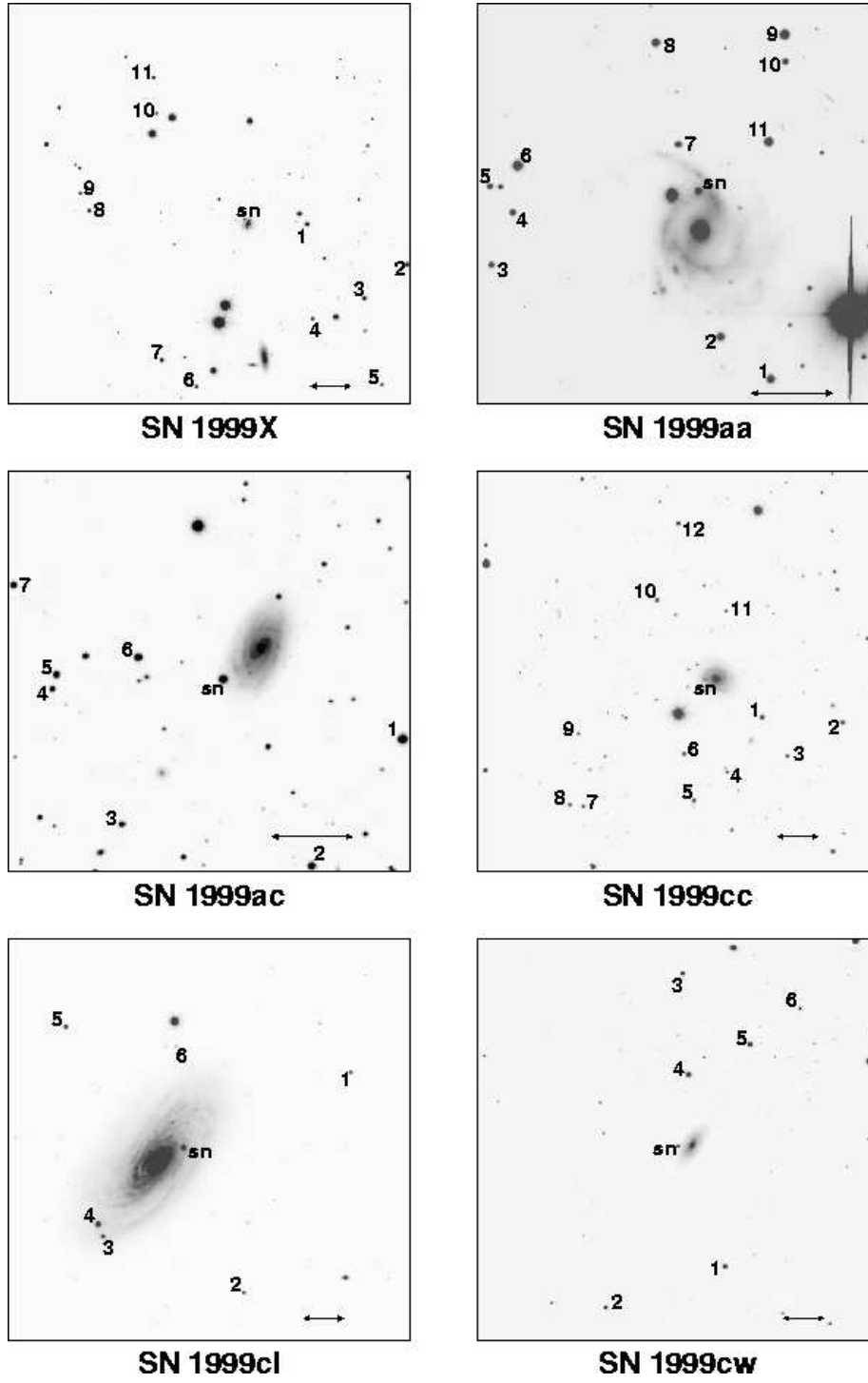


Fig. 1.— Continued

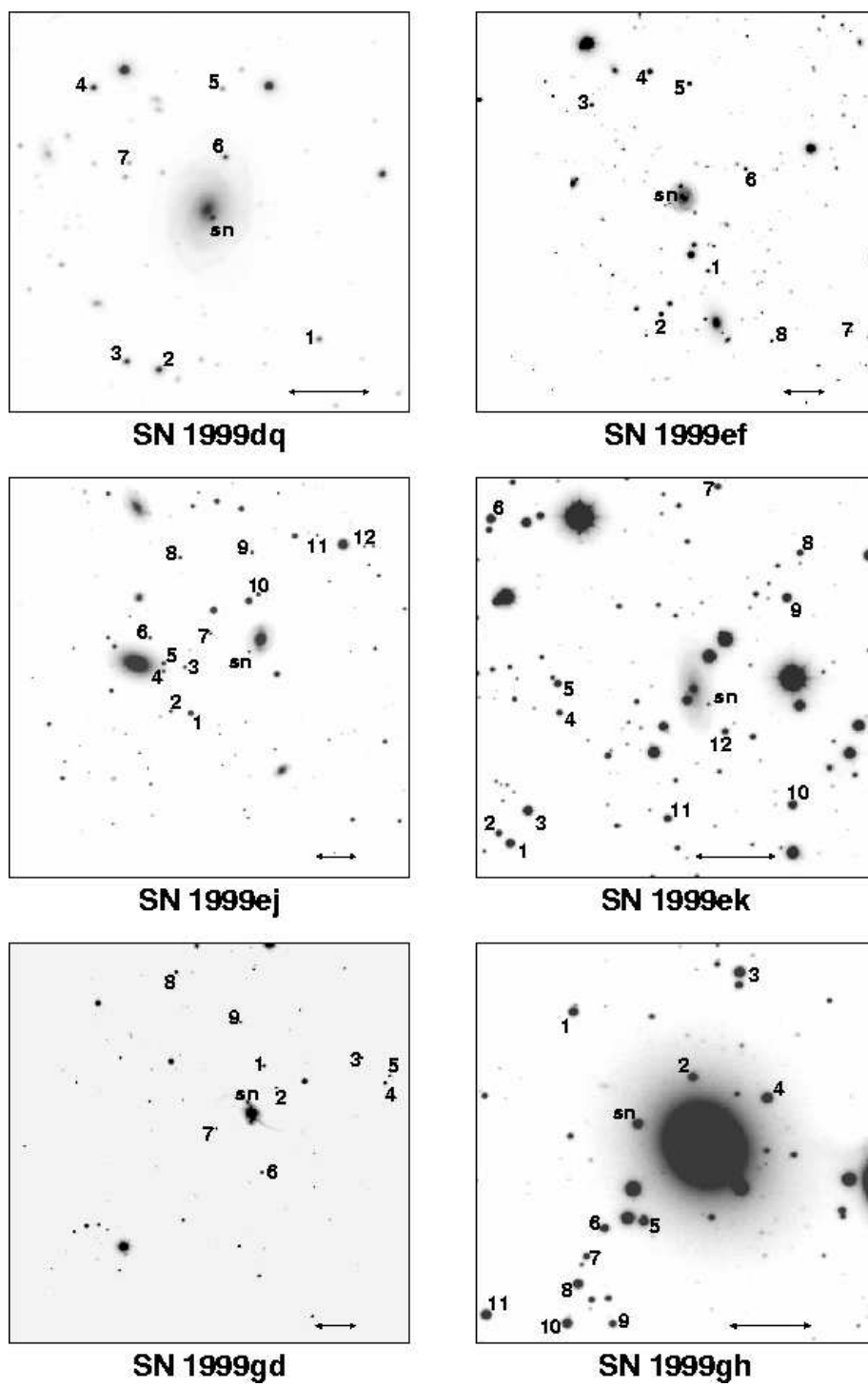


Fig. 1.— Continued

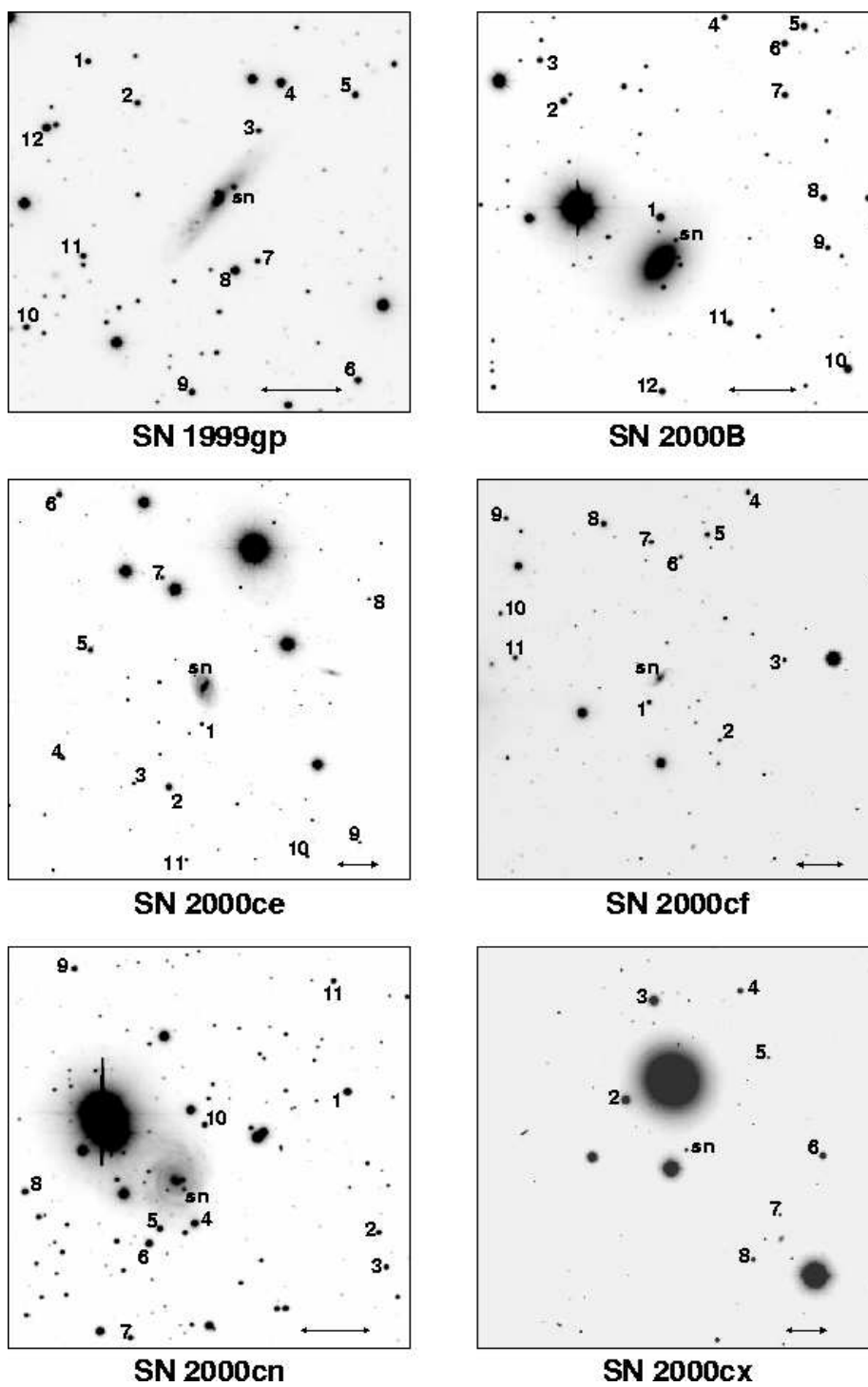


Fig. 1.— Continued

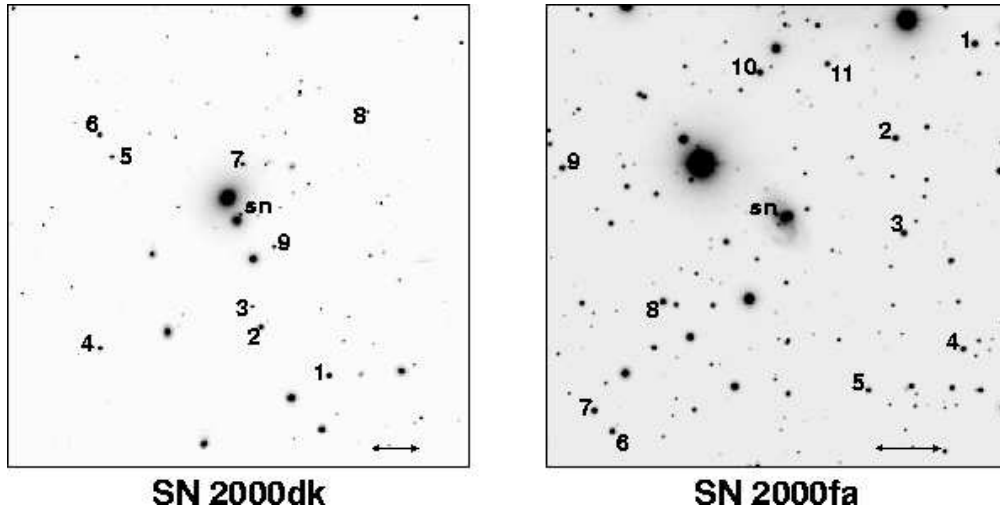


Fig. 1.— Continued

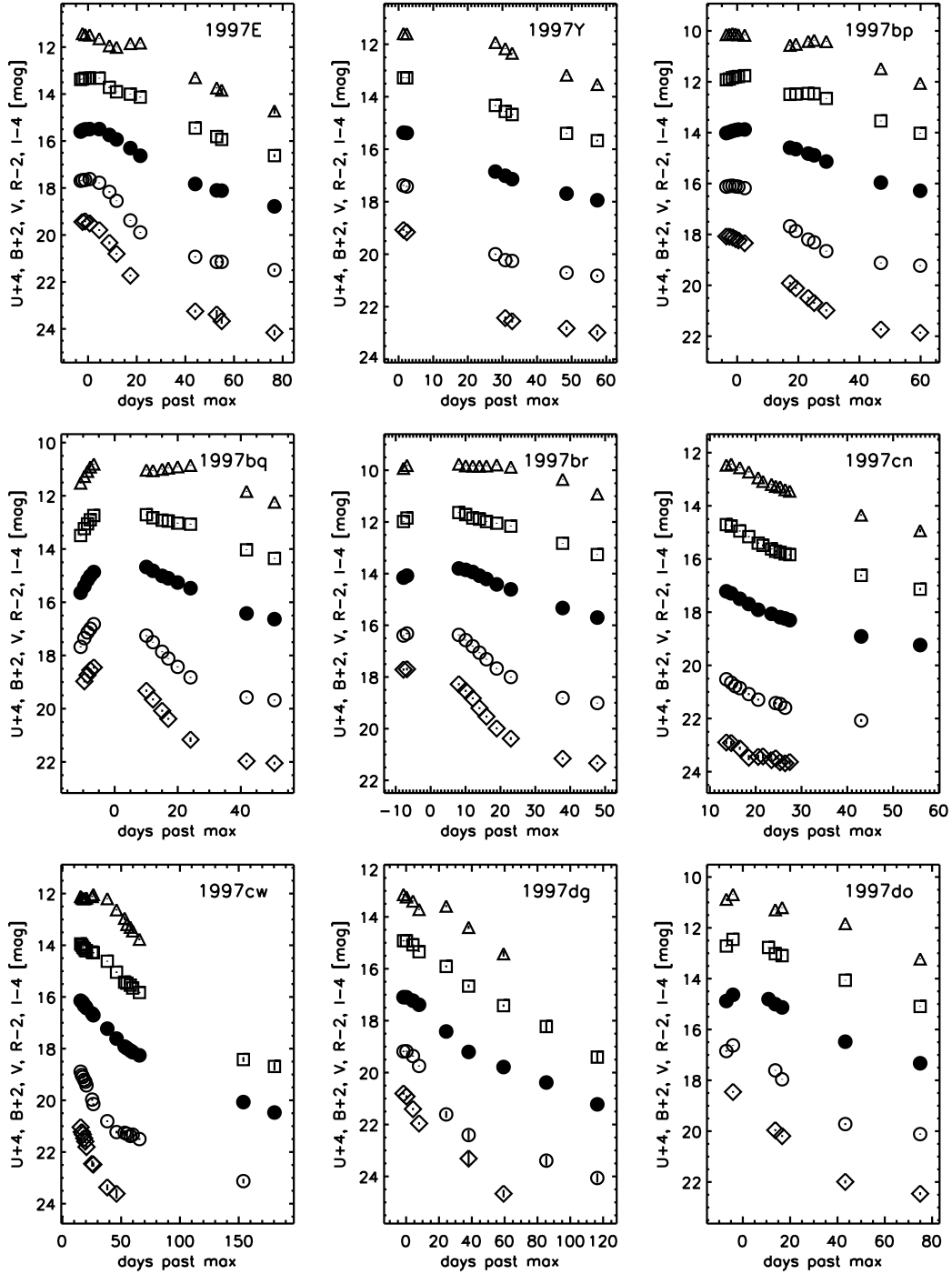


Fig. 2.— *UBVRI* photometry of 44 SN Ia. The *U* (diamonds), *B* (open circles), *V* (filled circles), *R* (squares), and *I* (triangles) light curves are shown shown relative to *B* maximum and have been corrected for time-dilation to the SN rest frame.

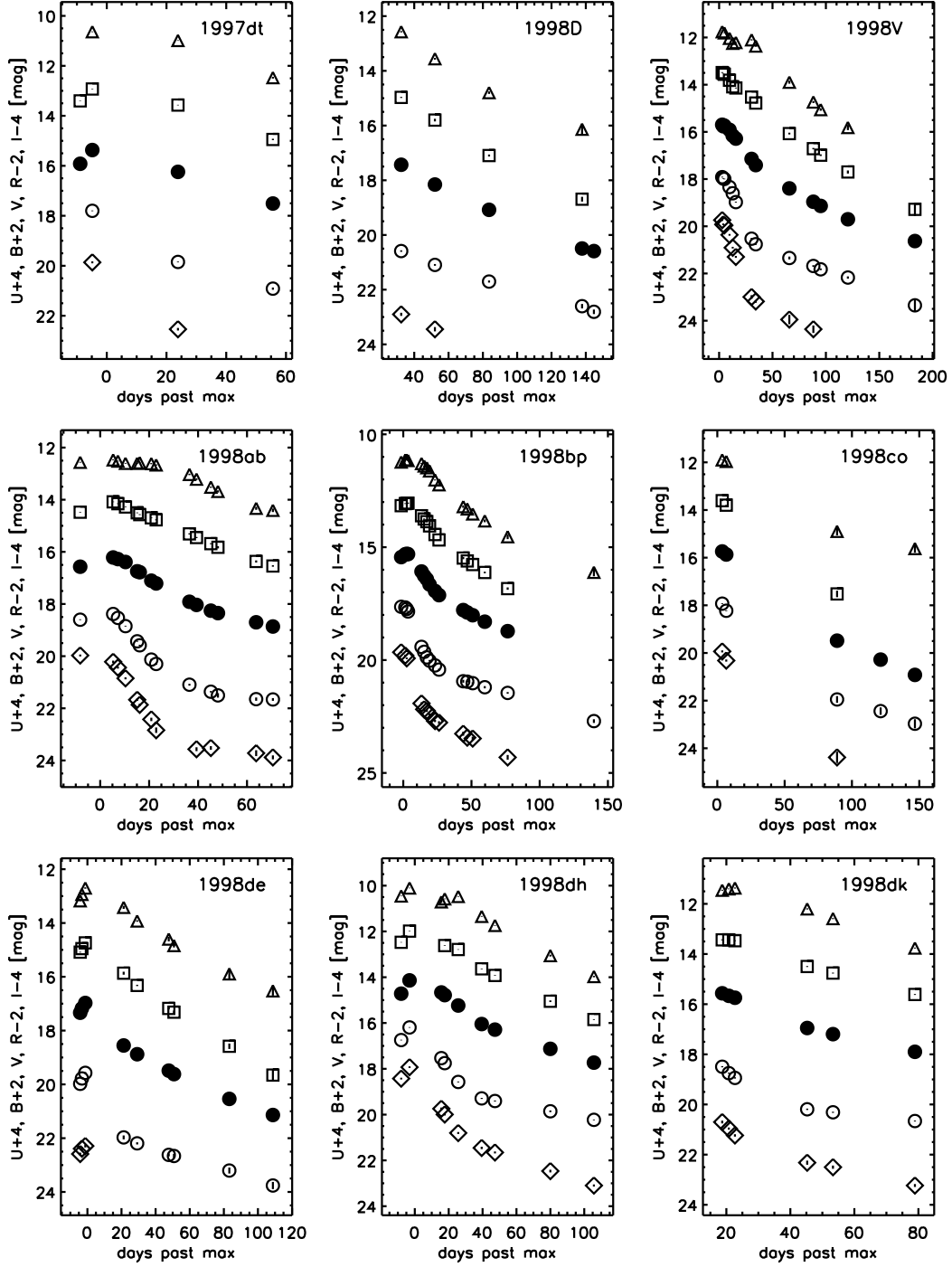


Fig. 2.— Continued

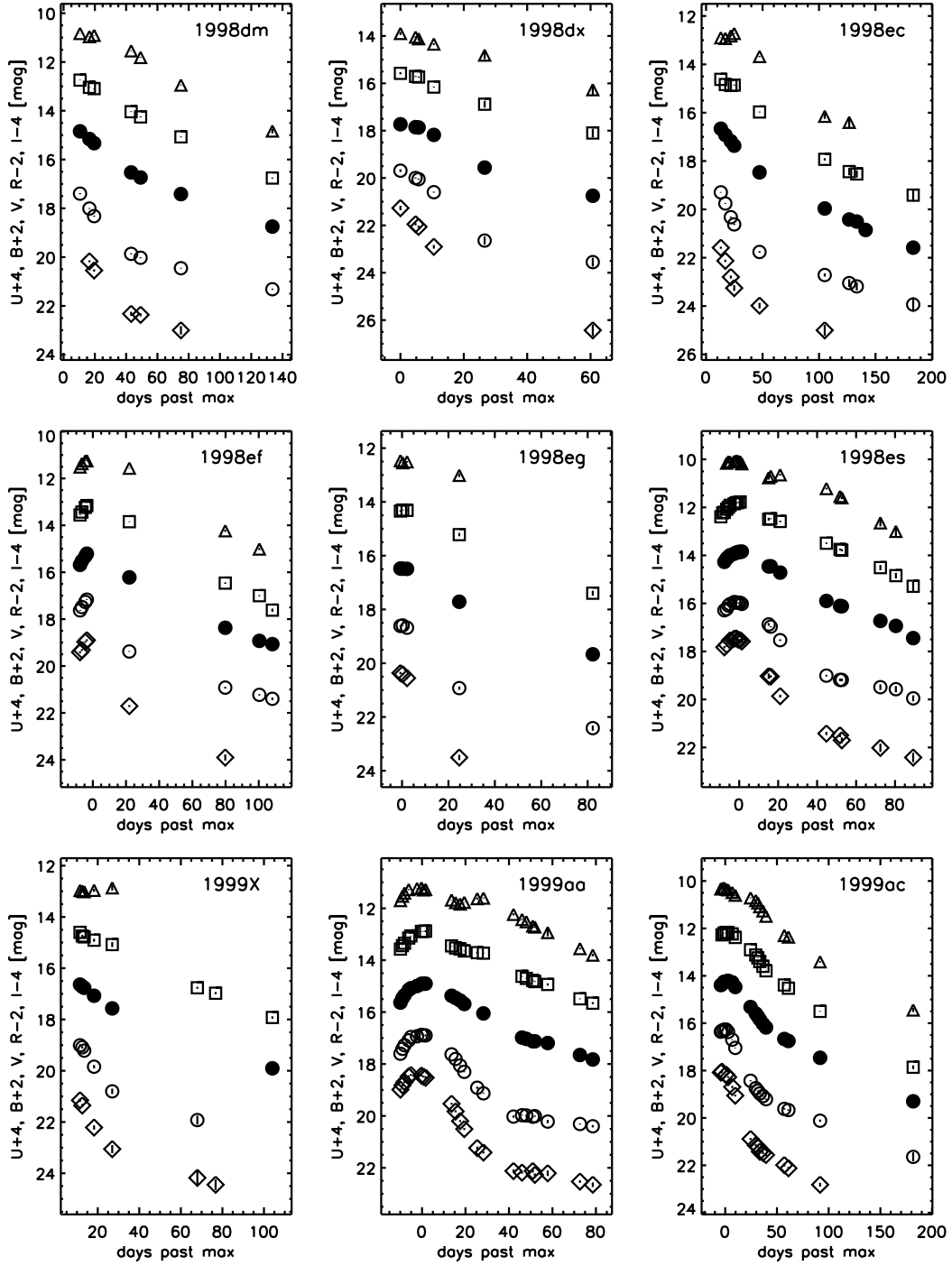


Fig. 2.— Continued

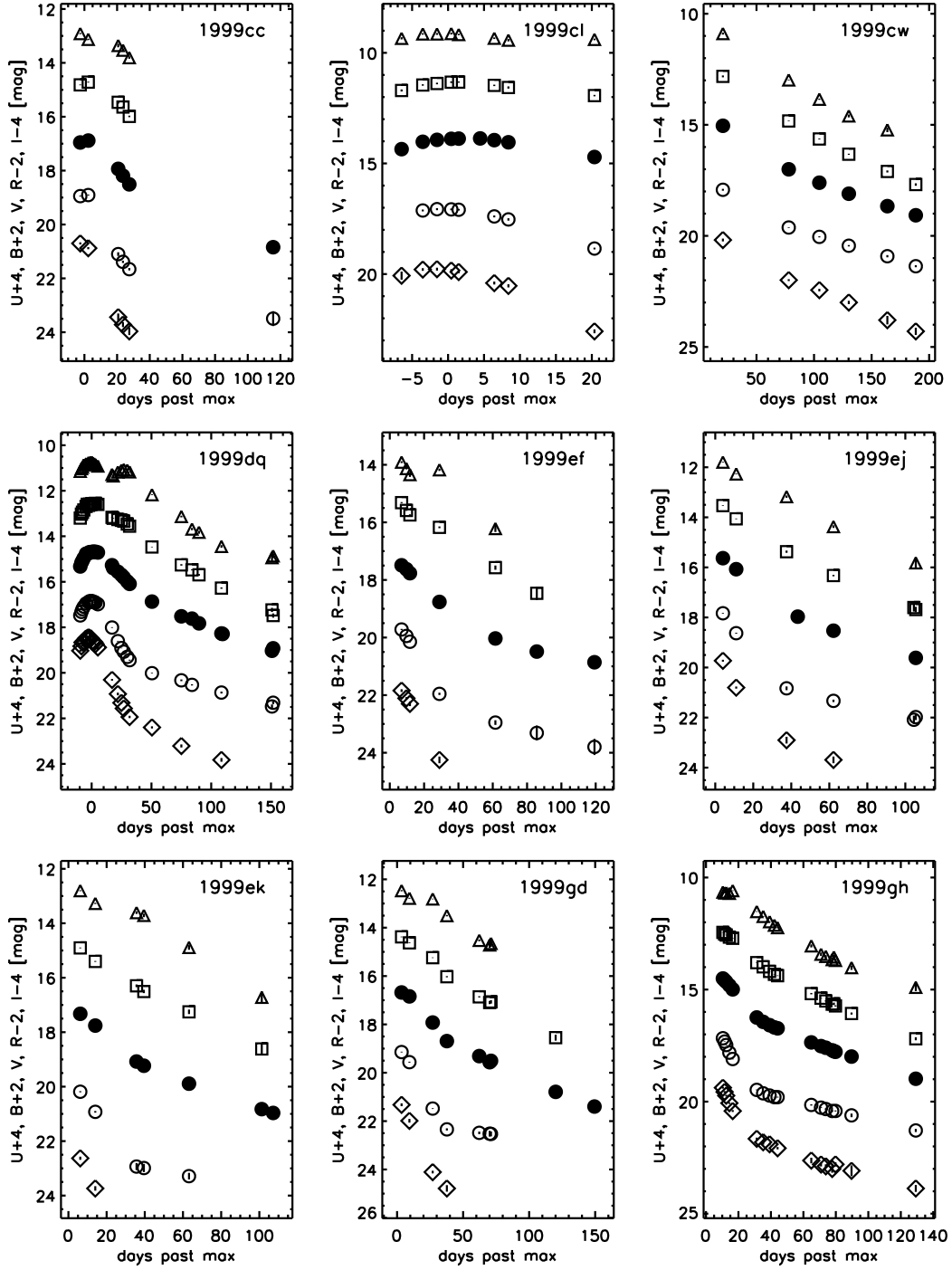


Fig. 2.— Continued

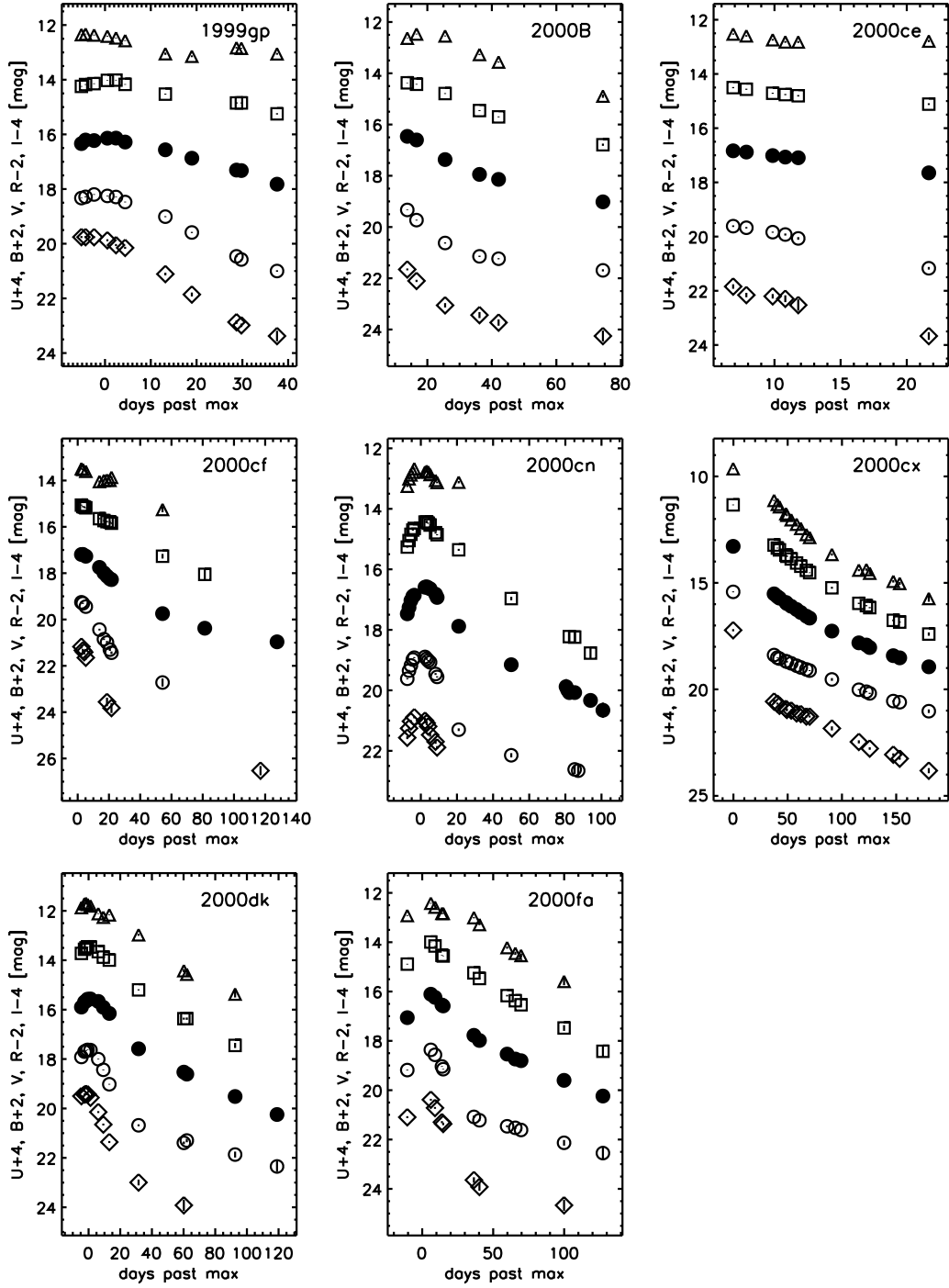


Fig. 2.— Continued

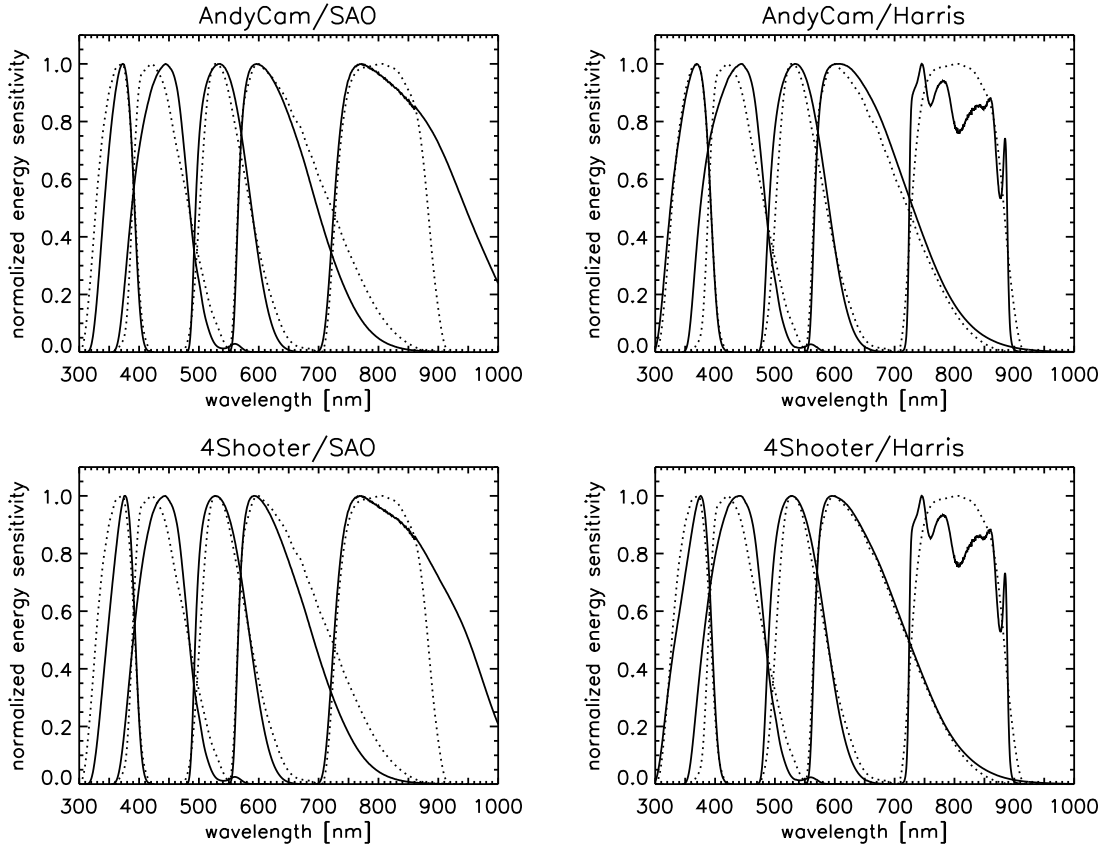


Fig. 3.— Synthesized natural system $UBVR$ passbands (*solid curves*) with the standard UX and $BVRI$ passbands (*dotted curves*) of Bessell (1990) shown for each detector/filterset combination.

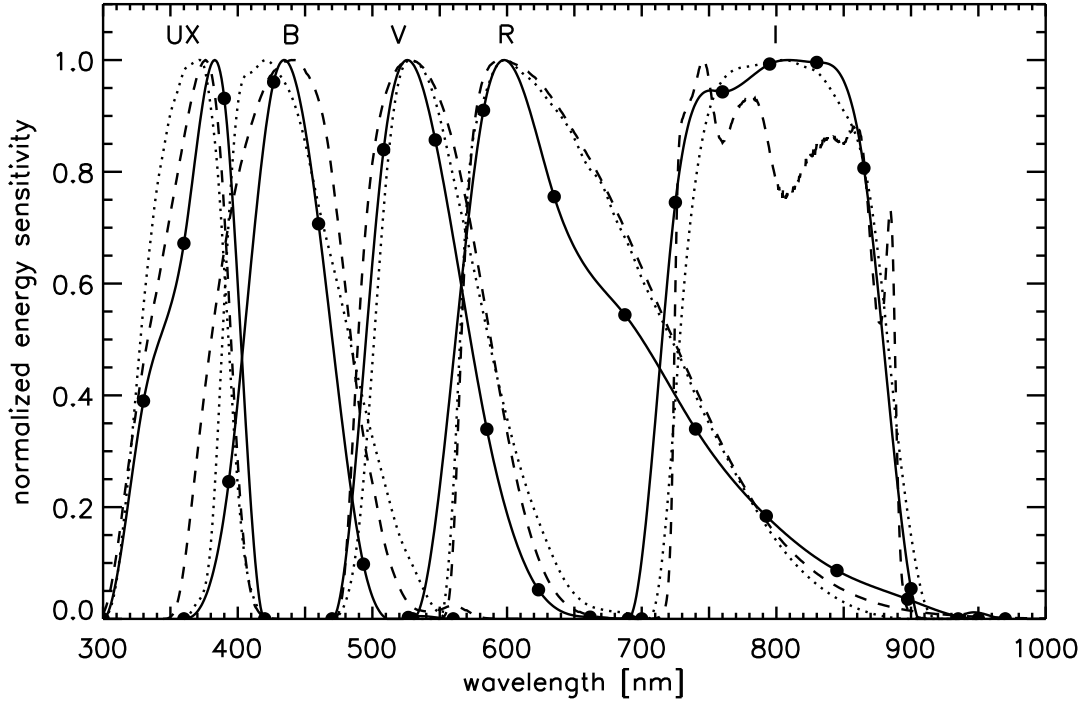


Fig. 4.— Model 4Shooter/Harris *UBVR* passbands derived from observations of spectrophotometric standard stars (*solid curves*), calculated passbands from optics + filter transmission + detector response (*dashed curves*), and the standard *UX* and *BVRI* passbands of Bessell (1990; *dotted curves*). The solid points show the location of the model spline points; see text for details.

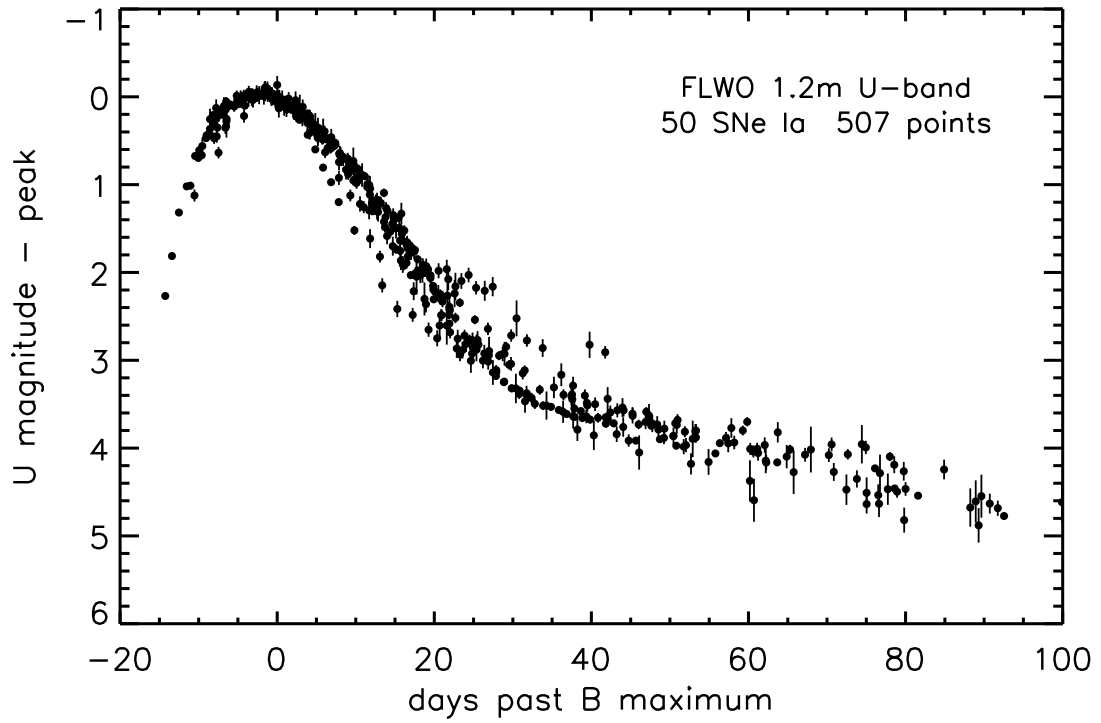


Fig. 5.— Composite *U*-band light curve of 50 SN Ia observed with the FLWO 1.2m telescope. The data were K-corrected and time-dilated to the SN rest frame. There are 507 individual points in the time interval displayed, from -20 to +100 days after maximum light in *B*.

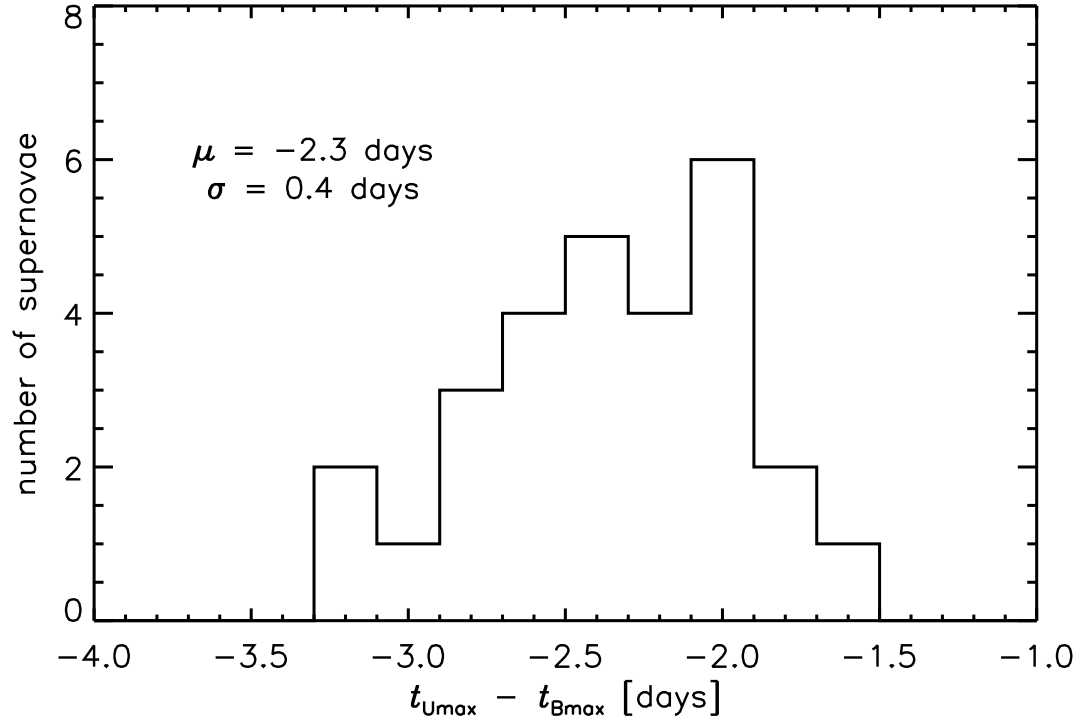


Fig. 6.— Distribution of the time of maximum light in U relative to the time of maximum light in B , measured in the SN rest frame.

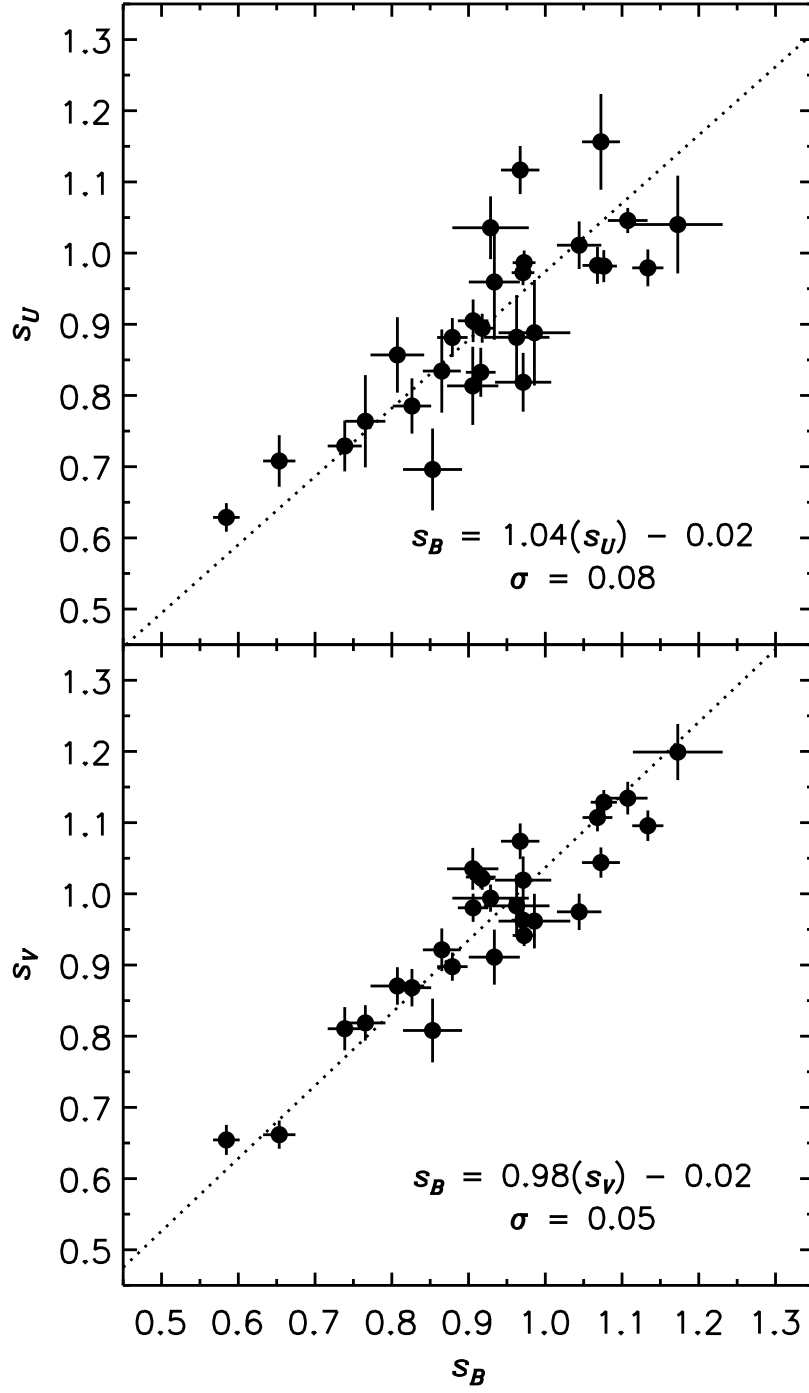


Fig. 7.— Relation between timescale stretch factors in UBV based on the stretch-corrected SN 1998aq templates (see text for details). The best linear fits are: $s_B = (1.04 \pm 0.06)s_U - (0.02 \pm 0.05)$ and $s_B = (0.98 \pm 0.05)s_V - (0.02 \pm 0.05)$.

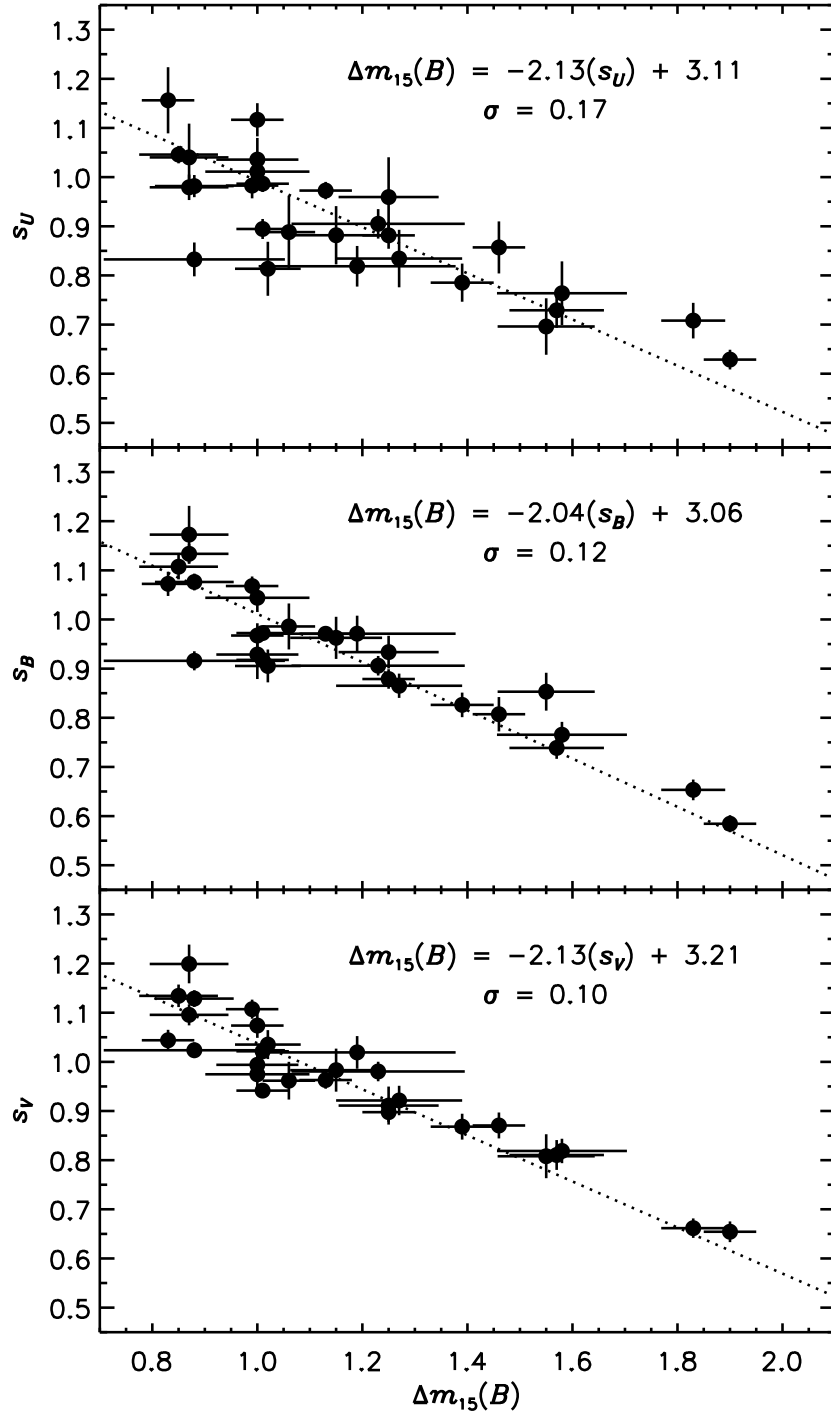


Fig. 8.— Relation between timescale stretch factors and $\Delta m_{15}(B)$. The best linear fits are $\Delta m_{15}(B) = (-2.13 \pm 0.14)s_U + (3.11 \pm 0.13)$, $\Delta m_{15}(B) = (-2.04 \pm 0.11)s_B + (3.06 \pm 0.10)$, and $\Delta m_{15}(B) = (-2.13 \pm 0.12)s_V + (3.21 \pm 0.11)$.

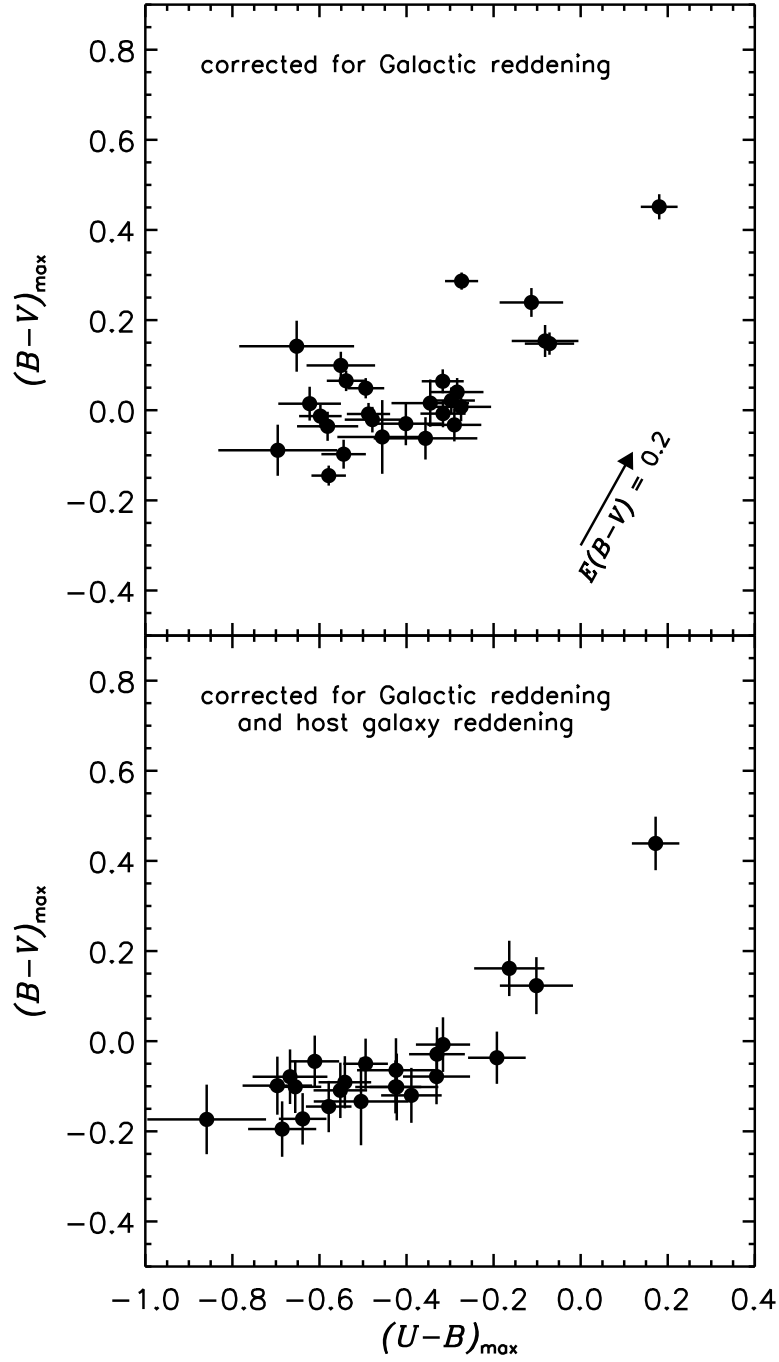


Fig. 9.— SN Ia colors at the epoch of maximum light in B . The top panel shows maximum light colors corrected for Galactic extinction, while the bottom panel includes a correction for extinction in the host galaxy. The arrow indicates a reddening vector corresponding to $E(B-V)_{\text{true}} = 0.2$ mag.

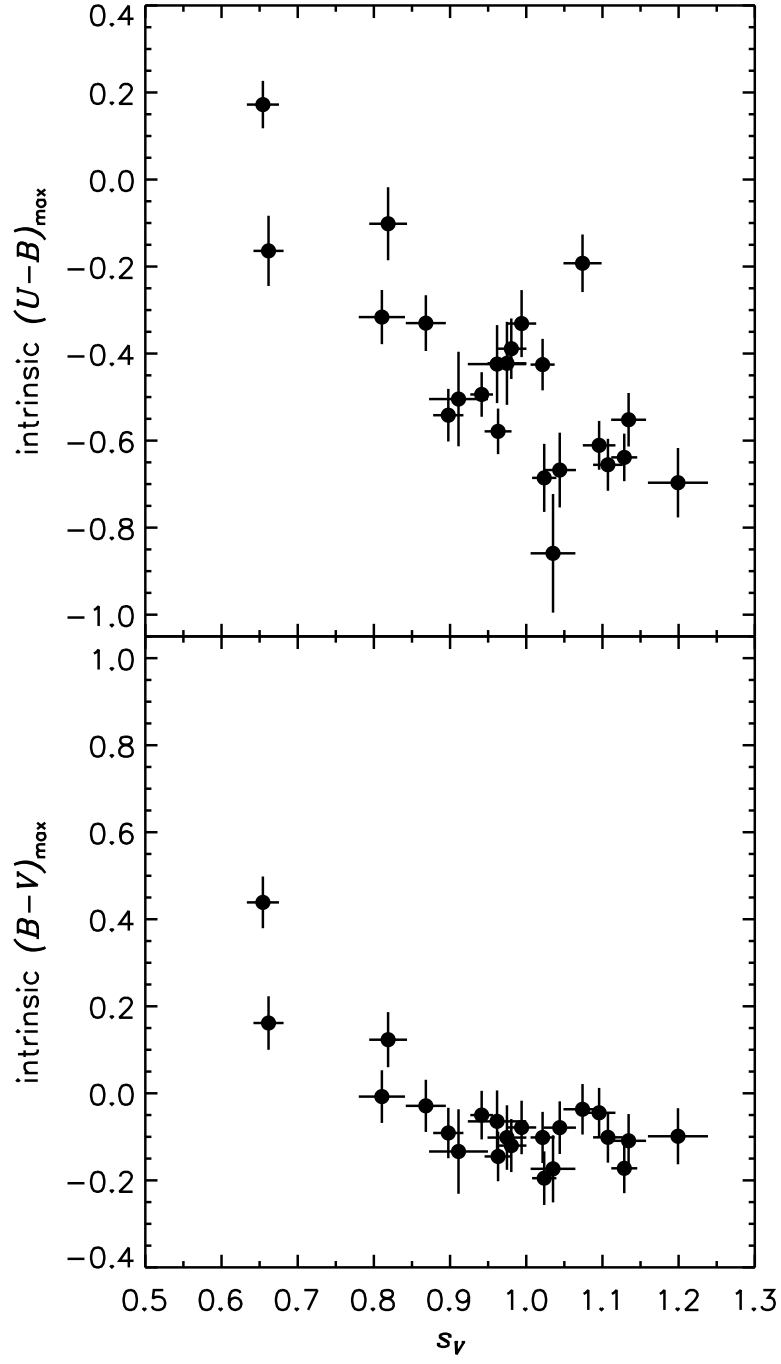


Fig. 10.— Relation between SN Ia UBV colors at maximum light in B and the V -band timescale stretch factor. The colors have been corrected for Galactic and host-galaxy reddening.

Table 1. SN Ia Discovery and Classification Data

SN Ia	Galaxy	Discovery Date	Discoverer	IAUC	Spectroscopic ID	IAUC
1997E	NGC 2258	1997-01-14.5	R. Kushida	6538	P. Garnavich & R. Kirshner (CfA)	6538
1997Y	NGC 4675	1997-02-02	W. Li et al. (BAO)	6556	A. Filippenko et al., P. Garnavich et al. (CfA)	6557
1997bp	NGC 4680	1997-04-06.5	R. Evans	6613	M. Phillips et al.	6613
1997bq	NGC 3147	1997-04-08.0	S. Laurie (UK)	6616	P. Challis (CfA)	6616
1997br	ESO 576-40	1997-04-10.6	Q. Qiao et al. (BAO)	6623	Q. Qiao et al.	6623
1997cn	NGC 5490	1997-05-14.6	W. Li et al. (BAO)	6661	M. Turatto et al.	6667
1997cw	NGC 105	1997-07-10.8	Q. Qiao et al. (BAO)	6699	Q. Qiao et al.	6699
1997dg	anonymous	1997-09-27.7	Q. Qiao et al. (BAO)	6749	S. Jha et al. (CfA)	6749
1997do	UGC 3845	1997-10-31	Y. Qiu et al. (BAO)	6766	Y. Qiu et al.	6766
1997dt	NGC 7448	1997-11-22.4	Q. Qiao et al. (BAO)	6775	Q. Qiao et al.	6775
1998D	NGC 5440	1998-01-28.9	Y. Qiu et al. (BAO)	6815	Y. Qiu et al.	6815
1998V	NGC 6627	1998-03-12.1	M. Armstrong (UK)	6841	S. Jha et al. (CfA)	6844
1998ab	NGC 4704	1998-04-01.7	J. Wei et al. (BAO)	6858	P. Garnavich et al. (CfA)	6858
1998bp	NGC 6495	1998-04-29.1	M. Armstrong (UK)	6890	F. Patat & M. Maia	6890
1998co	NGC 7131	1998-06-21	W. Johnson	6950	P. Garnavich et al. (CfA)	6950
1998de	NGC 252	1998-07-23	M. Modjaz et al. (LOSS)	6977	P. Garnavich et al. (CfA)	6980
1998dh	NGC 7541	1998-07-20.5	W. Li et al. (LOSS)	6978	P. Garnavich et al. (CfA)	6980
1998dk	UGC 139	1998-08-19.4	J. King et al. (LOSS)	6991	A. Filippenko	6997
1998dm	MCG-01-4-44	1998-08-22.5	M. Modjaz et al. (LOSS)	6993	A. Filippenko	6997
1998dx	UGC 11149	1998-09-10.2	M. Modjaz et al. (LOSS)	7011	S. Jha et al. (CfA)	7011
1998ec	UGC 3576	1998-09-26.8	Y. Qiu et al. (BAO)	7022	S. Jha et al. (CfA)	7024
1998ef	UGC 646	1998-10-18.3	W. Li et al. (LOSS)	7032	A. Filippenko	7032
1998eg	UGC 12133	1998-10-19.9	T. Boles (UK)	7033	M. Salvo et al., S. Jha et al. (CfA)	7037
1998es	NGC 632	1998-11-13.3	E. Halderson et al. (LOSS)	7050	S. Jha et al. (CfA)	7054
1999X	CGCG 180-22	1999-01-23.2	M. Schwartz (TO)	7105	P. Garnavich et al. (CfA)	7105
1999aa	NGC 2595	1999-02-11.0	R. Arbour (UK)	7108	A. Filippenko et al.	7108
1999ac	NGC 6063	1999-02-26.5	M. Modjaz et al. (LOSS)	7114	M. Phillips, A. Filippenko	7122
1999cc	NGC 6038	1999-05-08.3	M. Schwartz (TO)	7163	P. Garnavich et al. (CfA)	7169
1999cl	NGC 4501 (M88)	1999-05-29	M. Papenkova et al. (LOSS)	7185	P. Garnavich et al. (CfA)	7190
1999cw	MCG-01-02-001	1999-06-28.5	R. Johnson & W. Li (LOSS)	7211	L. Rizzi et al.	7216
1999dq	NGC 976	1999-09-02.5	W. Li (LOSS)	7247	S. Jha et al. (CfA)	7250
1999ef	UGC 607	1999-10-09	J. Mueller	7275	M. Kuchner & D. Branch	7275
1999ej	NGC 495	1999-10-18.3	A. Friedman et al. (LOSS)	7286	S. Jha et al. (CfA)	7298
1999ek	UGC 3329	1999-10-20.5	R. Johnson & W. Li (LOSS)	7286	L. Strolger et al., S. Jha et al. (CfA)	7300
1999gd	NGC 2623	1999-11-24.5	W. Li (LOSS)	7319	A. Filippenko & P. Garnavich	7328
1999gh	NGC 2986	1999-12-03.8	K. Takamizawa	7328	A. Filippenko & P. Garnavich	7328
1999gp	UGC 1993	1999-12-23.2	M. Papenkova & W. Li (LOSS)	7337	S. Jha et al. (CfA)	7341
2000B	NGC 2320	2000-01-11.0	P. Antonini et al.	7347	F. Colas et al.	7351
2000ce	UGC 4195	2000-05-08.1	T. Puckett (POSS)	7417	S. Jha et al. (CfA)	7422
2000cf	MCG+11-19-25	2000-05-09.2	T. Puckett & A. Sehgal (POSS)	7421	S. Jha et al. (CfA)	7423
2000cn	UGC 11064	2000-06-02.5	M. Papenkova & W. Li (LOSS)	7436	S. Jha et al. (CfA), M. Turatto et al.	7437
2000cx	NGC 524	2000-07-17.5	C. Yu et al. (LOSS)	7458	R. Chornock et al.	7463
2000dk	NGC 382	2000-09-18.3	S. Beckmann & W. Li (LOSS)	7493	S. Jha et al. (CfA)	7494
2000fa	UGC 3770	2000-11-30.5	A. Friedman & W. Li (LOSS)	7533	T. Matheson et al. (CfA)	7535

Table 2. Comparison Star Photometry

Star	α (J2000)	δ (J2000)	V	$U-B$	$B-V$	$V-R$	$V-I$	N
SN 1997E								
SN	06:47:38.16	+74:29:51.0						
1	06:47:27.41	+74:30:02.6	14.402(014)	0.086(041)	0.675(011)	0.427(007)	0.846(010)	3
2	06:47:52.40	+74:31:52.6	15.139(015)	0.123(040)	0.715(011)	0.436(007)	0.863(010)	3
3	06:47:18.41	+74:31:40.7	15.895(017)	0.018(040)	0.584(013)	0.365(008)	0.747(009)	3
4	06:47:23.92	+74:31:01.6	15.410(022)	0.580(045)	0.946(019)	0.539(007)	1.021(014)	3
5	06:47:00.39	+74:28:13.5	15.358(014)	0.594(041)	0.907(012)	0.511(009)	0.968(009)	3
6	06:47:03.36	+74:29:06.4	15.152(013)	0.143(040)	0.733(012)	0.439(008)	0.877(010)	3
7	06:46:49.48	+74:29:17.2	15.181(014)	0.390(042)	0.833(012)	0.481(009)	0.930(013)	3
8	06:47:25.35	+74:26:43.6	16.150(015)	0.231(045)	0.812(011)	0.476(009)	0.926(012)	3
9	06:47:48.60	+74:25:39.1	15.718(014)	0.055(040)	0.657(011)	0.399(007)	0.800(009)	3
SN 1997Y								
SN	12:45:31.46	+54:44:17.4						
1	12:45:50.75	+54:44:06.0	16.576(011)	0.563(061)	0.911(015)	0.544(010)	1.042(011)	2
2	12:45:44.09	+54:45:22.3	16.029(014)	0.428(040)	0.823(013)	0.470(010)	0.946(011)	2
3	12:45:26.06	+54:46:22.0	16.174(061)	0.177(042)	0.766(019)	0.425(008)	0.870(037)	2
4	12:45:05.99	+54:45:01.8	16.562(016)	1.209(119)	1.499(010)	0.941(025)	1.949(009)	2
5	12:45:18.05	+54:42:31.9	17.846(010)	1.081(195)	1.493(029)	1.025(057)	2.370(020)	2
6	12:45:23.93	+54:44:45.6	18.317(040)	0.216(238)	0.830(056)	0.449(013)	0.908(032)	2
SN 1997bp								
SN	12:46:53.78	-11:38:33.2						
1	12:46:48.63	-11:38:09.3	14.525(012)	-0.001(042)	0.610(014)	0.360(007)	0.717(014)	3
2	12:46:42.03	-11:37:27.5	14.840(014)	-0.036(043)	0.590(011)	0.353(009)	0.698(014)	3
3	12:46:42.53	-11:36:22.2	15.953(012)	0.234(041)	0.731(012)	0.436(007)	0.832(015)	3
4	12:47:04.62	-11:36:00.8	16.150(013)	0.090(043)	0.750(016)	0.447(014)	0.899(013)	3
5	12:47:05.48	-11:36:08.6	15.462(011)	0.789(044)	0.951(016)	0.552(008)	1.022(015)	3
6	12:47:09.57	-11:35:37.1	15.227(014)	0.003(048)	0.630(014)	0.408(012)	0.832(016)	3
7	12:47:07.87	-11:36:19.4	16.201(014)	0.106(042)	0.634(010)	0.379(012)	0.737(019)	3
8	12:47:08.39	-11:37:15.4	16.309(013)	-0.007(042)	0.604(015)	0.366(015)	0.723(024)	3
9	12:47:09.58	-11:38:32.9	14.889(011)	0.124(042)	0.688(011)	0.414(008)	0.799(011)	3
10	12:47:08.24	-11:38:36.4	15.463(011)	0.385(042)	0.821(013)	0.493(009)	0.963(011)	3
11	12:47:08.53	-11:39:31.1	16.236(013)	-0.278(042)	0.481(014)	0.331(016)	0.666(012)	3
12	12:47:03.38	-11:41:35.2	16.879(012)	0.099(041)	0.657(019)	0.375(021)	0.755(017)	3
13	12:46:57.05	-11:38:08.0	16.722(053)	-0.052(054)	0.585(034)	0.356(015)	0.691(036)	3
SN 1997bq								
SN	10:17:05.48	+73:23:01.5						
1	10:17:18.23	+73:25:38.3	15.948(032)	-0.108(041)	0.531(026)	0.344(007)	0.687(022)	2
2	10:17:20.64	+73:25:37.4	16.633(026)	0.861(041)	1.015(021)	0.620(011)	1.141(024)	2
3	10:17:33.01	+73:25:50.8	17.225(042)	-0.136(078)	0.506(017)	0.349(013)	0.724(032)	2
4	10:17:24.78	+73:25:08.2	16.621(023)	0.186(093)	0.740(023)	0.431(013)	0.827(021)	2
5	10:17:37.69	+73:24:46.0	17.991(056)	0.361(207)	0.590(233)	0.479(010)	...	2
6	10:17:29.91	+73:24:18.0	15.928(031)	0.197(040)	0.744(029)	0.445(007)	0.877(014)	2
7	10:17:37.52	+73:24:16.0	17.971(010)	...	0.968(042)	0.541(022)	1.050(011)	2
8	10:17:40.47	+73:24:13.5	16.432(014)	0.299(046)	0.746(018)	0.459(010)	0.890(014)	2
9	10:17:45.85	+73:23:56.5	16.004(039)	0.303(041)	0.816(013)	0.462(016)	0.912(014)	2
10	10:16:29.63	+73:23:33.6	18.017(027)	0.780(209)	0.875(028)	0.488(019)	0.987(044)	2
SN 1997br								
SN	13:20:42.38	-22:02:12.7						
1	13:20:40.15	-22:02:07.0	17.570(021)	...	0.900(017)	0.507(021)	0.914(090)	3
2	13:20:42.28	-22:01:27.6	16.014(017)	1.172(100)	1.187(010)	0.736(010)	1.362(010)	3
3	13:20:46.13	-22:01:21.4	19.816(078)	...	0.832(205)	0.638(154)	1.099(168)	2
4	13:20:45.81	-22:01:51.1	19.227(038)	...	0.873(016)	0.432(065)	0.898(257)	3
5	13:20:45.67	-22:02:22.2	18.330(011)	...	1.552(028)	1.191(007)	2.613(014)	3
6	13:20:46.75	-22:02:34.9	17.407(023)	0.423(163)	0.860(011)	0.508(029)	0.974(012)	3
7	13:20:50.08	-22:01:59.1	15.483(016)	0.655(051)	0.956(015)	0.544(007)	1.022(009)	3
8	13:20:52.84	-22:02:27.9	16.966(011)	...	1.168(016)	0.713(013)	1.315(023)	3
9	13:20:53.35	-22:02:49.2	15.608(015)	0.371(059)	0.903(012)	0.521(011)	1.013(019)	3
10	13:20:46.92	-22:02:45.2	0.775(197)	0.441(043)	1.086(102)	3
11	13:20:46.75	-22:03:01.9	17.709(014)	...	1.111(014)	0.702(028)	1.316(012)	3
12	13:20:49.68	-22:03:06.7	19.166(035)	...	1.062(027)	0.587(046)	1.249(073)	3
13	13:20:50.22	-22:03:58.2	16.404(018)	0.006(043)	0.734(013)	0.402(008)	0.776(018)	3
14	13:20:47.32	-22:04:15.8	15.600(021)	-0.053(046)	0.634(012)	0.380(008)	0.755(009)	3
15	13:20:45.89	-22:03:53.5	15.908(019)	0.031(083)	0.697(012)	0.427(007)	0.844(011)	3
16	13:20:41.71	-22:03:38.8	17.519(023)	...	0.879(017)	0.514(007)	0.983(018)	3
17	13:20:39.75	-22:02:54.3	19.337(197)	...	1.283(165)	0.884(014)	1.784(072)	3

Table 2—Continued

Star	α (J2000)	δ (J2000)	V	$U-B$	$B-V$	$V-R$	$V-I$	N
SN 1997cn								
SN	14:09:57.74	+17:32:32.2						
1	14:09:59.56	+17:35:18.1	17.456(014)	1.269(166)	1.322(024)	0.817(012)	1.562(013)	3
2	14:10:09.47	+17:33:38.0	16.137(011)	0.153(049)	0.726(015)	0.407(009)	0.813(013)	3
3	14:10:09.00	+17:30:57.3	17.694(012)	0.622(105)	0.876(013)	0.512(009)	0.988(017)	3
4	14:10:07.12	+17:30:00.0	16.150(011)	0.128(058)	0.677(013)	0.375(008)	0.753(016)	3
5	14:10:03.12	+17:30:03.5	15.966(011)	0.059(045)	0.653(013)	0.377(008)	0.753(011)	3
6	14:09:58.30	+17:30:22.4	17.694(018)	0.436(088)	0.798(014)	0.447(019)	0.885(010)	3
7	14:09:42.17	+17:28:41.7	16.683(016)	1.135(124)	1.111(011)	0.664(015)	1.230(033)	3
8	14:09:43.14	+17:29:19.9	16.975(012)	1.080(138)	1.448(017)	0.915(009)	1.804(023)	3
9	14:09:52.00	+17:33:02.7	18.516(015)	0.050(260)	0.622(032)	0.380(015)	0.696(069)	3
10	14:09:46.13	+17:33:59.5	17.894(025)	0.169(199)	0.719(029)	0.393(009)	0.831(022)	3
SN 1997cw								
SN	00:25:17.26	+12:53:06.4						
1	00:25:14.51	+12:56:11.1	15.147(029)	0.294(080)	0.797(031)	0.447(027)	0.877(028)	1
2	00:25:21.21	+12:55:18.5	17.368(063)	0.161(160)	0.721(069)	0.451(053)	0.874(058)	1
3	00:25:21.89	+12:54:31.0	16.035(038)	-0.018(100)	0.651(041)	0.385(033)	0.765(035)	1
4	00:25:23.36	+12:53:12.6	15.813(035)	0.085(094)	0.708(038)	0.406(031)	0.807(033)	1
5	00:25:26.06	+12:53:06.2	17.994(082)	1.684(207)	1.361(090)	0.846(069)	1.577(075)	1
6	00:25:25.54	+12:51:12.5	15.801(035)	0.160(094)	0.723(038)	0.420(031)	0.814(033)	1
7	00:25:21.96	+12:50:52.9	16.990(054)	0.091(139)	0.716(059)	0.405(046)	0.793(050)	1
SN 1997dg								
SN	23:40:14.28	+26:12:11.2						
1	23:40:05.02	+26:14:16.0	15.777(035)	0.001(093)	0.637(038)	0.383(031)	0.766(033)	1
3	23:40:14.02	+26:13:45.1	17.499(066)	0.820(169)	1.061(073)	0.653(056)	1.219(061)	1
4	23:40:20.99	+26:13:33.7	18.674(110)	0.205(278)	0.927(122)	0.508(093)	1.006(101)	1
6	23:40:16.90	+26:10:58.6	17.974(081)	0.605(206)	0.954(090)	0.540(069)	1.017(074)	1
7	23:40:21.45	+26:10:02.8	18.347(096)	...	1.406(106)	0.936(080)	1.782(087)	1
8	23:40:20.75	+26:10:01.4	18.857(120)	...	0.930(133)	0.533(100)	0.976(109)	1
9	23:40:10.41	+26:09:27.4	15.969(037)	0.083(098)	0.699(040)	0.416(033)	0.816(035)	1
10	23:40:06.33	+26:10:43.1	15.959(037)	-0.054(098)	0.558(040)	0.343(033)	0.698(035)	1
11	23:40:11.33	+26:11:39.0	17.698(072)	0.802(183)	1.018(080)	0.616(061)	1.121(066)	1
SN 1997do								
SN	07:26:42.59	+47:05:34.6						
1	07:26:30.31	+47:07:44.1	16.999(054)	0.206(139)	0.795(059)	0.448(046)	0.885(050)	1
2	07:26:31.90	+47:06:49.9	17.761(074)	-0.048(188)	0.616(082)	0.391(063)	0.738(068)	1
3	07:26:31.95	+47:06:16.2	17.294(061)	0.590(156)	0.893(067)	0.528(052)	1.016(056)	1
4	07:26:27.49	+47:04:06.3	16.194(040)	0.736(105)	1.011(043)	0.591(035)	1.151(037)	1
5	07:26:35.73	+47:03:20.7	16.362(042)	0.251(111)	0.774(046)	0.432(037)	0.858(039)	1
6	07:26:43.33	+47:03:31.7	15.545(033)	-0.008(088)	0.675(035)	0.361(029)	0.718(031)	1
7	07:26:45.40	+47:03:37.2	16.352(042)	0.072(111)	0.694(046)	0.388(037)	0.772(039)	1
8	07:26:55.57	+47:04:15.6	17.046(055)	0.454(142)	0.881(060)	0.506(047)	0.946(051)	1
9	07:26:48.30	+47:05:20.9	17.250(060)	0.431(153)	0.860(066)	0.464(051)	0.885(055)	1
10	07:26:48.46	+47:05:35.9	17.955(080)	1.550(204)	1.340(089)	0.897(068)	1.705(074)	1
11	07:26:40.59	+47:07:03.9	17.893(078)	0.607(199)	0.948(087)	0.547(066)	1.016(072)	1
SN 1997dt								
SN	23:00:02.97	+15:58:50.4						
1	22:59:55.18	+16:00:31.0	15.940(037)	-0.004(098)	0.581(040)	0.347(033)	0.682(034)	1
2	22:59:54.90	+15:59:23.2	18.007(082)	-0.213(208)	0.547(091)	0.332(069)	0.728(075)	1
3	22:59:57.02	+15:56:18.8	16.646(047)	0.167(122)	0.767(051)	0.434(041)	0.911(044)	1
4	23:00:07.16	+15:57:04.8	16.520(045)	0.894(117)	1.051(049)	0.639(039)	1.209(042)	1
5	23:00:15.93	+15:56:24.4	18.056(084)	-0.086(213)	0.543(093)	0.346(071)	0.734(077)	1
6	23:00:13.88	+15:57:11.1	15.256(030)	0.143(082)	0.790(032)	0.464(027)	0.951(029)	1
7	23:00:13.03	+15:58:55.3	16.807(050)	-0.182(130)	0.547(055)	0.338(043)	0.708(046)	1
8	23:00:14.85	+16:00:25.1	17.785(075)	-0.077(190)	0.573(083)	0.362(063)	0.711(069)	1
9	23:00:10.63	+15:59:45.5	17.496(066)	0.247(169)	0.785(073)	0.463(056)	0.883(061)	1
10	23:00:06.65	+15:59:43.2	17.146(057)	0.019(147)	0.659(063)	0.381(049)	0.808(053)	1

Table 2—Continued

Star	α (J2000)	δ (J2000)	V	$U-B$	$B-V$	$V-R$	$V-I$	N
SN 1998D								
SN	14:02:59.33	+34:44:54.6						
1	14:03:11.93	+34:49:23.6	15.350(013)	0.082(049)	0.672(014)	0.370(007)	0.755(029)	3
2	14:03:10.88	+34:48:48.1	16.041(012)	−0.059(042)	0.584(012)	0.354(010)	0.725(027)	4
3	14:02:57.85	+34:47:36.6	16.896(014)	0.037(067)	0.724(013)	0.427(009)	0.900(015)	4
4	14:02:53.98	+34:47:12.0	17.567(012)	−0.016(063)	0.038(015)	0.015(014)	0.123(045)	4
5	14:02:51.94	+34:47:00.5	15.281(014)	0.336(053)	0.780(016)	0.445(007)	0.878(029)	3
6	14:02:46.22	+34:46:31.8	15.687(013)	0.608(048)	0.904(016)	0.559(011)	1.057(032)	4
7	14:02:56.40	+34:43:34.8	15.889(015)	−0.054(041)	0.587(012)	0.348(008)	0.707(034)	4
8	14:02:55.85	+34:40:26.0	16.586(013)	−0.075(044)	0.587(010)	0.344(008)	0.703(019)	4
9	14:03:23.77	+34:43:51.6	15.522(013)	0.032(040)	0.600(011)	0.341(010)	0.707(031)	4
SN 1998V								
SN	18:22:37.40	+15:42:08.0						
1	18:22:42.93	+15:43:30.7	15.705(011)	0.434(050)	0.894(013)	0.516(007)	1.007(012)	5
2	18:22:39.60	+15:44:39.8	16.421(014)	0.169(051)	0.653(016)	0.409(008)	0.813(012)	5
3	18:22:33.94	+15:44:06.1	16.029(012)	0.156(053)	0.732(024)	0.425(013)	0.864(011)	5
4	18:22:29.21	+15:43:47.4	16.437(010)	0.194(048)	0.810(013)	0.480(007)	0.978(013)	5
5	18:22:31.58	+15:41:12.9	17.034(011)	0.246(045)	0.848(010)	0.524(009)	1.070(019)	5
6	18:22:34.57	+15:40:59.2	16.513(011)	0.616(058)	1.074(036)	0.639(009)	1.291(013)	5
7	18:22:35.69	+15:40:25.7	16.180(011)	0.381(042)	0.890(011)	0.529(007)	1.040(011)	5
8	18:22:37.15	+15:40:02.0	16.120(011)	0.208(043)	0.784(016)	0.479(008)	0.968(012)	5
9	18:22:39.65	+15:39:55.5	16.129(012)	0.746(044)	1.113(012)	0.642(007)	1.263(014)	5
10	18:22:43.56	+15:40:37.2	16.653(012)	0.678(041)	1.141(013)	0.664(008)	1.339(013)	5
11	18:22:39.20	+15:41:17.4	16.101(012)	0.957(042)	1.117(013)	0.670(008)	1.258(014)	5
SN 1998ab								
SN	12:48:47.28	+41:55:29.0						
1	12:48:27.54	+41:57:37.0	15.196(013)	0.306(044)	0.754(011)	0.420(009)	0.814(023)	4
2	12:48:29.50	+41:56:43.4	17.322(012)	0.612(043)	0.890(012)	0.538(009)	1.041(020)	5
3	12:48:35.46	+41:55:35.9	17.430(013)	−0.044(042)	0.671(016)	0.431(010)	0.899(034)	5
4	12:48:44.97	+41:53:37.3	18.253(013)	...	1.426(031)	0.894(013)	1.746(014)	5
5	12:48:47.63	+41:53:09.1	16.361(011)	−0.552(042)	0.135(011)	−0.038(013)	−0.055(028)	5
6	12:48:56.78	+41:52:30.7	15.648(010)	−0.055(041)	0.587(013)	0.337(009)	0.676(020)	5
7	12:49:02.45	+41:53:04.5	16.189(011)	0.408(042)	0.816(014)	0.449(008)	0.876(018)	5
8	12:49:02.01	+41:55:17.6	17.318(014)	1.194(095)	1.377(020)	0.879(010)	1.729(019)	5
9	12:48:59.07	+41:57:15.3	17.300(011)	1.311(272)	1.569(013)	1.010(013)	2.201(011)	5
SN 1998bp								
SN	17:54:50.73	+18:19:50.2						
1	17:54:50.25	+18:20:13.9	17.290(014)	1.276(117)	1.330(020)	0.814(014)	1.515(017)	6
2	17:54:48.77	+18:21:05.7	16.960(013)	0.062(049)	0.658(019)	0.378(008)	0.750(011)	6
3	17:54:48.24	+18:20:43.5	16.565(014)	0.094(044)	0.662(014)	0.387(009)	0.768(016)	6
4	17:54:44.94	+18:19:44.9	16.987(014)	0.597(044)	0.881(015)	0.508(010)	0.977(015)	6
5	17:54:44.30	+18:18:37.9	15.575(015)	0.389(044)	0.812(014)	0.466(008)	0.906(012)	6
6	17:54:46.13	+18:18:04.0	16.122(015)	0.285(042)	0.771(015)	0.443(008)	0.884(011)	6
7	17:54:52.68	+18:17:30.1	16.492(014)	0.142(045)	0.712(014)	0.408(007)	0.816(012)	6
8	17:54:54.92	+18:18:40.0	18.093(012)	0.052(041)	0.658(022)	0.381(011)	0.766(020)	6
9	17:54:52.72	+18:19:33.9	16.783(015)	0.275(047)	0.735(013)	0.411(009)	0.813(020)	6
10	17:54:55.65	+18:20:09.3	17.219(013)	0.105(045)	0.678(018)	0.411(008)	0.821(022)	6
11	17:54:56.27	+18:20:25.0	15.992(015)	−0.077(045)	0.500(013)	0.315(008)	0.653(013)	6
SN 1998co								
SN	21:47:36.27	−13:10:52.7						
1	21:47:44.17	−13:08:23.1	16.237(012)	0.539(042)	0.894(012)	0.535(012)	1.016(009)	3
2	21:47:47.13	−13:12:11.7	17.779(018)	0.053(059)	0.681(028)	0.416(012)	0.811(031)	3
3	21:47:45.79	−13:12:37.3	17.968(018)	1.240(247)	1.208(017)	0.751(007)	1.396(024)	3
4	21:47:42.14	−13:13:36.0	14.245(024)	−0.045(042)	0.568(025)	0.338(023)	0.667(024)	3
5	21:47:41.21	−13:13:08.7	16.837(011)	0.591(063)	0.815(069)	0.508(007)	0.944(012)	3
6	21:47:37.19	−13:11:27.8	14.691(011)	0.157(041)	0.715(011)	0.409(009)	0.797(025)	3
7	21:47:37.15	−13:11:48.8	16.011(012)	0.153(045)	0.705(013)	0.404(008)	0.777(020)	3
8	21:47:37.39	−13:12:58.6	16.248(011)	0.068(042)	0.659(011)	0.392(009)	0.768(019)	3
9	21:47:34.34	−13:13:20.7	16.371(012)	0.315(045)	0.801(011)	0.467(007)	0.912(013)	3
10	21:47:30.18	−13:11:08.3	16.583(014)	0.092(048)	0.655(010)	0.375(007)	0.747(017)	2

Table 2—Continued

Star	α (J2000)	δ (J2000)	V	$U-B$	$B-V$	$V-R$	$V-I$	N
SN 1998de								
SN	00:48:06.88	+27:37:29.9						
1	00:48:06.02	+27:37:47.0	17.247(017)	0.991(050)	1.059(013)	0.605(011)	1.140(014)	5
2	00:48:05.00	+27:37:16.0	17.968(015)	0.072(047)	0.622(012)	0.382(012)	0.794(015)	5
3	00:48:03.80	+27:39:24.4	17.898(012)	1.096(119)	1.490(017)	0.942(012)	1.870(013)	5
4	00:48:21.44	+27:35:50.6	17.620(012)	0.620(059)	0.962(012)	0.577(009)	1.110(011)	5
5	00:48:16.70	+27:33:55.2	17.795(015)	0.762(065)	0.992(012)	0.595(009)	1.136(020)	5
6	00:48:00.04	+27:33:48.7	16.941(013)	−0.058(048)	0.557(010)	0.340(008)	0.711(012)	5
7	00:47:47.53	+27:34:32.6	17.079(019)	1.217(227)	1.556(013)	0.992(026)	2.113(026)	3
8	00:47:50.70	+27:39:26.1	16.543(011)	0.543(068)	0.895(011)	0.522(009)	1.012(010)	5
SN 1998dh								
SN	23:14:40.31	+04:32:13.4						
1	23:14:27.33	+04:30:10.4	16.180(014)	1.228(044)	1.240(011)	0.775(008)	1.462(016)	5
2	23:14:39.10	+04:29:59.2	16.065(013)	0.557(085)	0.965(013)	0.543(008)	1.073(012)	5
3	23:14:43.25	+04:28:31.4	16.942(013)	0.165(042)	0.747(013)	0.428(008)	0.863(018)	5
4	23:14:50.84	+04:29:37.6	16.454(012)	0.560(073)	0.930(013)	0.556(009)	1.099(014)	5
5	23:14:49.56	+04:30:46.0	17.268(011)	0.375(043)	0.875(013)	0.533(008)	1.054(011)	5
6	23:14:57.13	+04:30:24.6	16.636(011)	−0.216(041)	0.604(010)	0.398(008)	0.831(013)	5
7	23:14:55.76	+04:30:56.2	16.036(011)	0.533(041)	0.917(011)	0.537(007)	1.036(012)	5
8	23:14:50.34	+04:33:22.8	17.539(011)	0.185(048)	0.768(011)	0.470(010)	0.927(016)	5
SN 1998dk								
SN	00:14:32.26	−00:44:12.6						
1	00:14:27.99	−00:44:47.9	17.367(012)	1.141(072)	1.186(012)	0.745(010)	1.401(010)	4
2	00:14:25.04	−00:45:04.2	17.751(011)	0.014(041)	0.671(012)	0.393(009)	0.804(014)	4
3	00:14:27.39	−00:45:32.6	16.248(020)	1.153(052)	1.478(015)	0.983(018)	2.124(015)	4
4	00:14:21.31	−00:47:59.2	17.197(014)	0.395(051)	0.806(015)	0.445(009)	0.875(019)	4
5	00:14:38.33	−00:46:56.6	17.374(018)	0.125(042)	0.717(011)	0.410(010)	0.809(010)	4
6	00:14:41.27	−00:40:36.5	17.349(019)	1.232(154)	1.537(024)	1.064(031)	2.425(014)	4
7	00:14:26.63	−00:41:15.9	16.705(014)	1.354(057)	1.307(014)	0.829(010)	1.581(013)	4
SN 1998dm								
SN	01:26:13.64	−06:06:13.7						
1	01:26:12.33	−06:06:01.0	16.125(011)	0.933(048)	1.036(010)	0.618(007)	1.146(012)	4
2	01:26:09.10	−06:05:58.2	16.953(012)	0.876(045)	1.046(011)	0.629(008)	1.181(013)	4
3	01:26:07.15	−06:05:32.7	17.633(013)	1.310(083)	1.460(017)	0.930(012)	1.875(010)	4
4	01:26:05.77	−06:05:58.9	17.742(012)	0.406(046)	0.826(011)	0.457(008)	0.910(014)	4
5	01:26:11.93	−06:01:46.8	17.304(017)	0.974(120)	1.525(015)	1.026(023)	2.239(016)	4
6	01:26:04.64	−06:02:06.3	15.238(011)	0.156(041)	0.674(012)	0.381(008)	0.753(011)	4
7	01:25:57.54	−06:07:33.3	16.063(015)	1.192(042)	1.359(012)	0.865(009)	1.656(010)	4
8	01:26:05.16	−06:09:10.3	16.170(013)	0.713(044)	0.937(012)	0.542(008)	1.048(010)	4
9	01:26:20.60	−06:03:32.5	16.699(018)	1.146(049)	1.471(011)	0.982(020)	2.117(011)	4
SN 1998dx								
SN	18:11:11.95	+49:51:40.9						
1	18:11:05.17	+49:50:20.8	15.413(010)	0.021(043)	0.625(014)	0.368(008)	0.734(021)	3
2	18:11:08.65	+49:49:43.8	15.808(011)	0.094(046)	0.680(014)	0.398(008)	0.781(014)	3
3	18:11:17.65	+49:49:47.6	16.869(011)	0.544(040)	0.844(014)	0.480(009)	0.891(025)	3
4	18:11:29.28	+49:50:03.9	16.360(010)	0.220(042)	0.740(017)	0.421(008)	0.800(011)	3
5	18:11:30.26	+49:51:53.9	16.429(012)	−0.068(046)	0.602(015)	0.364(010)	0.720(016)	3
6	18:11:30.58	+49:54:19.4	16.009(011)	−0.067(040)	0.616(014)	0.376(012)	0.748(014)	3
7	18:11:22.96	+49:53:00.6	15.312(010)	0.037(044)	0.650(014)	0.388(011)	0.751(017)	3
8	18:10:56.96	+49:53:15.1	15.152(012)	0.013(042)	0.566(014)	0.340(010)	0.663(022)	3
SN 1998ec								
SN	06:53:06.10	+50:02:22.8						
1	06:53:00.72	+50:03:50.2	16.886(011)	0.582(050)	0.937(012)	0.543(007)	1.045(010)	4
2	06:52:48.81	+50:04:05.6	16.139(011)	0.156(041)	0.716(013)	0.411(007)	0.821(011)	4
3	06:52:55.76	+50:02:40.8	17.628(010)	1.171(178)	1.483(016)	0.953(015)	1.903(010)	4
4	06:52:53.61	+50:01:07.9	16.845(011)	0.132(044)	0.712(015)	0.410(009)	0.804(016)	4
5	06:52:53.13	+50:00:53.5	18.101(010)	1.112(217)	1.238(025)	0.786(010)	1.454(020)	4
6	06:52:57.30	+49:59:59.4	17.243(014)	0.932(040)	1.105(013)	0.669(009)	1.270(014)	4
7	06:52:58.94	+49:58:57.6	16.018(012)	0.127(042)	0.713(012)	0.410(007)	0.804(016)	4
8	06:53:07.87	+50:01:29.3	17.788(014)	0.258(044)	0.779(019)	0.449(013)	0.912(011)	4
9	06:53:11.40	+50:01:06.1	16.161(012)	0.075(041)	0.711(013)	0.409(007)	0.818(010)	4
10	06:53:14.07	+50:00:54.6	17.367(013)	0.890(040)	1.055(014)	0.634(009)	1.199(013)	4
11	06:53:21.78	+50:00:41.7	16.206(012)	0.444(050)	0.867(014)	0.489(007)	0.950(012)	4
12	06:53:18.34	+50:01:32.1	16.723(013)	0.078(042)	0.660(016)	0.385(009)	0.764(015)	4
13	06:53:17.10	+50:04:26.3	16.563(011)	0.128(040)	0.712(013)	0.431(007)	0.879(012)	4

Table 2—Continued

Star	α (J2000)	δ (J2000)	V	$U-B$	$B-V$	$V-R$	$V-I$	N
SN 1998ef								
SN	01:03:26.80	+32:14:12.8						
1	01:03:28.07	+32:14:23.8	16.428(011)	0.394(060)	0.849(030)	0.498(020)	0.976(019)	2
2	01:03:15.87	+32:15:51.4	15.622(011)	0.003(042)	0.619(019)	0.378(016)	0.758(020)	2
3	01:03:21.89	+32:13:11.1	17.391(042)	0.636(162)	0.878(024)	0.450(008)	0.865(017)	2
4	01:03:19.05	+32:11:40.5	15.695(011)	0.373(040)	0.816(017)	0.463(014)	0.899(013)	2
5	01:03:24.54	+32:11:43.8	17.316(010)	0.123(059)	0.695(014)	0.430(007)	0.842(019)	2
6	01:03:28.39	+32:13:39.4	17.036(010)	0.312(041)	0.785(028)	0.447(020)	0.869(010)	2
7	01:03:38.20	+32:12:10.5	17.424(012)	0.747(164)	1.004(048)	0.608(013)	1.140(009)	2
8	01:03:34.44	+32:15:15.0	16.021(010)	0.166(048)	0.781(014)	0.459(015)	0.913(011)	2
9	01:03:33.59	+32:15:28.9	17.498(011)	0.973(169)	1.535(034)	1.067(057)	2.421(012)	2
SN 1998eg								
SN	22:39:30.34	+08:36:20.8						
1	22:39:42.06	+08:39:15.3	16.067(038)	0.153(101)	0.757(041)	0.425(034)	0.856(036)	1
2	22:39:40.85	+08:38:03.9	16.985(054)	0.174(138)	0.874(059)	0.516(046)	1.039(050)	1
3	22:39:31.99	+08:33:39.8	16.504(045)	0.103(117)	0.818(049)	0.471(039)	0.949(041)	1
4	22:39:27.33	+08:35:31.9	17.143(057)	1.151(147)	1.206(063)	0.715(049)	1.308(053)	1
5	22:39:24.30	+08:33:04.1	15.762(035)	0.698(093)	1.073(037)	0.590(031)	1.174(033)	1
6	22:39:22.24	+08:35:12.0	16.749(049)	0.488(127)	0.893(054)	0.540(042)	1.052(045)	1
7	22:39:17.61	+08:36:11.0	16.640(047)	0.819(122)	1.111(051)	0.604(041)	1.212(044)	1
8	22:39:17.74	+08:36:34.8	16.566(046)	0.400(119)	0.894(050)	0.500(040)	1.021(042)	1
SN 1998es								
SN	01:37:17.52	+05:52:50.2						
1	01:37:18.27	+05:52:55.6	15.423(011)	−0.023(041)	0.589(014)	0.367(009)	0.742(014)	4
2	01:37:27.84	+05:53:48.7	16.633(011)	−0.032(050)	0.635(012)	0.391(007)	0.783(012)	4
3	01:37:28.69	+05:53:56.3	17.006(011)	0.663(050)	0.937(022)	0.565(008)	1.088(014)	4
4	01:37:32.42	+05:51:35.6	15.932(010)	0.617(057)	0.921(017)	0.547(009)	1.041(015)	4
5	01:37:17.72	+05:50:51.4	16.745(011)	1.361(076)	1.385(025)	0.897(011)	1.755(014)	4
6	01:37:15.25	+05:49:34.3	16.841(010)	0.654(045)	0.899(018)	0.536(007)	1.005(013)	4
7	01:37:11.74	+05:48:35.2	16.162(015)	1.217(045)	1.445(020)	0.973(015)	1.996(019)	4
SN 1999X								
SN	08:54:32.28	+36:30:41.7						
1	08:54:24.12	+36:30:35.4	15.229(012)	0.478(040)	0.871(011)	0.539(010)	1.071(013)	3
2	08:54:11.00	+36:29:33.0	15.137(013)	0.184(041)	0.717(010)	0.416(010)	0.821(017)	3
3	08:54:16.57	+36:28:39.9	15.524(015)	0.119(053)	0.673(030)	0.399(013)	0.806(014)	2
4	08:54:23.31	+36:28:07.6	16.596(011)	0.496(042)	0.843(011)	0.488(007)	0.953(020)	3
5	08:54:14.21	+36:26:25.3	17.534(012)	...	1.448(013)	0.958(007)	1.971(016)	3
6	08:54:38.42	+36:26:20.2	16.801(013)	0.016(043)	0.575(011)	0.347(007)	0.700(031)	3
7	08:54:42.96	+36:27:01.3	16.026(013)	1.173(055)	1.463(017)	0.953(008)	1.930(018)	3
8	08:54:52.59	+36:30:54.5	16.711(012)	1.140(073)	1.122(011)	0.668(007)	1.236(018)	3
9	08:54:53.73	+36:31:21.1	16.884(014)	0.595(042)	0.892(011)	0.538(009)	1.050(012)	3
10	08:54:43.86	+36:33:26.8	16.979(014)	0.416(047)	0.820(012)	0.458(008)	0.903(012)	3
11	08:54:44.30	+36:34:22.8	17.323(011)	0.934(158)	1.424(014)	0.921(007)	1.826(020)	3
12	08:54:35.63	+36:31:13.4	17.068(011)	1.259(143)	1.256(011)	0.798(007)	1.496(018)	3
SN 1999aa								
SN	08:27:42.15	+21:29:15.6						
1	08:27:37.96	+21:26:48.5	15.595(028)	0.376(054)	0.758(019)	0.417(012)	0.805(014)	4
2	08:27:40.83	+21:27:21.3	15.835(015)	0.436(045)	0.828(011)	0.465(011)	0.908(011)	4
3	08:27:53.81	+21:28:15.8	16.854(015)	0.238(051)	0.754(011)	0.408(013)	0.817(012)	4
4	08:27:52.63	+21:28:57.1	16.543(014)	0.008(041)	0.599(012)	0.354(008)	0.705(010)	4
5	08:27:53.95	+21:29:17.4	16.876(013)	0.009(043)	0.631(013)	0.354(015)	0.731(025)	4
6	08:27:52.41	+21:29:34.1	14.572(010)	0.038(041)	0.578(011)	0.336(024)	0.667(019)	4
7	08:27:43.33	+21:29:52.2	16.764(024)	0.609(048)	0.834(016)	0.456(012)	0.859(016)	4
8	08:27:44.66	+21:31:11.8	15.380(014)	0.173(057)	0.727(013)	0.393(010)	0.781(012)	4
9	08:27:37.39	+21:31:19.2	14.492(011)	−0.062(041)	0.506(011)	0.304(024)	0.619(012)	4
10	08:27:37.33	+21:30:58.2	16.659(023)	0.937(059)	1.049(011)	0.622(008)	1.153(011)	4
11	08:27:38.22	+21:29:54.9	15.104(014)	0.119(041)	0.666(011)	0.393(009)	0.770(011)	4

Table 2—Continued

Star	α (J2000)	δ (J2000)	V	$U-B$	$B-V$	$V-R$	$V-I$	N
SN 1999ac								
SN	16:07:15.05	+07:58:20.1						
1	16:07:05.51	+07:57:33.2	14.776(010)	0.178(042)	0.673(010)	0.394(019)	0.743(011)	3
2	16:07:10.32	+07:55:53.8	15.728(011)	0.052(044)	0.653(012)	0.387(015)	0.748(011)	3
3	16:07:20.41	+07:56:26.2	16.888(013)	0.032(053)	0.775(013)	0.485(012)	0.973(024)	3
4	16:07:24.10	+07:58:12.3	16.869(011)	0.031(045)	0.688(016)	0.399(010)	0.770(013)	3
5	16:07:23.90	+07:58:23.6	16.192(010)	0.272(042)	0.742(011)	0.418(015)	0.785(011)	3
6	16:07:19.55	+07:58:37.3	15.839(010)	0.764(061)	1.104(014)	0.609(014)	1.179(011)	3
7	16:07:26.19	+07:59:33.9	16.286(011)	0.141(042)	0.696(010)	0.417(016)	0.803(010)	3
SN 1999cc								
SN	16:02:42.04	+37:21:33.7						
1	16:02:34.48	+37:20:34.6	15.663(011)	−0.155(044)	0.531(013)	0.362(009)	0.734(009)	2
2	16:02:23.86	+37:20:25.5	16.054(012)	1.276(056)	1.359(011)	0.867(009)	1.656(012)	2
3	16:02:31.18	+37:19:33.0	16.728(013)	0.329(040)	0.767(011)	0.450(014)	0.856(020)	2
4	16:02:39.12	+37:19:08.0	16.866(014)	0.141(044)	0.699(016)	0.412(010)	0.838(015)	2
5	16:02:43.52	+37:18:23.8	16.439(027)	0.285(041)	0.755(011)	0.427(008)	0.834(028)	2
6	16:02:44.80	+37:19:37.3	16.425(019)	0.531(067)	0.902(021)	0.538(011)	1.056(013)	2
7	16:02:58.15	+37:18:15.1	16.743(011)	0.054(040)	0.624(015)	0.363(013)	0.685(020)	2
8	16:02:59.90	+37:18:17.9	16.668(048)	...	0.851(052)	0.539(041)	1.097(044)	1
9	16:02:58.78	+37:20:09.8	17.185(016)	0.085(046)	0.666(012)	0.376(019)	0.708(025)	2
10	16:02:48.32	+37:23:39.2	16.545(010)	0.944(068)	1.181(016)	0.733(010)	1.392(011)	2
11	16:02:39.21	+37:23:21.6	17.160(013)	−0.213(148)	0.518(014)	0.347(007)	0.716(017)	2
12	16:02:45.46	+37:25:39.5	16.001(016)	−0.068(041)	0.560(010)	0.357(010)	0.710(010)	2
SN 1999cl								
SN	12:31:56.03	+14:25:35.1						
1	12:31:37.92	+14:27:33.1	15.374(028)	−0.095(043)	0.570(014)	0.341(011)	0.693(025)	3
2	12:31:49.45	+14:21:48.0	16.320(018)	0.470(058)	0.842(020)	0.473(010)	0.908(014)	3
3	12:32:04.75	+14:23:15.6	14.991(025)	0.257(045)	0.765(022)	0.438(009)	0.848(023)	3
4	12:32:05.24	+14:23:34.5	13.655(033)	0.490(053)	0.883(031)	0.509(022)	0.969(029)	3
5	12:32:08.80	+14:28:44.1	14.712(026)	−0.087(047)	0.577(014)	0.348(008)	0.695(019)	3
6	12:31:56.80	+14:28:12.9	17.561(016)	−0.026(043)	0.622(021)	0.347(016)	0.703(013)	3
SN 1999cw								
SN	00:20:01.46	−06:20:02.5						
1	00:19:56.46	−06:23:10.7	14.926(011)	−0.022(041)	0.596(010)	0.366(007)	0.730(011)	5
2	00:20:09.05	−06:24:15.6	16.608(016)	1.163(062)	1.501(023)	1.031(010)	2.224(014)	4
3	00:20:01.04	−06:15:31.5	15.696(011)	0.146(040)	0.712(010)	0.425(008)	0.837(012)	5
4	00:20:00.40	−06:18:09.9	14.719(013)	1.096(040)	1.107(011)	0.667(010)	1.226(018)	5
5	00:19:53.92	−06:17:22.2	14.723(011)	0.025(041)	0.611(011)	0.370(008)	0.734(011)	5
6	00:19:48.63	−06:16:26.0	16.742(011)	0.595(043)	1.015(011)	0.556(008)	1.093(014)	5
SN 1999dq								
SN	02:33:59.71	+20:58:30.2						
1	02:33:53.71	+20:56:54.5	16.537(011)	0.225(043)	0.745(012)	0.438(007)	0.849(011)	6
2	02:34:02.63	+20:56:29.0	14.976(011)	0.096(041)	0.695(011)	0.414(007)	0.829(012)	6
3	02:34:04.45	+20:56:35.5	15.791(011)	0.237(041)	0.761(012)	0.443(007)	0.865(011)	6
4	02:34:06.45	+21:00:12.9	15.497(010)	0.149(041)	0.716(011)	0.423(007)	0.833(011)	6
5	02:33:59.23	+21:00:12.8	17.540(011)	0.341(045)	0.966(013)	0.692(008)	1.527(015)	6
6	02:33:59.03	+20:59:18.6	16.780(011)	1.549(119)	1.429(016)	0.905(008)	1.743(014)	6
7	02:34:04.42	+20:59:13.1	17.802(012)	−0.152(044)	0.540(014)	0.369(010)	0.747(023)	6
SN 1999ef								
SN	00:58:46.39	+12:44:45.2						
1	00:58:42.23	+12:42:58.1	16.797(011)	0.047(041)	0.670(010)	0.405(008)	0.814(010)	6
2	00:58:47.26	+12:41:49.0	15.961(011)	−0.122(043)	0.588(011)	0.389(007)	0.792(011)	6
3	00:58:54.80	+12:47:21.6	16.871(011)	1.121(107)	1.210(014)	0.756(009)	1.433(013)	6
4	00:58:48.58	+12:48:15.4	15.142(010)	0.399(041)	0.851(012)	0.487(007)	0.943(010)	6
5	00:58:44.35	+12:47:56.1	16.254(010)	0.270(045)	0.793(012)	0.466(007)	0.914(011)	6
6	00:58:38.25	+12:45:40.7	17.183(014)	0.475(043)	0.921(015)	0.570(009)	1.093(012)	6
7	00:58:26.88	+12:41:22.7	17.775(011)	−0.158(045)	0.538(024)	0.356(013)	0.685(081)	5
8	00:58:35.40	+12:41:07.0	17.778(013)	0.787(189)	1.063(015)	0.658(012)	1.243(030)	6

Table 2—Continued

Star	α (J2000)	δ (J2000)	V	$U-B$	$B-V$	$V-R$	$V-I$	N
SN 1999ej								
SN	01:22:57.38	+33:27:57.4						
1	01:23:04.61	+33:26:18.9	14.843(010)	0.013(042)	0.654(011)	0.390(007)	0.779(014)	5
2	01:23:07.11	+33:26:21.4	16.608(011)	1.161(051)	1.154(015)	0.681(008)	1.250(012)	5
3	01:23:05.42	+33:27:32.0	16.368(011)	0.424(041)	0.842(011)	0.468(008)	0.912(013)	4
4	01:23:08.12	+33:27:25.2	16.588(013)	0.131(044)	0.698(011)	0.409(008)	0.808(015)	5
5	01:23:08.12	+33:27:38.1	16.292(012)	0.828(047)	1.001(017)	0.573(008)	1.086(012)	5
6	01:23:09.86	+33:28:18.0	17.134(014)	0.401(043)	0.890(013)	0.517(010)	0.999(013)	5
7	01:23:02.20	+33:28:26.4	16.865(011)	0.222(042)	0.810(012)	0.480(007)	0.933(013)	5
8	01:23:06.16	+33:30:26.1	16.537(012)	0.106(041)	0.724(013)	0.418(010)	0.839(011)	5
9	01:22:57.10	+33:30:35.6	16.634(011)	1.075(070)	1.580(017)	1.012(008)	2.110(020)	5
10	01:22:56.29	+33:29:28.9	15.959(011)	0.237(042)	0.719(012)	0.408(007)	0.797(011)	5
11	01:22:48.92	+33:31:04.0	17.435(014)	0.449(049)	0.896(023)	0.509(013)	0.992(015)	5
12	01:22:43.02	+33:30:46.9	17.501(017)	-0.011(053)	0.619(017)	0.364(009)	0.736(017)	5
SN 1999ek								
SN	05:36:31.55	+16:38:17.1						
1	05:36:42.31	+16:36:24.5	15.152(012)	0.281(046)	0.840(022)	0.543(007)	1.089(009)	4
2	05:36:42.94	+16:36:32.7	16.480(011)	1.159(078)	1.422(027)	0.850(008)	1.663(013)	4
3	05:36:41.35	+16:36:50.9	15.130(012)	1.720(072)	1.627(029)	0.926(027)	1.778(015)	4
4	05:36:39.67	+16:38:09.1	16.485(011)	0.394(044)	0.983(024)	0.607(008)	1.202(011)	4
5	05:36:39.79	+16:38:32.5	15.681(012)	0.276(045)	0.690(022)	0.440(008)	0.909(013)	4
6	05:36:43.52	+16:40:43.4	15.095(011)	0.520(047)	1.016(023)	0.609(008)	1.205(010)	4
7	05:36:31.16	+16:41:10.8	16.302(011)	0.267(052)	0.873(022)	0.564(007)	1.140(009)	4
8	05:36:26.63	+16:40:18.5	16.368(012)	0.294(060)	0.914(024)	0.590(008)	1.164(011)	4
9	05:36:27.33	+16:39:42.6	15.165(011)	0.431(048)	0.996(021)	0.614(008)	1.209(010)	4
10	05:36:26.91	+16:36:57.4	15.330(012)	0.344(046)	0.924(024)	0.598(008)	1.195(011)	4
11	05:36:33.73	+16:36:45.6	15.737(012)	0.461(041)	0.784(022)	0.493(007)	0.993(011)	4
12	05:36:30.63	+16:37:55.4	16.282(012)	0.266(049)	0.847(018)	0.561(007)	1.116(011)	4
SN 1999gd								
SN	08:38:24.57	+25:45:33.8						
1	08:38:22.74	+25:46:32.3	16.157(011)	0.291(043)	0.775(011)	0.443(008)	0.867(010)	7
2	08:38:21.31	+25:45:57.2	17.472(011)	0.273(053)	0.797(012)	0.457(009)	0.894(012)	7
3	08:38:11.48	+25:46:46.9	16.574(011)	0.206(043)	0.751(011)	0.433(007)	0.848(011)	7
4	08:38:08.68	+25:46:06.2	15.832(011)	-0.095(040)	0.559(011)	0.346(009)	0.684(010)	7
5	08:38:08.13	+25:46:18.4	16.904(011)	0.013(043)	0.629(011)	0.384(007)	0.754(012)	7
6	08:38:22.88	+25:43:42.2	17.581(012)	...	1.582(020)	1.125(010)	2.500(014)	7
7	08:38:28.18	+25:44:51.6	17.577(011)	0.371(050)	0.841(012)	0.497(008)	0.943(018)	7
8	08:38:33.00	+25:49:00.2	16.343(011)	-0.051(042)	0.603(011)	0.361(007)	0.717(010)	7
9	08:38:25.52	+25:47:41.7	17.077(011)	-0.040(043)	0.587(012)	0.350(007)	0.699(009)	7
SN 1999gh								
SN	09:44:19.73	-21:16:25.3						
1	09:44:23.52	-21:14:57.1	16.305(011)	1.183(042)	1.268(014)	0.832(008)	1.597(010)	5
2	09:44:16.73	-21:15:46.6	16.766(022)	1.125(069)	1.150(016)	0.712(010)	1.376(017)	5
3	09:44:14.27	-21:14:21.9	15.283(012)	1.029(041)	1.052(012)	0.596(008)	1.090(010)	5
4	09:44:12.53	-21:16:01.8	15.470(012)	0.257(040)	0.730(012)	0.412(008)	0.791(011)	5
5	09:44:19.24	-21:17:43.0	15.683(011)	-0.073(040)	0.571(011)	0.349(008)	0.700(009)	5
6	09:44:21.44	-21:17:49.4	16.504(013)	1.082(105)	1.076(013)	0.647(008)	1.194(011)	5
7	09:44:22.40	-21:18:12.3	17.084(015)	0.375(055)	0.795(013)	0.449(009)	0.846(018)	5
8	09:44:22.84	-21:18:34.5	15.635(011)	0.055(041)	0.638(011)	0.367(009)	0.725(012)	5
9	09:44:20.84	-21:19:05.5	17.120(012)	0.910(081)	1.049(012)	0.636(010)	1.182(020)	5
10	09:44:23.39	-21:19:06.2	15.611(012)	0.243(041)	0.733(012)	0.419(008)	0.807(009)	5
11	09:44:27.93	-21:19:01.0	15.681(011)	0.963(049)	1.065(011)	0.673(009)	1.288(009)	5
SN 1999gp								
SN	02:31:39.08	+39:22:52.4						
1	02:31:48.99	+39:24:30.0	16.469(011)	0.077(041)	0.682(010)	0.403(009)	0.790(014)	5
2	02:31:45.65	+39:23:57.6	16.547(011)	1.124(076)	1.156(012)	0.697(009)	1.272(013)	5
3	02:31:37.46	+39:23:36.8	16.838(011)	0.686(050)	0.960(010)	0.549(008)	1.021(016)	5
4	02:31:36.00	+39:24:14.8	14.364(011)	0.330(041)	0.794(010)	0.440(007)	0.852(011)	4
5	02:31:30.97	+39:24:05.8	15.836(011)	-0.019(041)	0.577(011)	0.361(008)	0.712(013)	5
6	02:31:30.61	+39:20:21.3	15.800(011)	0.410(042)	0.880(011)	0.496(007)	0.957(012)	5
7	02:31:37.44	+39:21:54.3	16.846(012)	0.526(045)	0.869(011)	0.510(008)	0.984(015)	5
8	02:31:38.95	+39:21:46.6	14.481(010)	0.024(040)	0.571(011)	0.334(007)	0.658(015)	5
9	02:31:41.78	+39:20:10.8	16.214(011)	0.822(042)	1.025(011)	0.614(007)	1.137(011)	5
10	02:31:52.97	+39:21:00.5	16.280(011)	0.599(051)	0.932(013)	0.532(008)	0.996(013)	5
11	02:31:49.18	+39:21:56.9	16.272(014)	-0.015(041)	0.461(011)	0.318(008)	0.666(015)	5
12	02:31:51.74	+39:23:37.5	14.874(010)	0.571(042)	0.893(011)	0.500(007)	0.941(012)	5

Table 2—Continued

Star	α (J2000)	δ (J2000)	V	$U-B$	$B-V$	$V-R$	$V-I$	N
SN 2000B								
SN	07:05:40.49	+50:35:12.3						
1	07:05:42.01	+50:35:32.5	14.637(012)	0.037(040)	0.623(011)	0.366(009)	0.743(009)	6
2	07:05:51.38	+50:37:15.6	15.252(012)	−0.087(040)	0.511(010)	0.315(008)	0.641(009)	6
3	07:05:53.69	+50:37:52.2	16.087(012)	0.202(040)	0.757(011)	0.427(007)	0.836(010)	6
4	07:05:36.09	+50:38:31.8	16.073(013)	0.364(042)	0.849(011)	0.499(008)	0.968(010)	6
5	07:05:28.49	+50:38:24.7	15.394(012)	0.056(040)	0.646(011)	0.372(007)	0.739(011)	6
6	07:05:30.35	+50:38:09.1	15.330(013)	−0.090(040)	0.530(011)	0.326(008)	0.659(010)	6
7	07:05:30.27	+50:37:23.1	15.521(012)	0.039(040)	0.606(011)	0.347(007)	0.689(010)	6
8	07:05:26.45	+50:35:51.4	15.855(012)	0.725(045)	0.979(012)	0.570(007)	1.088(011)	6
9	07:05:26.01	+50:35:06.8	16.517(011)	0.116(040)	0.658(011)	0.378(007)	0.731(010)	6
10	07:05:24.05	+50:33:18.8	14.606(011)	−0.074(040)	0.487(011)	0.292(012)	0.585(009)	6
11	07:05:35.32	+50:33:58.8	15.636(012)	−0.039(042)	0.540(011)	0.322(008)	0.647(011)	6
12	07:05:41.67	+50:32:56.9	15.592(012)	0.609(042)	0.945(011)	0.517(007)	0.998(010)	6
SN 2000ce								
SN	08:05:09.40	+66:47:16.2						
1	08:05:07.45	+66:46:00.0	15.821(035)	−0.008(094)	0.699(038)	0.416(031)	0.805(033)	1
2	08:05:15.94	+66:44:21.3	13.455(022)	0.134(065)	0.703(023)	1
3	08:05:25.21	+66:44:26.3	15.782(035)	−0.023(093)	0.609(038)	0.355(031)	0.704(033)	1
4	08:05:43.87	+66:45:05.1	15.031(028)	0.118(079)	0.700(030)	0.399(026)	0.776(027)	1
5	08:05:37.00	+66:47:54.7	13.955(024)	−0.087(067)	0.526(024)	0.328(022)	0.651(023)	1
6	08:05:45.57	+66:51:58.7	14.093(024)	0.692(068)	1.005(025)	0.549(023)	1.060(023)	1
7	08:05:18.27	+66:49:49.7	15.277(030)	0.195(083)	0.721(032)	0.401(028)	0.777(029)	1
8	08:04:23.74	+66:49:18.3	14.314(025)	0.059(070)	0.676(026)	0.376(023)	0.743(024)	1
9	08:04:25.82	+66:42:56.3	15.480(032)	0.404(087)	0.936(034)	0.525(029)	1.031(030)	1
10	08:04:39.59	+66:42:33.8	15.416(031)	−0.028(085)	0.599(034)	0.350(028)	0.672(030)	1
11	08:05:11.23	+66:42:26.9	14.942(028)	0.285(077)	0.743(029)	0.432(026)	0.820(027)	1
SN 2000cf								
SN	15:52:56.33	+65:56:13.2						
1	15:52:58.02	+65:55:36.0	15.914(016)	0.174(062)	0.704(012)	0.419(014)	0.789(028)	2
2	15:52:42.68	+65:54:45.7	17.080(015)	...	1.342(010)	0.869(016)	1.620(012)	2
3	15:52:28.84	+65:56:33.7	15.848(012)	0.990(095)	1.138(014)	0.728(008)	1.333(010)	2
4	15:52:37.02	+66:00:18.0	15.353(014)	0.056(042)	0.669(014)	0.411(010)	0.773(009)	2
5	15:52:45.76	+65:59:20.4	15.490(012)	0.625(248)	0.926(014)	0.551(008)	0.991(010)	2
6	15:52:51.53	+65:58:51.0	16.598(023)	0.638(120)	0.923(010)	0.529(015)	0.957(024)	2
7	15:52:57.95	+65:59:10.2	16.015(024)	0.546(040)	0.874(016)	0.526(021)	0.975(020)	2
8	15:53:08.27	+65:59:34.1	14.739(018)	−0.022(045)	0.568(011)	0.344(008)	0.650(017)	2
9	15:53:29.51	+65:59:40.1	16.130(013)	0.225(054)	0.754(011)	0.435(008)	0.805(018)	2
10	15:53:30.37	+65:57:32.5	16.378(013)	0.739(112)	1.000(024)	0.585(009)	1.059(012)	2
11	15:53:27.12	+65:56:33.5	15.797(020)	0.284(055)	0.746(017)	0.428(014)	0.793(018)	2
SN 2000cn								
SN	17:57:40.47	+27:49:58.0						
1	17:57:29.79	+27:51:24.1	14.643(018)	0.337(041)	0.734(010)	0.403(024)	0.781(012)	2
2	17:57:27.62	+27:49:22.8	16.512(021)	0.886(046)	0.989(010)	0.619(015)	1.158(016)	2
3	17:57:27.11	+27:48:52.9	16.289(018)	0.514(065)	0.848(010)	0.488(016)	0.921(011)	2
4	17:57:39.73	+27:49:28.5	14.873(018)	−0.005(041)	0.592(011)	0.365(014)	0.720(010)	2
5	17:57:42.03	+27:49:23.8	15.624(019)	0.336(040)	0.732(013)	0.418(008)	0.793(011)	2
6	17:57:42.73	+27:49:10.8	15.068(021)	0.816(040)	0.990(010)	0.560(015)	1.071(010)	2
7	17:57:43.88	+27:47:49.1	15.905(012)	−0.120(042)	0.570(012)	0.387(012)	0.779(012)	2
8	17:57:50.93	+27:49:54.5	15.441(018)	0.097(044)	0.629(012)	0.383(012)	0.742(011)	2
9	17:57:47.87	+27:53:07.8	16.096(017)	0.099(055)	0.748(014)	0.461(016)	0.920(011)	2
10	17:57:39.15	+27:50:54.1	15.960(020)	−0.007(042)	0.603(017)	0.360(010)	0.720(010)	2
11	17:57:30.79	+27:52:59.8	16.328(020)	−0.005(045)	0.606(010)	0.368(017)	0.719(011)	2

Table 2—Continued

Star	α (J2000)	δ (J2000)	V	$U-B$	$B-V$	$V-R$	$V-I$	N
SN 2000cx								
SN	01:24:46.15	+09:30:31.1						
2	01:24:52.67	+09:31:48.9	13.490(022)	0.303(045)	0.804(023)	3
3	01:24:49.71	+09:34:24.1	...	0.051(040)	2
4	01:24:40.49	+09:34:39.8	14.538(010)	0.334(043)	0.818(011)	0.470(007)	0.920(010)	3
5	01:24:37.44	+09:32:55.8	17.199(011)	0.285(118)	0.754(014)	0.432(013)	0.854(015)	3
6	01:24:31.62	+09:30:23.1	13.746(010)	0.340(045)	0.763(010)	...	0.798(012)	3
7	01:24:36.20	+09:28:50.3	17.147(010)	0.010(042)	0.699(010)	0.422(013)	0.949(141)	3
8	01:24:39.00	+09:27:40.2	15.636(010)	1.129(078)	1.170(013)	0.709(009)	1.299(010)	3
SN 2000dk								
SN	01:07:23.53	+32:24:23.4						
1	01:07:13.76	+32:20:46.7	14.312(010)	0.212(041)	0.719(013)	0.409(023)	0.785(011)	2
2	01:07:21.20	+32:21:51.0	14.582(010)	0.448(044)	0.831(011)	0.457(008)	0.868(013)	2
3	01:07:22.16	+32:22:18.6	15.972(011)	0.121(042)	0.673(017)	0.395(010)	0.775(009)	2
4	01:07:38.60	+32:21:20.3	15.382(011)	0.022(040)	0.621(015)	0.373(007)	0.737(009)	2
5	01:07:37.54	+32:25:39.0	16.083(010)	1.211(106)	1.522(012)	0.994(015)	2.066(017)	2
6	01:07:38.92	+32:26:08.6	14.805(011)	0.600(047)	0.942(012)	0.525(007)	1.007(011)	2
7	01:07:23.40	+32:25:31.2	15.991(010)	1.085(045)	1.116(013)	0.681(007)	1.239(009)	2
8	01:07:09.84	+32:26:43.6	16.059(010)	0.593(041)	0.861(063)	0.495(007)	0.939(010)	2
9	01:07:19.88	+32:23:39.9	15.794(011)	-0.037(040)	0.544(012)	0.331(012)	0.669(012)	2
SN 2000fa								
SN	07:15:29.87	+23:25:42.4						
1	07:15:15.98	+23:28:24.3	15.206(013)	0.108(041)	0.687(010)	0.394(008)	0.771(011)	4
2	07:15:21.55	+23:26:54.6	15.511(012)	0.007(041)	0.647(010)	0.389(007)	0.778(010)	4
3	07:15:21.01	+23:25:23.5	15.444(013)	0.178(041)	0.713(011)	0.403(008)	0.781(011)	4
4	07:15:16.94	+23:23:32.5	15.736(012)	0.029(041)	0.580(010)	0.345(007)	0.674(010)	4
5	07:15:23.53	+23:22:53.6	15.890(013)	0.001(041)	0.533(011)	0.327(007)	0.643(014)	4
6	07:15:41.39	+23:22:15.8	15.395(010)	-0.010(048)	0.563(010)	0.349(008)	0.694(012)	3
7	07:15:42.66	+23:22:35.8	15.497(012)	0.007(043)	0.644(011)	0.391(007)	0.775(013)	4
8	07:15:37.82	+23:24:19.5	15.317(011)	0.795(043)	0.978(011)	0.577(008)	1.076(010)	4
9	07:15:44.77	+23:26:28.0	15.686(013)	0.301(044)	0.749(015)	0.435(008)	0.849(010)	4
10	07:15:30.96	+23:27:58.0	15.801(012)	1.235(041)	1.222(012)	0.762(008)	1.448(010)	4
11	07:15:26.26	+23:28:05.9	16.169(014)	-0.082(043)	0.553(013)	0.364(016)	0.708(013)	4

Table 3. Photometric Color Terms

Detector/Filterset	Color Term	Value	Nights
AndyCam/SAO	$(v-V)/(B-V)$	$+0.0340 \pm 0.0042$	7
AndyCam/SAO	$(u-b)/(U-B)$	0.9312 ± 0.0039	6
AndyCam/SAO	$(b-v)/(B-V)$	0.9293 ± 0.0029	7
AndyCam/SAO	$(v-r)/(V-R)$	0.9824 ± 0.0053	7
AndyCam/SAO	$(v-i)/(V-I)$	1.0739 ± 0.0040	7
AndyCam/Harris+ I_{SAO} ^a	$(v-i)/(V-I)$	1.0639 ± 0.0124	2 ^b
AndyCam/Harris	$(v-V)/(B-V)$	$+0.0441 \pm 0.0061$	3 ^b
AndyCam/Harris	$(u-b)/(U-B)$	0.9617 ± 0.0130	3 ^b
AndyCam/Harris	$(b-v)/(B-V)$	0.9631 ± 0.0149	3 ^b
AndyCam/Harris	$(v-r)/(V-R)$	1.0947 ± 0.0203	3 ^b
AndyCam/Harris	$(v-i)/(V-I)$	0.9899 ± 0.0224	1 ^b
4Sh-chip1/SAO	$(v-V)/(B-V)$	$+0.0423 \pm 0.0043$	3
4Sh-chip1/SAO	$(u-b)/(U-B)$	0.9433 ± 0.0111	3
4Sh-chip1/SAO	$(b-v)/(B-V)$	0.8937 ± 0.0171	3
4Sh-chip1/SAO	$(v-r)/(V-R)$	0.9873 ± 0.0126	3
4Sh-chip1/SAO	$(v-i)/(V-I)$	1.0837 ± 0.0206	3
4Sh-chip3/SAO	$(v-V)/(B-V)$	$+0.0398 \pm 0.0052$	4
4Sh-chip3/SAO	$(u-b)/(U-B)$	0.9650 ± 0.0156	1
4Sh-chip3/SAO	$(b-v)/(B-V)$	0.8830 ± 0.0100	4
4Sh-chip3/SAO	$(v-r)/(V-R)$	0.9685 ± 0.0190	2
4Sh-chip3/SAO	$(v-i)/(V-I)$	1.0725 ± 0.0024	4
4Sh-chip3/Harris+ I_{SAO} ^a	$(v-i)/(V-I)$	1.0900 ± 0.0149	1
4Sh-chip3/Harris	$(v-V)/(B-V)$	0.0447 ± 0.0009	19
4Sh-chip3/Harris	$(u-b)/(U-B)$	0.9638 ± 0.0081	18
4Sh-chip3/Harris	$(b-v)/(B-V)$	0.9155 ± 0.0035	19
4Sh-chip3/Harris	$(v-r)/(V-R)$	1.0812 ± 0.0026	19
4Sh-chip3/Harris	$(v-i)/(V-I)$	1.0284 ± 0.0016	17

Note. — The lowercase/uppercase letters in the color terms refer to instrumental/standard magnitudes. All color terms implicitly contain an additive constant. For example, for the AndyCam/SAO combination: $(v-V) = +0.0340(B-V) + \text{const}$, and $(u-b) = 0.9312(U-B) + \text{const}$.

^aThis filterset consists of the Harris $UBVR$ filters and the SAO I filter.

^bThese nights were not photometric; the color terms were derived from the calibrated comparison stars. See text for details.

Table 4. Photometry of SN 1997E

HJD	<i>U</i>	<i>B</i>	<i>V</i>	<i>R</i>	<i>I</i>	Detector/Filterset
2450464.92	...	15.694(017)	15.598(011)	15.377(015)	...	AndyCam/SAO
2450465.69	15.441(038)	15.667(015)	15.544(010)	15.357(013)	15.423(014)	AndyCam/SAO
2450466.78	15.414(036)	15.656(013)	15.502(008)	15.323(011)	15.468(011)	AndyCam/SAO
2450468.66	15.500(037)	15.620(014)	15.492(010)	15.322(012)	15.480(013)	AndyCam/SAO
2450472.66	15.789(037)	15.779(013)	15.491(008)	15.323(013)	15.638(012)	AndyCam/SAO
2450476.89	16.330(061)	16.166(032)	15.741(023)	15.716(030)	15.940(032)	AndyCam/SAO
2450479.87	16.802(037)	16.547(013)	15.933(008)	15.906(011)	16.006(011)	AndyCam/SAO
2450485.62	17.725(041)	17.381(015)	16.301(009)	16.003(013)	15.847(018)	AndyCam/SAO
2450489.77	...	17.891(022)	16.627(014)	16.131(019)	15.823(019)	AndyCam/SAO
2450512.65	19.247(060)	18.929(025)	17.829(016)	17.448(026)	17.296(023)	AndyCam/SAO
2450521.62	19.383(186)	19.147(028)	18.101(016)	17.811(023)	17.736(024)	AndyCam/SAO
2450523.66	19.668(114)	19.147(051)	18.113(034)	17.933(048)	17.831(074)	AndyCam/SAO
2450545.65	20.159(120)	19.495(070)	18.783(046)	18.622(066)	18.717(129)	AndyCam/SAO

Table 5. Photometry of SN 1997Y

HJD	<i>U</i>	<i>B</i>	<i>V</i>	<i>R</i>	<i>I</i>	Detector/Filterset
2450488.96	15.073(037)	15.379(015)	15.368(010)	15.278(015)	15.592(014)	AndyCam/SAO
2450489.91	15.157(038)	15.421(016)	15.384(011)	15.284(016)	15.600(015)	AndyCam/SAO
2450515.94	...	18.000(025)	16.852(013)	16.332(019)	15.928(018)	AndyCam/SAO
2450518.84	18.429(056)	18.225(022)	17.012(010)	16.563(015)	16.168(014)	AndyCam/SAO
2450520.86	18.549(056)	18.256(024)	17.141(012)	16.681(023)	16.339(017)	AndyCam/SAO
2450536.84	18.827(069)	18.707(030)	17.690(011)	17.396(018)	17.174(020)	AndyCam/SAO
2450545.87	18.989(099)	18.821(046)	17.944(024)	17.672(037)	17.530(032)	AndyCam/SAO

Table 6. Photometry of SN 1997bp

HJD	<i>U</i>	<i>B</i>	<i>V</i>	<i>R</i>	<i>I</i>	Detector/Filterset
2450546.79	14.077(036)	14.122(012)	14.018(007)	13.921(010)	14.144(011)	AndyCam/SAO
2450547.80	14.079(038)	14.097(014)	13.980(009)	13.894(012)	14.133(014)	AndyCam/SAO
2450548.79	14.110(036)	14.085(012)	13.934(007)	13.838(009)	14.105(011)	AndyCam/SAO
2450549.80	14.175(037)	14.109(014)	13.902(009)	13.812(015)	14.119(013)	AndyCam/SAO
2450550.76	14.229(035)	14.124(013)	13.879(008)	13.792(013)	14.150(018)	AndyCam/SAO
2450552.82	14.340(037)	14.179(015)	13.875(009)	13.762(012)	14.169(013)	AndyCam/SAO
2450567.77	15.914(039)	15.680(017)	14.594(010)	14.494(015)	14.564(024)	AndyCam/SAO
2450569.71	16.114(037)	15.866(016)	14.648(011)	14.483(014)	14.523(014)	AndyCam/SAO
2450573.79	16.494(037)	16.200(012)	14.822(007)	14.461(009)	14.412(010)	AndyCam/SAO
2450575.73	16.689(039)	16.311(015)	14.890(008)	14.475(013)	14.366(012)	AndyCam/SAO
2450579.74	16.983(046)	16.655(016)	15.135(010)	14.655(013)	14.417(015)	AndyCam/SAO
2450597.73	17.733(041)	17.118(016)	15.962(009)	15.540(013)	15.482(012)	AndyCam/SAO
2450610.69	17.859(040)	17.226(020)	16.284(013)	16.025(017)	16.058(018)	AndyCam/SAO

Table 7. Photometry of SN 1997bq

HJD	<i>U</i>	<i>B</i>	<i>V</i>	<i>R</i>	<i>I</i>	Detector/Filterset
2450547.62	...	15.676(020)	15.641(012)	15.493(016)	15.522(017)	AndyCam/SAO
2450548.81	14.971(042)	15.350(023)	15.401(017)	15.234(022)	15.270(021)	AndyCam/SAO
2450549.82	14.735(043)	15.135(023)	15.168(017)	15.054(023)	15.080(023)	AndyCam/SAO
2450550.70	14.551(070)	14.994(042)	15.013(020)	14.902(028)	14.914(027)	AndyCam/SAO
2450551.83	14.451(044)	14.824(021)	14.865(009)	14.740(012)	14.807(014)	AndyCam/SAO
2450568.66	15.323(046)	15.255(018)	14.675(011)	14.711(015)	15.032(017)	AndyCam/SAO
2450570.76	15.650(039)	15.501(012)	14.819(007)	14.827(010)	15.052(011)	AndyCam/SAO
2450573.70	16.078(041)	15.860(016)	15.009(011)	14.918(014)	15.000(016)	AndyCam/SAO
2450575.68	16.380(038)	16.114(014)	15.102(008)	14.951(012)	14.954(013)	AndyCam/SAO
2450578.66	...	16.429(020)	15.259(011)	15.027(019)	14.908(014)	AndyCam/SAO
2450582.78	17.162(089)	16.824(022)	15.473(013)	15.068(017)	14.853(018)	AndyCam/SAO
2450600.72	17.968(045)	17.575(017)	16.422(011)	16.030(015)	15.834(015)	AndyCam/SAO
2450609.66	18.047(054)	17.679(021)	16.636(011)	16.355(016)	16.237(016)	AndyCam/SAO

Table 8. Photometry of SN 1997br

HJD	<i>U</i>	<i>B</i>	<i>V</i>	<i>R</i>	<i>I</i>	Detector/Filterset
2450551.84	13.713(045)	14.397(016)	14.154(008)	13.983(011)	13.922(011)	AndyCam/SAO
2450552.83	13.695(053)	14.317(028)	14.078(016)	13.847(023)	13.811(021)	AndyCam/SAO
2450567.79	14.278(043)	14.371(015)	13.800(009)	13.637(013)	13.759(012)	AndyCam/SAO
2450569.79	14.537(042)	14.574(014)	13.855(008)	13.717(012)	13.825(012)	AndyCam/SAO
2450571.81	14.826(037)	14.811(016)	13.936(010)	13.849(013)	13.833(015)	AndyCam/SAO
2450573.75	15.205(039)	15.060(015)	14.080(009)	13.890(012)	13.838(014)	AndyCam/SAO
2450575.76	15.532(041)	15.315(014)	14.208(008)	13.985(012)	13.828(014)	AndyCam/SAO
2450578.73	15.988(040)	15.672(019)	14.416(013)	14.048(017)	13.789(017)	AndyCam/SAO
2450582.80	16.381(056)	16.002(021)	14.609(012)	14.162(017)	13.875(017)	AndyCam/SAO
2450597.75	17.156(046)	16.810(017)	15.331(009)	14.825(012)	14.350(014)	AndyCam/SAO
2450607.75	17.334(046)	17.009(017)	15.701(009)	15.262(013)	14.915(013)	AndyCam/SAO

Table 9. Photometry of SN 1997cn

HJD	<i>U</i>	<i>B</i>	<i>V</i>	<i>R</i>	<i>I</i>	Detector/Filterset
2450597.76	18.897(068)	18.523(027)	17.216(014)	16.708(019)	16.465(019)	AndyCam/SAO
2450598.83	18.915(068)	18.653(029)	17.291(012)	16.761(016)	16.428(016)	AndyCam/SAO
2450599.71	...	18.780(048)	AndyCam/SAO
2450600.75	19.119(060)	18.858(026)	17.497(014)	16.948(019)	16.563(021)	AndyCam/SAO
2450602.73	19.471(099)	19.081(038)	17.694(016)	17.160(022)	16.724(022)	AndyCam/SAO
2450604.82	19.440(076)	19.290(037)	17.911(020)	17.402(028)	16.941(031)	AndyCam/SAO
2450605.88	19.422(099)	17.487(041)	17.078(039)	AndyCam/SAO
2450607.77	19.559(080)	...	18.062(014)	17.623(018)	17.191(021)	AndyCam/SAO
2450608.70	19.493(072)	19.421(045)	...	17.710(039)	17.265(039)	AndyCam/SAO
2450609.67	19.643(065)	19.454(030)	18.189(020)	17.746(026)	17.286(027)	AndyCam/SAO
2450610.79	19.679(106)	19.595(053)	18.238(023)	17.810(030)	17.391(031)	AndyCam/SAO
2450611.82	19.632(101)	...	18.301(019)	17.837(025)	17.447(029)	AndyCam/SAO
2450627.67	...	20.076(051)	18.911(020)	18.616(031)	18.345(029)	AndyCam/SAO
2450640.75	19.238(034)	19.135(052)	18.932(063)	AndyCam/SAO

Table 10. Photometry of SN 1997cw

HJD	<i>U</i>	<i>B</i>	<i>V</i>	<i>R</i>	<i>I</i>	Detector/Filterset
2450642.94	17.041(039)	16.892(016)	16.146(008)	15.948(011)	16.109(014)	AndyCam/SAO
2450643.88	17.227(038)	17.024(015)	16.184(009)	16.002(012)	16.155(013)	AndyCam/SAO
2450644.85	17.319(056)	17.096(027)	16.222(015)	16.079(020)	16.189(024)	AndyCam/SAO
2450645.98	17.469(048)	17.213(020)	16.341(010)	16.132(014)	16.197(020)	AndyCam/SAO
2450646.98	17.594(059)	17.282(019)	16.359(009)	16.199(012)	16.182(013)	AndyCam/SAO
2450647.98	17.804(076)	17.424(045)	16.429(008)	16.215(014)	16.167(013)	AndyCam/SAO
2450652.92	18.453(119)	17.971(046)	16.643(018)	16.268(024)	16.113(027)	AndyCam/SAO
2450653.94	18.484(079)	18.145(028)	16.707(018)	16.290(025)	16.038(025)	AndyCam/SAO
2450665.99	19.368(116)	18.808(033)	17.227(013)	16.619(019)	16.196(018)	AndyCam/SAO
2450673.99	19.612(187)	19.229(050)	17.612(021)	17.044(027)	16.627(027)	AndyCam/SAO
2450680.99	...	19.258(097)	17.920(058)	17.427(075)	16.956(073)	AndyCam/SAO
2450682.97	...	19.293(094)	17.983(057)	17.469(072)	17.194(070)	AndyCam/SAO
2450685.97	...	19.379(051)	18.075(030)	17.545(042)	17.299(040)	AndyCam/SAO
2450688.00	...	19.329(051)	18.138(037)	17.655(047)	17.444(047)	AndyCam/SAO
2450693.79	...	19.499(036)	18.260(021)	17.828(028)	17.769(040)	AndyCam/SAO
2450783.74	...	21.126(092)	20.068(051)	20.421(093)	...	AndyCam/SAO
2450810.62	20.472(086)	20.690(160)	...	AndyCam/SAO

Table 11. Photometry of SN 1997dg

HJD	<i>U</i>	<i>B</i>	<i>V</i>	<i>R</i>	<i>I</i>	Detector/Filterset
2450720.90	16.806(047)	17.186(027)	17.095(018)	16.921(024)	17.141(026)	AndyCam/SAO
2450722.74	16.919(044)	17.178(021)	17.098(014)	16.927(019)	17.231(023)	AndyCam/SAO
2450726.83	17.405(044)	17.364(022)	17.230(013)	17.078(019)	17.392(022)	AndyCam/SAO
2450730.65	17.958(049)	17.745(022)	17.387(012)	17.344(017)	17.714(024)	AndyCam/SAO
2450747.71	...	19.612(132)	18.416(029)	17.910(038)	17.587(039)	AndyCam/SAO
2450761.79	19.311(275)	20.406(191)	19.205(047)	18.668(066)	18.406(063)	AndyCam/SAO
2450783.72	20.664(144)	...	19.786(034)	19.420(046)	19.424(111)	AndyCam/SAO
2450810.60	...	21.392(192)	20.383(116)	20.227(183)	...	AndyCam/SAO
2450842.61	...	22.062(176)	21.224(127)	21.404(222)	...	4Sh-chip1/SAO

Table 12. Photometry of SN 1997do

HJD	<i>U</i>	<i>B</i>	<i>V</i>	<i>R</i>	<i>I</i>	Detector/Filterset
2450760.01	...	14.849(029)	14.880(022)	14.716(028)	14.873(027)	AndyCam/SAO
2450762.84	14.455(038)	14.626(014)	14.635(008)	14.454(011)	14.691(013)	AndyCam/SAO
2450778.02	14.807(009)	14.773(012)	...	AndyCam/SAO
2450780.90	15.959(037)	15.607(013)	15.003(007)	15.021(009)	15.288(010)	AndyCam/SAO
2450783.81	16.190(038)	15.960(013)	15.131(008)	15.096(011)	15.203(011)	AndyCam/SAO
2450810.78	17.991(065)	17.722(039)	16.480(008)	16.063(012)	15.833(013)	AndyCam/SAO
2450842.74	18.458(059)	18.116(024)	17.329(009)	17.093(014)	17.223(019)	4Sh-chip1/SAO

Table 13. Photometry of SN 1997dt

HJD	<i>U</i>	<i>B</i>	<i>V</i>	<i>R</i>	<i>I</i>	Detector/Filterset
2450777.60	15.919(007)	15.402(010)	...	AndyCam/SAO
2450781.68	15.863(038)	15.801(014)	15.369(009)	14.928(011)	14.636(013)	AndyCam/SAO
2450810.58	18.539(051)	17.847(015)	16.242(008)	15.570(011)	14.986(012)	AndyCam/SAO
2450842.59	...	18.915(044)	17.510(019)	16.945(027)	16.474(035)	4Sh-chip1/SAO

Table 14. Photometry of SN 1998D

HJD	<i>U</i>	<i>B</i>	<i>V</i>	<i>R</i>	<i>I</i>	Detector/Filterset
2450874.04	18.902(057)	18.588(028)	17.433(013)	16.971(020)	16.571(024)	4Sh-chip1/SAO
2450893.93	19.445(079)	19.094(032)	18.156(022)	17.801(048)	17.558(031)	AndyCam/SAO
2450925.89	...	19.703(037)	19.081(021)	19.096(036)	18.797(045)	4Sh-chip1/SAO
2450980.80	...	20.604(082)	20.494(059)	20.692(086)	20.134(198)	4Sh-chip1/SAO
2450987.78	...	20.809(083)	20.590(060)	4Sh-chip1/SAO

Table 15. Photometry of SN 1998V

HJD	<i>U</i>	<i>B</i>	<i>V</i>	<i>R</i>	<i>I</i>	Detector/Filterset
2450894.00	15.738(039)	15.917(016)	15.698(010)	15.486(017)	15.757(015)	AndyCam/SAO
2450894.98	15.918(037)	15.972(014)	15.761(009)	15.521(011)	...	AndyCam/SAO
2450896.01	15.960(038)	15.996(014)	15.736(007)	15.558(010)	15.807(011)	AndyCam/SAO
2450900.93	16.362(036)	16.337(011)	15.913(007)	15.812(008)	16.036(012)	AndyCam/SAO
2450904.00	16.906(036)	16.601(011)	16.159(007)	16.090(010)	16.248(013)	AndyCam/SAO
2450906.99	17.296(041)	16.975(018)	16.285(012)	16.140(016)	16.213(018)	AndyCam/SAO
2450921.99	18.995(076)	18.526(032)	17.147(011)	16.526(017)	16.100(025)	4Sh-chip1/SAO
2450925.95	19.186(056)	18.761(028)	17.408(010)	16.779(016)	16.364(022)	4Sh-chip1/SAO
2450957.98	19.952(199)	19.345(060)	18.395(022)	18.072(038)	17.895(063)	4Sh-chip1/SAO
2450980.86	20.362(160)	19.683(035)	18.960(021)	18.710(030)	18.735(043)	4Sh-chip1/SAO
2450987.83	...	19.823(035)	19.137(018)	18.987(036)	19.057(049)	4Sh-chip1/SAO
2451013.79	...	20.172(049)	19.702(032)	19.700(065)	19.815(111)	AndyCam/SAO
2451077.66	...	21.350(266)	20.626(199)	21.282(280)	...	4Sh-chip1/SAO

Table 16. Photometry of SN 1998ab

HJD	<i>U</i>	<i>B</i>	<i>V</i>	<i>R</i>	<i>I</i>	Detector/Filterset
2450906.82	15.974(038)	16.602(015)	16.570(008)	16.478(013)	16.565(015)	AndyCam/SAO
2450920.66	16.216(044)	16.384(019)	16.216(008)	16.082(011)	16.473(017)	4Sh-chip1/SAO
2450922.65	16.438(040)	16.533(015)	16.277(009)	16.153(012)	16.520(014)	4Sh-chip1/SAO
2450925.84	16.850(040)	16.850(015)	16.388(008)	16.280(012)	16.606(014)	4Sh-chip1/SAO
2450930.76	17.673(045)	17.431(018)	16.746(009)	16.503(013)	16.605(015)	4Sh-chip1/SAO
2450931.81	17.865(046)	17.583(020)	16.781(011)	16.571(015)	16.583(017)	4Sh-chip1/SAO
2450936.68	18.425(065)	18.132(027)	17.106(011)	16.695(017)	16.617(021)	4Sh-chip1/SAO
2450938.71	18.840(104)	18.300(032)	17.211(015)	16.772(021)	16.668(023)	4Sh-chip1/SAO
2450952.69	...	19.096(037)	17.914(015)	17.311(024)	17.030(028)	4Sh-chip1/SAO
2450955.65	19.568(075)	...	18.035(012)	17.452(021)	17.213(031)	4Sh-chip1/SAO
2450961.69	19.522(071)	19.365(028)	18.255(013)	17.686(019)	17.520(024)	AndyCam/SAO
2450964.65	...	19.505(086)	18.349(029)	17.824(043)	17.683(042)	4Sh-chip1/SAO
2450980.69	19.721(113)	19.649(063)	18.702(026)	18.369(042)	18.330(058)	4Sh-chip1/SAO
2450987.73	19.882(075)	19.661(052)	18.863(016)	18.542(028)	18.406(067)	4Sh-chip1/SAO

Table 17. Photometry of SN 1998bp

HJD	<i>U</i>	<i>B</i>	<i>V</i>	<i>R</i>	<i>I</i>	Detector/Filterset
2450934.88	15.655(037)	15.641(014)	15.439(008)	15.162(011)	15.230(014)	4Sh-chip1/SAO
2450937.90	15.801(040)	15.672(017)	15.313(010)	15.070(015)	15.134(016)	4Sh-chip1/SAO
2450938.95	15.923(037)	15.739(014)	15.298(008)	15.054(012)	15.135(013)	4Sh-chip1/SAO
2450939.93	...	15.849(029)	15.307(019)	15.052(026)	15.160(025)	4Sh-chip1/SAO
2450949.93	17.921(053)	17.416(026)	16.077(011)	15.607(015)	15.295(019)	4Sh-chip1/SAO
2450951.87	18.184(069)	17.636(038)	16.266(013)	15.751(021)	15.403(025)	4Sh-chip1/SAO
2450953.85	18.250(049)	17.883(029)	16.416(012)	15.870(019)	15.482(023)	4Sh-chip1/SAO
2450955.89	18.417(053)	18.028(032)	16.653(013)	16.058(019)	15.622(022)	4Sh-chip1/SAO
2450959.94	18.700(046)	18.239(023)	16.941(016)	16.441(021)	16.022(022)	AndyCam/SAO
2450962.88	18.770(062)	18.422(042)	17.125(019)	16.680(026)	16.237(035)	4Sh-chip1/SAO
2450980.84	19.263(088)	18.939(064)	17.787(039)	17.481(051)	17.203(053)	4Sh-chip1/SAO
2450983.81	19.434(053)	18.958(031)	17.891(013)	17.610(022)	17.307(029)	4Sh-chip1/SAO
2450987.82	19.476(083)	19.025(038)	18.014(017)	17.770(027)	17.529(038)	4Sh-chip1/SAO
2450996.78	...	19.204(049)	18.301(025)	18.121(036)	17.836(059)	4Sh-chip1/SAO
2451013.74	20.311(106)	19.456(037)	18.721(025)	18.835(053)	18.538(106)	AndyCam/SAO
2451077.63	...	20.705(082)	20.114(175)	4Sh-chip1/SAO

Table 18. Photometry of SN 1998co

HJD	<i>U</i>	<i>B</i>	<i>V</i>	<i>R</i>	<i>I</i>	Detector/Filterset
2450990.90	15.934(042)	15.930(016)	15.739(010)	15.608(017)	15.897(016)	4Sh-chip1/SAO
2450993.96	16.319(045)	16.228(016)	15.867(009)	15.796(012)	15.961(020)	4Sh-chip1/SAO
2451077.71	20.381(238)	19.951(141)	19.484(084)	19.522(135)	18.896(173)	4Sh-chip1/SAO
2451110.66	...	20.441(156)	20.279(100)	4sh-chip3/SAO
2451136.58	...	20.971(192)	20.920(134)	...	19.618(175)	AndyCam/SAO

Table 19. Photometry of SN 1998de

HJD	<i>U</i>	<i>B</i>	<i>V</i>	<i>R</i>	<i>I</i>	Detector/Filterset
2451021.95	18.587(049)	17.979(019)	17.336(010)	17.085(015)	17.175(016)	4Sh-chip1/SAO
2451022.96	18.389(064)	17.781(022)	17.176(011)	16.952(024)	16.937(021)	4Sh-chip1/SAO
2451024.98	18.291(056)	17.572(029)	16.974(017)	16.740(023)	16.701(026)	4Sh-chip1/SAO
2451047.85	...	19.972(072)	18.554(042)	17.866(056)	17.419(057)	4Sh-chip1/SAO
2451055.90	...	20.193(040)	18.879(017)	18.321(024)	17.925(028)	4Sh-chip1/SAO
2451074.74	...	20.621(055)	19.489(027)	19.176(037)	18.598(085)	4Sh-chip1/SAO
2451077.84	...	20.663(075)	19.619(046)	19.315(060)	18.839(071)	4Sh-chip1/SAO
2451110.84	...	21.203(112)	20.540(067)	20.582(101)	19.893(188)	4sh-chip3/SAO
2451136.81	...	21.760(133)	21.139(085)	21.654(198)	20.523(175)	AndyCam/SAO

Table 20. Photometry of SN 1998dh

HJD	<i>U</i>	<i>B</i>	<i>V</i>	<i>R</i>	<i>I</i>	Detector/Filterset
2451021.94	14.427(039)	14.745(015)	14.718(007)	14.475(010)	14.453(012)	4Sh-chip1/SAO
2451026.89	13.929(038)	14.193(013)	14.138(008)	13.987(011)	14.105(011)	4Sh-chip1/SAO
2451045.84	15.743(052)	15.534(036)	14.665(024)	...	14.709(047)	4Sh-chip1/SAO
2451047.84	15.994(045)	15.753(021)	14.782(009)	14.618(014)	14.580(015)	4Sh-chip1/SAO
2451055.89	16.804(042)	16.574(019)	15.235(007)	14.790(011)	14.472(015)	4Sh-chip1/SAO
2451069.87	17.455(051)	17.293(023)	16.045(010)	15.634(014)	15.343(016)	4Sh-chip1/SAO
2451077.76	17.652(042)	17.407(022)	16.289(010)	15.922(014)	15.739(016)	4Sh-chip1/SAO
2451110.75	18.467(059)	17.855(038)	17.128(025)	17.049(036)	17.058(040)	4sh-chip3/SAO
2451136.68	19.097(045)	18.229(017)	17.730(011)	17.847(015)	17.971(032)	AndyCam/SAO

Table 21. Photometry of SN 1998dk

HJD	<i>U</i>	<i>B</i>	<i>V</i>	<i>R</i>	<i>I</i>	Detector/Filterset
2451075.72	16.700(055)	16.494(023)	15.566(012)	15.434(020)	15.456(019)	4Sh-chip1/SAO
2451077.82	16.961(042)	16.750(020)	15.667(008)	15.435(013)	15.402(014)	4Sh-chip1/SAO
2451079.76	17.234(048)	16.941(026)	15.743(013)	15.469(017)	15.369(021)	4Sh-chip1/SAO
2451102.62	18.321(081)	18.192(028)	16.951(013)	16.498(020)	16.200(023)	4sh-chip3/SAO
2451110.79	18.500(065)	18.311(022)	17.196(013)	16.760(019)	16.588(021)	4sh-chip3/SAO
2451136.73	19.231(058)	18.661(018)	17.899(011)	17.613(018)	17.762(018)	AndyCam/SAO

Table 22. Photometry of SN 1998dm

HJD	<i>U</i>	<i>B</i>	<i>V</i>	<i>R</i>	<i>I</i>	Detector/Filterset
2451071.82	...	15.398(023)	14.843(006)	14.743(010)	14.832(011)	4Sh-chip1/SAO
2451077.86	16.171(040)	16.008(017)	15.158(008)	15.040(013)	14.962(014)	4Sh-chip1/SAO
2451080.88	16.545(046)	16.321(021)	15.328(009)	15.094(015)	14.909(014)	4Sh-chip1/SAO
2451104.74	18.325(083)	17.866(022)	16.529(008)	16.037(016)	15.544(012)	4sh-chip3/SAO
2451110.80	18.363(062)	18.027(021)	16.736(011)	16.251(019)	15.816(017)	4sh-chip3/SAO
2451136.77	19.000(173)	18.454(017)	17.417(011)	17.071(016)	16.947(016)	AndyCam/SAO
2451195.64	...	19.317(023)	18.749(014)	18.759(021)	18.831(094)	4sh-chip3/Harris+ <i>I</i> _{SAO}

Table 23. Photometry of SN 1998dx

HJD	<i>U</i>	<i>B</i>	<i>V</i>	<i>R</i>	<i>I</i>	Detector/Filterset
2451072.62	17.269(095)	17.689(057)	17.729(030)	17.578(045)	17.895(062)	4Sh-chip1/SAO
2451077.64	17.951(046)	17.999(023)	17.852(014)	17.708(020)	18.046(027)	4Sh-chip1/SAO
2451078.64	18.059(046)	18.050(024)	17.865(015)	17.735(022)	18.118(085)	4Sh-chip1/SAO
2451083.73	18.904(078)	18.598(021)	18.179(012)	18.158(019)	18.343(036)	AndyCam/SAO
2451100.62	...	20.642(175)	19.559(093)	18.882(142)	18.808(174)	4sh-chip3/SAO
2451136.60	22.432(242)	21.552(184)	20.751(123)	20.097(181)	20.270(212)	AndyCam/SAO

Table 24. Photometry of SN 1998ec

HJD	<i>U</i>	<i>B</i>	<i>V</i>	<i>R</i>	<i>I</i>	Detector/Filterset
2451101.96	17.587(044)	17.296(014)	16.663(008)	16.620(011)	16.901(014)	4sh-chip3/SAO
2451106.02	18.128(049)	17.757(017)	16.920(009)	16.836(013)	16.928(017)	4sh-chip3/SAO
2451110.97	18.800(059)	18.324(024)	17.182(013)	16.873(019)	16.823(018)	4sh-chip3/SAO
2451114.01	19.255(116)	18.622(026)	17.366(013)	16.859(019)	16.724(020)	4sh-chip3/SAO
2451136.88	19.983(113)	19.762(032)	18.469(012)	17.972(019)	17.678(023)	AndyCam/SAO
2451195.74	21.003(226)	20.717(064)	19.964(036)	19.929(048)	20.149(108)	4sh-chip3/Harris+ <i>I</i> _{SAO}
2451217.84	...	21.050(160)	20.421(121)	20.439(151)	20.401(210)	AndyCam/Harris+ <i>I</i> _{SAO}
2451224.68	...	21.187(171)	20.504(121)	20.535(152)	...	AndyCam/Harris+ <i>I</i> _{SAO}
2451232.67	20.853(298)	4sh-chip3/Harris+ <i>I</i> _{SAO}
2451275.62	...	21.938(296)	21.584(153)	21.411(261)	...	4sh-chip3/Harris+ <i>I</i> _{SAO}

Table 25. Photometry of SN 1998ef

HJD	<i>U</i>	<i>B</i>	<i>V</i>	<i>R</i>	<i>I</i>	Detector/Filterset
2451106.62	15.412(043)	15.628(018)	15.684(011)	15.557(016)	15.513(017)	4sh-chip3/SAO
2451107.75	15.317(040)	15.487(013)	15.521(007)	15.431(010)	15.367(012)	AndyCam/SAO
2451109.86	14.972(038)	15.266(016)	15.320(010)	15.233(013)	15.251(014)	AndyCam/SAO
2451110.78	14.898(039)	15.167(016)	15.209(010)	15.157(013)	15.242(013)	4sh-chip3/SAO
2451136.86	17.707(041)	17.380(014)	16.220(008)	15.845(013)	15.564(014)	AndyCam/SAO
2451195.70	19.901(130)	18.921(038)	18.369(023)	18.465(031)	18.233(047)	4sh-chip3/Harris+ <i>I</i> _{SAO}
2451216.62	...	19.230(030)	18.928(017)	19.000(024)	19.011(046)	AndyCam/Harris+ <i>I</i> _{SAO}
2451224.59	...	19.399(056)	19.066(034)	19.618(067)	...	AndyCam/Harris+ <i>I</i> _{SAO}

Table 26. Photometry of SN 1998eg

HJD	<i>U</i>	<i>B</i>	<i>V</i>	<i>R</i>	<i>I</i>	Detector/Filterset
2451110.67	16.367(042)	16.615(022)	16.480(014)	16.340(021)	16.467(020)	4sh-chip3/SAO
2451111.66	16.409(041)	16.594(019)	16.486(011)	16.303(017)	16.545(018)	4sh-chip3/SAO
2451113.58	16.552(043)	16.680(022)	16.490(012)	16.314(018)	16.510(028)	4sh-chip3/SAO
2451136.64	19.506(099)	18.926(064)	17.714(048)	17.217(062)	17.014(062)	AndyCam/SAO
2451195.61	...	20.415(096)	19.669(062)	19.397(093)	...	4sh-chip3/Harris+ <i>I</i> _{SAO}

Table 27. Photometry of SN 1998es

HJD	<i>U</i>	<i>B</i>	<i>V</i>	<i>R</i>	<i>I</i>	Detector/Filterset
2451133.84	14.391(039)	...	AndyCam/SAO
2451134.80	14.228(039)	...	AndyCam/SAO
2451135.67	13.827(045)	14.288(021)	14.270(012)	14.205(018)	...	AndyCam/SAO
2451136.84	13.725(084)	14.231(032)	14.131(019)	14.073(031)	14.159(027)	AndyCam/SAO
2451137.77	...	14.090(027)	14.061(014)	13.994(021)	14.095(019)	4sh-chip3/SAO
2451138.64	13.537(047)	14.032(022)	13.995(013)	13.913(023)	14.110(021)	4sh-chip3/SAO
2451140.78	13.461(045)	13.945(023)	13.927(016)	13.850(024)	14.079(027)	4sh-chip3/SAO
2451141.82	13.450(065)	13.958(026)	13.889(019)	13.807(025)	14.056(027)	4sh-chip3/SAO
2451142.84	13.507(041)	13.975(022)	13.857(015)	13.801(022)	14.072(030)	4sh-chip3/SAO
2451143.86	13.524(039)	13.974(017)	13.857(008)	13.773(014)	14.100(018)	4sh-chip3/SAO
2451144.72	13.584(042)	14.022(025)	13.841(017)	...	14.184(023)	4sh-chip3/SAO
2451158.65	15.029(113)	14.877(059)	14.459(040)	14.492(058)	14.765(079)	4sh-chip3/Harris+ <i>I</i> _{SAO}
2451159.71	15.045(053)	14.970(022)	14.453(013)	14.475(018)	14.703(034)	4sh-chip3/Harris+ <i>I</i> _{SAO}
2451164.62	15.863(063)	15.532(036)	14.718(023)	14.587(031)	14.644(040)	4sh-chip3/Harris+ <i>I</i> _{SAO}
2451188.58	17.419(066)	17.009(036)	15.897(023)	15.493(030)	15.218(037)	4sh-chip3/Harris+ <i>I</i> _{SAO}
2451195.66	17.492(084)	17.187(051)	16.106(028)	15.754(039)	15.544(047)	4sh-chip3/Harris+ <i>I</i> _{SAO}
2451196.60	17.702(119)	17.187(059)	16.120(034)	15.787(047)	15.601(054)	4sh-chip3/Harris+ <i>I</i> _{SAO}
2451216.60	18.016(171)	17.490(115)	16.728(079)	16.510(109)	16.647(144)	AndyCam/Harris+ <i>I</i> _{SAO}
2451224.63	...	17.573(131)	16.938(074)	16.845(116)	17.001(202)	AndyCam/Harris+ <i>I</i> _{SAO}
2451233.60	18.418(195)	17.954(125)	17.446(088)	17.287(207)	...	4sh-chip3/Harris+ <i>I</i> _{SAO}

Table 28. Photometry of SN 1999X

HJD	<i>U</i>	<i>B</i>	<i>V</i>	<i>R</i>	<i>I</i>	Detector/Filterset
2451217.81	17.150(065)	17.007(041)	16.640(031)	16.602(046)	16.969(054)	AndyCam/Harris+ <i>I</i> _{SAO}
2451218.89	17.356(063)	17.086(046)	16.717(034)	16.744(042)	16.991(043)	AndyCam/Harris+ <i>I</i> _{SAO}
2451219.86	...	17.215(043)	16.765(032)	16.779(038)	17.016(038)	AndyCam/Harris+ <i>I</i> _{SAO}
2451224.71	18.214(082)	17.842(067)	17.074(047)	16.907(058)	16.963(059)	AndyCam/Harris+ <i>I</i> _{SAO}
2451233.68	19.056(158)	18.803(105)	17.568(080)	17.078(097)	16.867(103)	4sh-chip3/Harris+ <i>I</i> _{SAO}
2451275.67	20.175(259)	19.924(172)	...	18.764(038)	...	4sh-chip3/Harris+ <i>I</i> _{SAO}
2451284.69	20.444(209)	18.976(046)	...	4sh-chip3/Harris+ <i>I</i> _{SAO}
2451312.68	19.906(031)	19.922(045)	...	4sh-chip3/Harris

Table 29. Photometry of SN 1999aa

HJD	<i>U</i>	<i>B</i>	<i>V</i>	<i>R</i>	<i>I</i>	Detector/Filterset
2451222.90	14.986(036)	15.603(013)	15.633(008)	15.573(011)	15.704(013)	AndyCam/Harris+ <i>I</i> _{SAO}
2451223.84	14.818(037)	15.417(012)	15.466(007)	15.439(009)	15.534(011)	AndyCam/Harris+ <i>I</i> _{SAO}
2451224.79	14.693(043)	15.276(022)	15.351(009)	15.346(012)	15.415(020)	AndyCam/Harris+ <i>I</i> _{SAO}
2451226.76	14.477(041)	15.088(021)	15.147(016)	15.145(019)	15.282(020)	AndyCam/Harris+ <i>I</i> _{SAO}
2451227.80	14.422(036)	14.960(013)	15.079(009)	15.064(012)	...	AndyCam/Harris+ <i>I</i> _{SAO}
2451230.64	...	14.933(014)	14.994(007)	...	15.238(010)	4sh-chip3/Harris+ <i>I</i> _{SAO}
2451232.69	14.442(038)	14.876(015)	14.911(007)	14.890(008)	15.214(010)	4sh-chip3/Harris+ <i>I</i> _{SAO}
2451233.62	14.486(036)	14.895(012)	14.909(008)	14.888(011)	15.290(023)	4sh-chip3/Harris+ <i>I</i> _{SAO}
2451234.64	14.526(055)	14.899(037)	14.905(029)	14.882(035)	15.277(038)	4sh-chip3/Harris+ <i>I</i> _{SAO}
2451246.75	15.531(036)	15.629(012)	15.371(007)	15.448(010)	15.682(010)	4sh-chip3/Harris+ <i>I</i> _{SAO}
2451248.63	15.826(036)	15.806(012)	15.454(007)	15.531(009)	15.779(012)	4sh-chip3/Harris+ <i>I</i> _{SAO}
2451250.74	16.199(037)	16.058(013)	15.554(008)	15.572(010)	15.837(011)	AndyCam/Harris+ <i>I</i> _{SAO}
2451252.69	16.506(038)	16.302(016)	15.688(008)	15.646(011)	15.772(012)	AndyCam/Harris+ <i>I</i> _{SAO}
2451258.72	17.236(055)	16.914(040)	...	15.710(037)	15.630(039)	4sh-chip3/Harris+ <i>I</i> _{SAO}
2451261.62	17.409(040)	17.130(015)	16.051(010)	15.729(013)	15.609(017)	4sh-chip3/Harris+ <i>I</i> _{SAO}
2451275.65	18.123(060)	18.025(043)	16.235(041)	4sh-chip3/Harris+ <i>I</i> _{SAO}
2451279.64	18.184(042)	17.973(018)	16.982(010)	16.622(013)	16.432(024)	4sh-chip3/Harris+ <i>I</i> _{SAO}
2451281.64	...	17.983(017)	17.033(010)	16.700(013)	16.517(019)	4sh-chip3/Harris+ <i>I</i> _{SAO}
2451284.67	18.123(058)	18.032(024)	17.123(011)	16.787(017)	16.684(067)	4sh-chip3/Harris+ <i>I</i> _{SAO}
2451285.61	18.271(054)	18.009(023)	17.124(014)	16.825(017)	16.722(025)	4sh-chip3/Harris+ <i>I</i> _{SAO}
2451291.62	18.210(107)	18.218(065)	17.192(029)	16.934(045)	16.933(143)	4sh-chip3/Harris+ <i>I</i> _{SAO}
2451306.66	18.529(049)	18.311(020)	17.654(011)	17.489(017)	17.554(032)	4sh-chip3/Harris
2451312.65	18.650(090)	18.399(046)	17.826(033)	17.655(041)	17.804(046)	4sh-chip3/Harris

Table 30. Photometry of SN 1999ac

HJD	<i>U</i>	<i>B</i>	<i>V</i>	<i>R</i>	<i>I</i>	Detector/Filterset
2451246.89	14.081(035)	14.361(012)	14.392(007)	...	14.335(011)	4sh-chip3/Harris+ <i>I</i> _{SAO}
2451247.95	14.039(046)	14.316(028)	14.356(022)	14.271(027)	14.303(027)	4sh-chip3/Harris+ <i>I</i> _{SAO}
2451249.99	...	14.274(012)	14.253(007)	14.200(010)	14.290(011)	AndyCam/Harris+ <i>I</i> _{SAO}
2451252.00	14.168(037)	14.270(012)	14.237(008)	14.167(010)	14.344(012)	AndyCam/Harris+ <i>I</i> _{SAO}
2451253.99	14.276(038)	14.372(015)	14.211(008)	14.178(012)	14.373(013)	AndyCam/Harris+ <i>I</i> _{SAO}
2451258.00	14.690(045)	14.698(015)	14.278(010)	14.237(012)	14.482(014)	4sh-chip3/Harris+ <i>I</i> _{SAO}
2451260.96	15.057(038)	15.043(013)	14.473(007)	14.383(010)	14.600(011)	4sh-chip3/Harris+ <i>I</i> _{SAO}
2451275.90	16.888(047)	16.430(022)	15.319(009)	14.901(024)	14.712(017)	4sh-chip3/Harris+ <i>I</i> _{SAO}
2451280.98	17.153(043)	16.743(022)	15.593(012)	15.123(017)	14.826(023)	4sh-chip3/Harris+ <i>I</i> _{SAO}
2451282.98	17.205(043)	16.853(020)	15.711(008)	15.246(010)	14.927(017)	4sh-chip3/Harris+ <i>I</i> _{SAO}
2451284.92	17.424(044)	16.969(022)	15.843(009)	15.400(012)	15.085(018)	4sh-chip3/Harris+ <i>I</i> _{SAO}
2451287.97	17.471(053)	17.078(028)	16.028(016)	15.603(020)	15.262(029)	4sh-chip3/Harris+ <i>I</i> _{SAO}
2451290.97	17.560(050)	17.208(024)	16.180(009)	15.789(011)	15.486(017)	4sh-chip3/Harris+ <i>I</i> _{SAO}
2451308.85	17.988(058)	17.616(033)	16.668(007)	16.387(009)	16.298(013)	4sh-chip3/Harris
2451312.86	18.120(058)	17.667(033)	16.751(007)	16.525(010)	16.365(014)	4sh-chip3/Harris
2451343.78	18.816(080)	18.116(048)	17.461(011)	17.501(015)	17.411(032)	4sh-chip3/Harris
2451434.62	...	19.643(191)	19.297(050)	19.860(079)	19.444(085)	4sh-chip3/Harris

Table 31. Photometry of SN 1999cc

HJD	<i>U</i>	<i>B</i>	<i>V</i>	<i>R</i>	<i>I</i>	Detector/Filterset
2451312.84	16.702(039)	16.947(017)	16.955(011)	16.818(015)	16.914(022)	4sh-chip3/Harris
2451317.90	16.878(040)	16.907(019)	16.884(013)	16.716(017)	17.128(025)	4sh-chip3/Harris
2451336.80	19.439(136)	19.099(068)	17.935(042)	17.462(051)	17.355(067)	4sh-chip3/Harris
2451339.79	19.718(091)	19.386(042)	18.190(021)	17.640(026)	17.530(037)	4sh-chip3/Harris
2451343.79	19.966(139)	19.659(046)	18.510(023)	17.987(028)	17.809(039)	4sh-chip3/Harris
2451434.65	...	21.494(276)	20.843(181)	4sh-chip3/Harris

Table 32. Photometry of SN 1999cl

HJD	<i>U</i>	<i>B</i>	<i>V</i>	<i>R</i>	<i>I</i>	Detector/Filterset
2451335.69	16.071(184)	...	14.354(035)	13.702(046)	13.346(049)	4sh-chip3/Harris
2451338.65	15.793(061)	15.126(043)	14.022(028)	13.455(034)	13.147(035)	4sh-chip3/Harris
2451340.65	15.777(064)	15.066(046)	13.933(030)	13.387(036)	13.147(042)	4sh-chip3/Harris
2451342.65	15.838(060)	15.076(041)	13.887(027)	13.326(038)	13.131(041)	4sh-chip3/Harris
2451343.69	15.904(060)	15.091(037)	13.878(022)	13.323(028)	13.175(031)	4sh-chip3/Harris
2451346.70	13.869(031)	4sh-chip3/Harris
2451348.68	16.405(066)	15.395(043)	13.946(027)	13.471(032)	13.340(035)	4sh-chip3/Harris
2451350.66	16.531(072)	15.530(054)	14.044(036)	13.567(051)	13.429(054)	4sh-chip3/Harris
2451362.72	18.588(087)	16.846(040)	14.709(026)	13.934(032)	13.394(036)	4sh-chip3/Harris

Table 33. Photometry of SN 1999cw

HJD	<i>U</i>	<i>B</i>	<i>V</i>	<i>R</i>	<i>I</i>	Detector/Filterset
2451376.96	16.185(064)	15.925(043)	15.044(022)	14.821(041)	14.895(044)	4sh-chip3/Harris
2451434.86	17.991(042)	17.624(016)	17.003(007)	16.828(015)	16.982(019)	4sh-chip3/Harris
2451461.79	18.441(057)	18.044(023)	17.606(016)	17.639(020)	17.849(028)	4sh-chip3/Harris
2451487.71	18.998(074)	18.445(030)	18.103(018)	18.325(024)	18.602(065)	4sh-chip3/Harris
2451521.60	19.794(190)	18.916(050)	18.663(033)	19.102(046)	19.229(103)	4sh-chip3/Harris
2451546.62	20.297(161)	19.367(045)	19.073(030)	19.689(056)	...	4sh-chip3/Harris

Table 34. Photometry of SN 1999dq

HJD	<i>U</i>	<i>B</i>	<i>V</i>	<i>R</i>	<i>I</i>	Detector/Filterset
2451426.99	15.027(043)	15.477(022)	15.325(014)	15.202(017)	15.147(022)	4sh-chip3/Harris
2451427.97	14.831(037)	15.322(015)	15.162(010)	15.027(013)	15.029(015)	4sh-chip3/Harris
2451428.88	14.663(054)	15.199(021)	15.074(014)	14.943(018)	14.960(020)	4sh-chip3/Harris
2451429.99	14.613(038)	15.092(018)	14.955(010)	14.843(014)	14.861(017)	4sh-chip3/Harris
2451431.93	14.491(046)	14.953(023)	14.766(016)	14.689(020)	14.808(026)	4sh-chip3/Harris
2451432.97	14.472(064)	14.594(038)	...	4sh-chip3/Harris
2451434.00	14.431(040)	14.895(020)	14.740(013)	14.644(016)	14.760(021)	4sh-chip3/Harris
2451434.95	14.466(039)	14.853(021)	14.697(015)	14.587(021)	14.788(021)	4sh-chip3/Harris
2451435.90	14.481(036)	14.864(014)	14.710(010)	14.608(015)	14.743(015)	4sh-chip3/Harris
2451436.87	14.619(064)	14.845(039)	14.696(015)	14.563(019)	14.749(021)	4sh-chip3/Harris
2451437.86	14.621(038)	14.892(017)	14.675(011)	14.565(016)	14.783(016)	4sh-chip3/Harris
2451438.89	14.652(038)	14.889(012)	14.697(008)	14.565(010)	14.813(013)	4sh-chip3/Harris
2451439.91	14.738(038)	14.918(018)	14.681(013)	14.555(018)	14.851(019)	4sh-chip3/Harris
2451441.92	14.883(111)	14.985(015)	14.712(010)	14.601(014)	14.914(019)	4sh-chip3/Harris
2451453.94	16.306(038)	16.009(015)	15.273(007)	15.168(010)	15.280(016)	4sh-chip3/Harris
2451454.90	15.396(012)	15.210(015)	15.349(017)	AndyCam/Harris
2451458.89	16.928(057)	16.608(015)	15.558(010)	15.263(013)	15.178(014)	4sh-chip3/Harris
2451461.89	17.319(036)	16.911(011)	15.698(007)	15.298(009)	15.098(011)	4sh-chip3/Harris
2451463.90	17.565(039)	17.071(014)	15.808(009)	15.337(011)	15.068(013)	4sh-chip3/Harris
2451466.87	...	17.299(022)	15.983(012)	15.461(016)	15.094(016)	4sh-chip3/Harris
2451468.85	17.939(051)	17.443(021)	16.092(013)	15.556(017)	15.172(018)	4sh-chip3/Harris
2451487.83	18.397(047)	18.016(016)	16.871(010)	16.470(012)	16.174(017)	4sh-chip3/Harris
2451512.78	19.212(067)	18.329(038)	17.518(026)	17.258(032)	17.133(037)	4sh-chip3/Harris
2451521.78	...	18.528(026)	17.619(013)	17.476(019)	17.683(049)	4sh-chip3/Harris
2451527.72	17.825(028)	17.694(035)	17.824(065)	4sh-chip3/Harris
2451546.76	19.824(082)	18.867(041)	18.270(023)	18.277(032)	18.446(059)	4sh-chip3/Harris
2451547.74	18.292(029)	4sh-chip3/Harris
2451589.65	...	19.479(090)	19.031(065)	19.235(092)	18.941(148)	4sh-chip3/Harris
2451590.65	...	19.315(059)	18.922(038)	19.483(092)	18.862(094)	4sh-chip3/Harris

Table 35. Photometry of SN 1999ef

HJD	<i>U</i>	<i>B</i>	<i>V</i>	<i>R</i>	<i>I</i>	Detector/Filterset
2451464.81	17.842(047)	17.720(022)	17.491(015)	17.316(019)	17.909(031)	4sh-chip3/Harris
2451467.73	18.109(041)	17.945(018)	17.627(011)	17.586(016)	18.131(029)	4sh-chip3/Harris
2451469.85	18.301(081)	18.146(020)	17.765(012)	17.742(020)	18.343(080)	4sh-chip3/Harris
2451487.74	20.248(116)	19.955(039)	18.763(024)	18.173(031)	18.174(041)	4sh-chip3/Harris
2451521.62	...	20.953(081)	20.032(046)	19.573(074)	20.215(120)	4sh-chip3/Harris
2451546.68	...	21.313(258)	20.487(177)	20.464(234)	...	4sh-chip3/Harris
2451581.62	...	21.798(280)	20.858(177)	4sh-chip3/Harris

Table 36. Photometry of SN 1999ej

HJD	<i>U</i>	<i>B</i>	<i>V</i>	<i>R</i>	<i>I</i>	Detector/Filterset
2451487.75	15.728(038)	15.833(016)	15.632(010)	15.531(013)	15.795(014)	4sh-chip3/Harris
2451494.83	16.801(041)	16.629(018)	16.072(011)	16.060(014)	16.267(016)	4sh-chip3/Harris
2451521.70	18.902(135)	18.831(075)	...	17.373(044)	17.174(045)	4sh-chip3/Harris
2451527.64	17.968(256)	4sh-chip3/Harris
2451546.71	19.690(133)	19.332(048)	18.529(019)	18.326(029)	18.372(052)	4sh-chip3/Harris
2451589.59	...	20.087(164)	...	19.604(161)	...	4sh-chip3/Harris
2451590.61	...	19.981(118)	19.615(074)	19.684(110)	19.818(197)	4sh-chip3/Harris

Table 37. Photometry of SN 1999ek

HJD	<i>U</i>	<i>B</i>	<i>V</i>	<i>R</i>	<i>I</i>	Detector/Filterset
2451487.91	18.629(058)	18.186(021)	17.324(011)	16.905(015)	16.803(017)	4sh-chip3/Harris
2451495.91	19.737(083)	18.924(030)	17.757(012)	17.401(016)	17.272(022)	4sh-chip3/Harris
2451517.87	...	20.934(130)	19.077(038)	18.296(049)	17.609(049)	4sh-chip3/Harris
2451521.81	...	20.988(150)	19.231(044)	18.505(060)	17.712(064)	4sh-chip3/Harris
2451545.84	...	21.286(121)	19.890(067)	19.251(083)	18.888(085)	4sh-chip3/Harris
2451584.62	20.825(161)	20.616(209)	20.719(224)	4sh-chip3/Harris
2451590.70	20.966(201)	4sh-chip3/Harris

Table 38. Photometry of SN 1999gd

HJD	<i>U</i>	<i>B</i>	<i>V</i>	<i>R</i>	<i>I</i>	Detector/Filterset
2451521.93	17.325(059)	17.144(015)	16.680(010)	16.381(014)	16.470(027)	4sh-chip3/Harris
2451527.95	17.987(078)	17.563(020)	16.842(011)	16.627(014)	16.783(019)	4sh-chip3/Harris
2451545.91	20.109(055)	19.482(016)	17.923(007)	17.242(011)	16.812(012)	4sh-chip3/Harris
2451556.84	20.785(135)	20.343(045)	18.691(021)	18.028(026)	17.502(028)	4sh-chip3/Harris
2451581.82	...	20.486(052)	19.312(021)	18.860(027)	18.525(038)	4sh-chip3/Harris
2451589.86	...	20.521(118)	19.563(046)	19.096(065)	18.716(120)	4sh-chip3/Harris
2451590.89	...	20.531(101)	19.508(045)	19.068(071)	18.651(140)	4sh-chip3/Harris
2451640.77	20.791(091)	20.549(123)	...	4sh-chip3/Harris
2451670.68	21.398(257)	4sh-chip3/Harris

Table 39. Photometry of SN 1999gh

HJD	<i>U</i>	<i>B</i>	<i>V</i>	<i>R</i>	<i>I</i>	Detector/Filterset
2451520.95	15.381(040)	15.172(011)	14.507(007)	14.450(008)	14.651(013)	4sh-chip3/Harris
2451522.01	15.568(040)	15.321(011)	14.587(007)	14.524(011)	14.687(015)	4sh-chip3/Harris
2451523.00	15.733(037)	15.477(014)	14.657(010)	14.570(012)	14.679(015)	4sh-chip3/Harris
2451524.97	16.067(038)	15.814(015)	14.813(010)	14.661(012)	14.707(015)	4sh-chip3/Harris
2451527.04	16.420(043)	16.099(016)	14.991(009)	14.712(012)	14.589(014)	4sh-chip3/Harris
2451541.95	17.656(051)	17.477(017)	16.247(009)	15.799(012)	15.520(016)	4sh-chip3/Harris
2451545.95	17.810(113)	17.631(015)	16.442(010)	15.986(014)	15.737(019)	4sh-chip3/Harris
2451549.92	17.902(052)	17.728(019)	16.589(008)	16.190(012)	15.973(020)	4sh-chip3/Harris
2451552.93	...	17.800(017)	16.688(007)	16.320(011)	16.129(026)	4sh-chip3/Harris
2451554.89	18.079(051)	17.800(018)	16.730(009)	16.382(014)	16.238(019)	4sh-chip3/Harris
2451575.81	18.628(125)	18.148(028)	17.359(019)	17.182(030)	17.052(067)	4sh-chip3/Harris
2451581.85	18.804(091)	18.270(019)	17.524(009)	17.386(019)	17.424(076)	4sh-chip3/Harris
2451584.82	18.885(087)	18.331(031)	17.596(021)	17.509(029)	17.521(059)	4sh-chip3/Harris
2451588.79	19.003(172)	18.419(039)	17.711(023)	17.653(033)	17.664(097)	4sh-chip3/Harris
2451589.81	17.749(028)	17.638(054)	17.550(113)	4sh-chip3/Harris
2451590.83	18.800(095)	18.417(023)	17.777(015)	17.730(026)	17.701(065)	4sh-chip3/Harris
2451600.79	19.087(240)	18.614(079)	17.990(023)	18.070(046)	18.023(099)	4sh-chip3/Harris
2451640.68	19.873(154)	19.287(069)	18.980(042)	19.197(068)	18.902(168)	4sh-chip3/Harris

Table 40. Photometry of SN 1999gp

HJD	<i>U</i>	<i>B</i>	<i>V</i>	<i>R</i>	<i>I</i>	Detector/Filterset
2451545.81	15.756(037)	16.330(012)	16.338(008)	16.243(011)	16.352(012)	4sh-chip3/Harris
2451546.74	15.758(041)	16.285(016)	16.206(008)	16.177(012)	16.330(012)	4sh-chip3/Harris
2451548.65	15.760(036)	16.199(013)	16.226(009)	16.145(012)	16.366(015)	4sh-chip3/Harris
2451551.63	15.874(037)	16.251(013)	16.140(007)	16.023(011)	16.406(016)	4sh-chip3/Harris
2451553.57	16.050(038)	16.291(013)	16.136(008)	16.015(011)	16.472(014)	4sh-chip3/Harris
2451555.62	16.150(037)	16.475(014)	16.280(009)	16.171(012)	16.568(014)	4sh-chip3/Harris
2451564.64	17.109(048)	17.011(019)	16.564(012)	16.527(017)	17.048(041)	4sh-chip3/Harris
2451570.58	17.857(072)	17.589(021)	16.872(011)	...	17.142(033)	4sh-chip3/Harris
2451580.58	18.870(066)	18.463(031)	17.306(017)	16.851(026)	16.831(029)	4sh-chip3/Harris
2451581.67	18.985(063)	18.578(017)	17.324(010)	16.849(017)	16.850(017)	4sh-chip3/Harris
2451589.67	19.378(193)	18.999(028)	17.822(016)	17.249(024)	17.053(032)	4sh-chip3/Harris

Table 41. Photometry of SN 2000B

HJD	<i>U</i>	<i>B</i>	<i>V</i>	<i>R</i>	<i>I</i>	Detector/Filterset
2451578.83	17.654(036)	17.333(012)	16.462(007)	16.374(010)	16.632(013)	4sh-chip3/Harris
2451581.74	18.102(043)	17.731(017)	16.603(010)	16.429(014)	16.470(016)	4sh-chip3/Harris
2451590.78	19.055(086)	18.624(024)	17.368(012)	16.793(016)	16.544(019)	4sh-chip3/Harris
2451601.65	19.436(118)	19.145(025)	17.946(014)	17.455(018)	17.268(023)	4sh-chip3/Harris
2451607.67	19.728(123)	19.238(024)	18.141(011)	17.701(016)	17.562(022)	4sh-chip3/Harris
2451640.66	20.254(212)	19.691(042)	19.018(030)	18.789(043)	18.892(066)	4sh-chip3/Harris

Table 42. Photometry of SN 2000ce

HJD	<i>U</i>	<i>B</i>	<i>V</i>	<i>R</i>	<i>I</i>	Detector/Filterset
2451674.63	17.842(083)	17.615(030)	16.835(016)	16.504(022)	16.528(024)	4sh-chip3/Harris
2451675.64	18.156(081)	17.674(028)	16.882(015)	16.564(021)	16.595(029)	4sh-chip3/Harris
2451677.66	18.202(083)	17.837(020)	17.010(012)	16.711(019)	16.739(031)	4sh-chip3/Harris
2451678.63	18.292(126)	17.924(038)	17.067(015)	16.761(022)	16.818(033)	4sh-chip3/Harris
2451679.63	18.525(210)	18.068(050)	17.091(021)	16.804(027)	16.821(036)	4sh-chip3/Harris
2451689.66	19.669(141)	19.169(048)	17.648(026)	17.113(033)	16.787(040)	4sh-chip3/Harris

Table 43. Photometry of SN 2000cf

HJD	<i>U</i>	<i>B</i>	<i>V</i>	<i>R</i>	<i>I</i>	Detector/Filterset
2451676.85	17.173(077)	17.256(022)	17.194(012)	17.063(020)	17.491(037)	4sh-chip3/Harris
2451677.80	17.334(063)	17.302(027)	17.191(018)	17.126(024)	17.524(034)	4sh-chip3/Harris
2451678.74	17.410(097)	17.151(038)	...	4sh-chip3/Harris
2451679.78	17.648(085)	17.445(023)	17.270(014)	17.180(018)	17.604(027)	4sh-chip3/Harris
2451688.81	...	18.437(038)	17.751(020)	17.648(029)	18.046(045)	4sh-chip3/Harris
2451691.79	...	18.851(035)	17.989(015)	17.731(023)	17.993(041)	4sh-chip3/Harris
2451693.83	19.559(185)	18.996(070)	18.128(023)	17.778(031)	17.980(059)	4sh-chip3/Harris
2451695.73	...	19.302(053)	18.245(022)	17.793(028)	17.995(043)	4sh-chip3/Harris
2451696.78	19.822(216)	19.436(057)	18.278(022)	17.844(031)	17.864(038)	4sh-chip3/Harris
2451730.67	...	20.721(176)	19.746(069)	19.269(099)	19.252(118)	4sh-chip3/Harris
2451758.68	20.377(174)	20.052(236)	...	4sh-chip3/Harris
2451795.67	22.525(201)	4sh-chip3/Harris
2451806.62	20.964(205)	4sh-chip3/Harris

Table 44. Photometry of SN 2000cn

HJD	<i>U</i>	<i>B</i>	<i>V</i>	<i>R</i>	<i>I</i>	Detector/Filterset
2451699.85	17.567(047)	17.618(020)	17.471(013)	17.264(019)	17.254(025)	4sh-chip3/Harris
2451700.84	17.258(043)	17.349(024)	17.260(018)	17.049(023)	17.008(028)	4sh-chip3/Harris
2451701.90	17.024(038)	17.178(017)	17.033(011)	16.843(015)	16.879(017)	4sh-chip3/Harris
2451702.98	...	16.982(028)	16.892(016)	16.701(021)	16.789(027)	4sh-chip3/Harris
2451703.80	16.888(039)	16.921(018)	16.856(013)	16.647(017)	16.673(022)	4sh-chip3/Harris
2451709.89	17.003(090)	16.896(018)	16.591(012)	16.437(017)	16.785(027)	4sh-chip3/Harris
2451710.83	17.085(070)	16.958(037)	16.580(026)	16.432(041)	16.751(051)	4sh-chip3/Harris
2451711.71	17.195(049)	17.017(022)	16.611(014)	16.476(019)	16.781(023)	4sh-chip3/Harris
2451712.78	17.474(061)	17.074(028)	16.645(018)	16.538(024)	16.867(031)	4sh-chip3/Harris
2451715.86	17.698(071)	17.460(030)	16.821(020)	16.790(028)	17.061(046)	4sh-chip3/Harris
2451716.74	17.889(047)	17.557(020)	16.930(013)	16.857(018)	17.128(027)	4sh-chip3/Harris
2451728.97	...	19.301(044)	17.883(027)	17.355(033)	17.119(039)	4sh-chip3/Harris
2451758.72	...	20.148(070)	19.154(038)	18.967(059)	...	4sh-chip3/Harris
2451789.79	19.879(252)	4sh-chip3/Harris
2451790.67	19.992(244)	4sh-chip3/Harris
2451791.64	20.076(104)	20.225(206)	...	4sh-chip3/Harris
2451794.65	...	20.616(147)	20.075(101)	20.242(167)	...	4sh-chip3/Harris
2451796.66	...	20.656(182)	4sh-chip3/Harris
2451803.62	20.333(101)	20.769(175)	...	4sh-chip3/Harris
2451810.65	20.659(251)	4sh-chip3/Harris

Table 45. Photometry of SN 2000cx

HJD	<i>U</i>	<i>B</i>	<i>V</i>	<i>R</i>	<i>I</i>	Detector/Filterset
2451751.97	13.223(051)	13.422(021)	13.285(013)	13.338(017)	13.639(029)	4sh-chip3/Harris
2451789.96	16.571(092)	16.390(035)	15.516(012)	15.227(016)	15.129(028)	4sh-chip3/Harris
2451792.99	16.667(046)	16.512(018)	15.643(010)	15.365(015)	15.315(028)	4sh-chip3/Harris
2451794.95	16.768(049)	16.555(018)	15.718(010)	15.452(014)	15.429(025)	4sh-chip3/Harris
2451800.96	16.911(072)	16.677(048)	15.919(024)	15.700(030)	15.753(060)	4sh-chip3/Harris
2451801.88	16.961(065)	16.701(039)	15.973(028)	15.751(035)	15.828(041)	4sh-chip3/Harris
2451805.86	16.990(050)	16.780(026)	16.099(017)	15.877(024)	16.038(030)	4sh-chip3/Harris
2451810.85	17.126(047)	16.889(021)	16.250(012)	16.067(017)	16.248(027)	4sh-chip3/Harris
2451814.76	17.157(061)	16.971(016)	16.391(009)	16.219(012)	16.446(021)	4sh-chip3/Harris
2451819.93	17.271(047)	17.063(021)	16.563(010)	16.412(014)	16.730(025)	4sh-chip3/Harris
2451822.99	17.275(048)	17.120(021)	16.654(011)	16.524(016)	16.868(028)	4sh-chip3/Harris
2451843.64	17.833(095)	17.535(064)	17.263(033)	17.231(044)	17.667(054)	4sh-chip3/Harris
2451868.70	18.465(073)	18.018(030)	17.816(020)	17.963(029)	18.403(050)	4sh-chip3/Harris
2451875.70	...	18.111(027)	17.918(016)	18.071(027)	18.377(055)	4sh-chip3/Harris
2451878.77	18.779(060)	18.189(029)	18.036(020)	18.164(029)	18.548(050)	4sh-chip3/Harris
2451900.66	19.063(057)	18.550(031)	18.418(020)	18.760(038)	18.929(058)	4sh-chip3/Harris
2451906.64	19.252(055)	18.604(026)	18.520(017)	18.842(029)	19.026(066)	4sh-chip3/Harris
2451933.64	19.817(120)	19.025(084)	18.942(063)	19.404(077)	19.734(152)	4sh-chip3/Harris

Table 46. Photometry of SN 2000dk

HJD	<i>U</i>	<i>B</i>	<i>V</i>	<i>R</i>	<i>I</i>	Detector/Filterset
2451807.88	15.500(038)	15.917(016)	15.896(010)	15.724(012)	15.871(016)	4sh-chip3/Harris
2451809.88	15.431(037)	15.699(012)	15.692(007)	15.558(009)	15.713(011)	4sh-chip3/Harris
2451810.80	15.405(037)	15.664(015)	15.652(009)	15.498(011)	15.696(014)	4sh-chip3/Harris
2451811.84	15.423(036)	15.630(012)	15.578(007)	15.456(008)	15.742(012)	4sh-chip3/Harris
2451813.71	15.562(037)	15.637(014)	15.568(008)	15.468(011)	15.803(014)	4sh-chip3/Harris
2451818.71	16.146(038)	16.004(015)	15.667(009)	15.653(011)	16.114(014)	4sh-chip3/Harris
2451821.97	16.650(039)	16.435(017)	15.906(010)	15.876(013)	16.260(018)	4sh-chip3/Harris
2451825.81	17.359(040)	17.021(015)	16.153(009)	15.996(011)	16.166(016)	4sh-chip3/Harris
2451844.60	18.995(117)	18.682(039)	17.585(016)	17.201(024)	16.970(042)	4sh-chip3/Harris
2451873.73	19.918(229)	19.392(052)	18.529(027)	18.366(041)	18.422(066)	4sh-chip3/Harris
2451875.64	...	19.296(070)	18.610(032)	18.364(047)	18.567(068)	4sh-chip3/Harris
2451906.66	...	19.866(121)	19.515(067)	19.450(103)	19.371(137)	4sh-chip3/Harris
2451933.61	...	20.347(215)	20.245(143)	4sh-chip3/Harris

Table 47. Photometry of SN 2000fa

HJD	<i>U</i>	<i>B</i>	<i>V</i>	<i>R</i>	<i>I</i>	Detector/Filterset
2451881.91	17.095(041)	17.184(017)	17.059(011)	16.889(016)	16.919(019)	4sh-chip3/Harris
2451898.83	16.386(036)	16.364(011)	16.110(007)	15.993(010)	16.424(015)	4sh-chip3/Harris
2451901.83	16.718(037)	16.566(013)	16.237(008)	16.155(011)	16.580(018)	4sh-chip3/Harris
2451906.82	17.295(041)	17.039(015)	16.546(010)	16.531(012)	16.833(021)	4sh-chip3/Harris
2451907.74	17.368(052)	17.148(012)	16.584(007)	16.560(010)	16.836(017)	4sh-chip3/Harris
2451929.83	19.642(113)	19.082(054)	17.777(014)	17.246(019)	17.007(025)	4sh-chip3/Harris
2451933.83	19.921(159)	19.220(031)	17.984(017)	17.472(021)	17.284(025)	4sh-chip3/Harris
2451953.73	...	19.463(040)	18.537(024)	18.167(030)	18.219(044)	4sh-chip3/Harris
2451959.61	...	19.526(048)	18.737(034)	18.372(043)	18.451(063)	4sh-chip3/Harris
2451963.76	...	19.613(043)	18.804(020)	18.537(027)	18.541(080)	4sh-chip3/Harris
2451994.70	20.665(226)	20.133(114)	19.601(076)	19.478(116)	19.591(153)	4sh-chip3/Harris
2452022.66	...	20.550(239)	20.237(155)	20.422(227)	...	4sh-chip3/Harris

Table 48. Natural System *UBVRI* passbands

Wavelength (nm)	Detector/filterset normalized response			
	AndyCam/SAO	AndyCam/Harris	4Shooter/SAO	4Shooter/Harris
U				
295	0.000	0.000	0.000	0.000
300	0.000	0.011	0.000	0.009
305	0.000	0.060	0.000	0.048
310	0.000	0.149	0.000	0.117
315	0.002	0.264	0.002	0.206
320	0.023	0.381	0.018	0.296
325	0.089	0.493	0.067	0.382
330	0.194	0.592	0.148	0.459
335	0.326	0.673	0.250	0.527
340	0.465	0.745	0.362	0.591
345	0.595	0.815	0.472	0.659
350	0.713	0.876	0.581	0.727
355	0.814	0.924	0.686	0.794
360	0.897	0.965	0.786	0.861
365	0.960	0.991	0.878	0.924
370	0.997	1.000	0.953	0.974
375	1.000	0.981	1.000	1.000
380	0.943	0.924	0.985	0.983
385	0.816	0.808	0.888	0.896
390	0.616	0.632	0.696	0.727
395	0.384	0.421	0.448	0.501
400	0.189	0.230	0.226	0.281
405	0.071	0.101	0.086	0.125
410	0.020	0.035	0.025	0.045
415	0.005	0.011	0.006	0.014
420	0.001	0.003	0.001	0.004
425	0.000	0.001	0.000	0.001
430	0.000	0.000	0.000	0.000
B				
345	0.000	0.000	0.000	0.000
350	0.000	0.005	0.000	0.004
355	0.000	0.040	0.000	0.027
360	0.007	0.130	0.005	0.092
365	0.040	0.255	0.030	0.188
370	0.113	0.383	0.087	0.296
375	0.215	0.494	0.174	0.399
380	0.331	0.586	0.280	0.494
385	0.443	0.661	0.390	0.581
390	0.545	0.723	0.498	0.660
395	0.631	0.774	0.597	0.729
400	0.705	0.816	0.683	0.789
405	0.767	0.851	0.758	0.840
410	0.821	0.884	0.823	0.884
415	0.866	0.913	0.876	0.921
420	0.907	0.940	0.921	0.952
425	0.938	0.960	0.953	0.973
430	0.963	0.978	0.977	0.989
435	0.981	0.990	0.991	0.997
440	0.994	0.997	0.999	1.000
445	1.000	1.000	1.000	0.997
450	0.991	0.989	0.986	0.981
455	0.977	0.973	0.967	0.961
460	0.948	0.944	0.935	0.929
465	0.896	0.894	0.882	0.877
470	0.814	0.814	0.799	0.797
475	0.711	0.715	0.696	0.698
480	0.602	0.608	0.588	0.592
485	0.488	0.497	0.475	0.482
490	0.386	0.396	0.374	0.383
495	0.305	0.315	0.295	0.303
500	0.246	0.254	0.236	0.244

Table 48—Continued

Wavelength (nm)	Detector/filterset normalized response			
	AndyCam/SAO	AndyCam/Harris	4Shooter/SAO	4Shooter/Harris
505	0.183	0.191	0.174	0.182
510	0.126	0.133	0.119	0.126
515	0.087	0.093	0.082	0.087
520	0.056	0.060	0.052	0.056
525	0.034	0.037	0.031	0.034
530	0.021	0.023	0.019	0.021
535	0.015	0.018	0.013	0.016
540	0.013	0.015	0.012	0.013
545	0.014	0.015	0.012	0.014
550	0.018	0.018	0.016	0.016
555	0.025	0.024	0.022	0.021
560	0.029	0.027	0.025	0.024
565	0.025	0.024	0.022	0.021
570	0.018	0.018	0.015	0.015
575	0.009	0.009	0.008	0.008
580	0.004	0.004	0.003	0.003
585	0.001	0.001	0.001	0.001
590	0.000	0.001	0.000	0.000
595	0.000	0.000	0.000	0.000
V				
470	0.000	0.000	0.000	0.000
475	0.000	0.010	0.000	0.011
480	0.001	0.094	0.001	0.100
485	0.040	0.285	0.043	0.304
490	0.245	0.496	0.260	0.527
495	0.531	0.662	0.562	0.700
500	0.732	0.777	0.770	0.817
505	0.845	0.854	0.883	0.892
510	0.908	0.907	0.942	0.941
515	0.946	0.944	0.975	0.971
520	0.971	0.970	0.992	0.990
525	0.988	0.987	1.000	0.999
530	0.997	0.998	1.000	1.000
535	1.000	1.000	0.994	0.994
540	0.994	0.995	0.980	0.980
545	0.981	0.981	0.959	0.959
550	0.958	0.960	0.930	0.931
555	0.925	0.930	0.891	0.895
560	0.882	0.891	0.845	0.852
565	0.829	0.841	0.789	0.800
570	0.768	0.787	0.727	0.744
575	0.700	0.723	0.659	0.680
580	0.625	0.654	0.586	0.612
585	0.548	0.581	0.511	0.541
590	0.470	0.508	0.435	0.471
595	0.393	0.435	0.363	0.401
600	0.321	0.365	0.295	0.335
605	0.256	0.300	0.233	0.273
610	0.198	0.241	0.180	0.219
615	0.149	0.190	0.134	0.171
620	0.108	0.146	0.097	0.131
625	0.076	0.110	0.068	0.098
630	0.052	0.081	0.046	0.072
635	0.034	0.058	0.030	0.051
640	0.021	0.041	0.019	0.036
645	0.013	0.028	0.011	0.024
650	0.008	0.019	0.007	0.016
655	0.004	0.013	0.004	0.012
660	0.002	0.009	0.002	0.007
665	0.001	0.005	0.001	0.005
670	0.001	0.003	0.000	0.003
675	0.000	0.002	0.000	0.002
680	0.000	0.001	0.000	0.001
685	0.000	0.001	0.000	0.001
690	0.000	0.000	0.000	0.000

Table 48—Continued

Wavelength (nm)	Detector/filterset normalized response			
	AndyCam/SAO	AndyCam/Harris	4Shooter/SAO	4Shooter/Harris
R				
540	0.000	0.000	0.000	0.000
550	0.001	0.000	0.001	0.000
560	0.173	0.129	0.179	0.135
570	0.718	0.690	0.735	0.711
580	0.944	0.927	0.958	0.947
590	0.996	0.986	1.000	0.997
600	1.000	0.999	0.994	1.000
610	0.986	1.000	0.969	0.989
620	0.960	0.993	0.933	0.971
630	0.922	0.977	0.886	0.944
640	0.876	0.952	0.833	0.910
650	0.823	0.920	0.775	0.871
660	0.764	0.883	0.713	0.830
670	0.701	0.842	0.651	0.786
680	0.633	0.794	0.584	0.738
690	0.559	0.739	0.514	0.685
700	0.486	0.681	0.446	0.629
710	0.417	0.621	0.383	0.574
720	0.353	0.562	0.324	0.519
730	0.294	0.505	0.270	0.466
740	0.240	0.448	0.221	0.413
750	0.193	0.391	0.177	0.361
760	0.152	0.337	0.139	0.310
770	0.117	0.287	0.106	0.263
780	0.088	0.241	0.080	0.221
790	0.065	0.201	0.059	0.184
800	0.048	0.165	0.044	0.151
810	0.035	0.135	0.032	0.124
820	0.025	0.110	0.023	0.101
830	0.018	0.088	0.016	0.081
840	0.012	0.070	0.011	0.065
850	0.009	0.056	0.008	0.052
860	0.005	0.044	0.005	0.041
870	0.004	0.034	0.003	0.032
880	0.002	0.027	0.002	0.024
890	0.002	0.021	0.002	0.019
900	0.001	0.016	0.001	0.015
910	0.000	0.012	0.000	0.011
920	0.000	0.009	0.000	0.008
930	0.000	0.007	0.000	0.007
940	0.000	0.005	0.000	0.005
950	0.000	0.004	0.000	0.004
960	0.000	0.003	0.000	0.003
970	0.000	0.002	0.000	0.002
980	0.000	0.002	0.000	0.001
990	0.000	0.001	0.000	0.001
1000	0.000	0.001	0.000	0.001
1010	0.000	0.001	0.000	0.000
1020	0.000	0.000	0.000	0.000
I				
690	0.000	0.000	0.000	0.000
700	0.003	0.000	0.003	0.000
710	0.077	0.001	0.077	0.001
720	0.326	0.073	0.328	0.073
730	0.630	0.927	0.634	0.928
740	0.841	0.993	0.846	0.994
750	0.946	1.000	0.950	1.000
760	0.989	0.886	0.992	0.885
770	1.000	0.945	1.000	0.940
780	0.994	0.976	0.991	0.969
790	0.979	0.938	0.976	0.930

Table 48—Continued

Wavelength (nm)	AndyCam/SAO	Detector/filterset normalized response		
		AndyCam/Harris	4Shooter/SAO	4Shooter/Harris
800	0.970	0.826	0.967	0.819
810	0.950	0.799	0.948	0.795
820	0.932	0.837	0.935	0.836
830	0.916	0.879	0.923	0.882
840	0.895	0.886	0.905	0.892
850	0.876	0.875	0.886	0.881
860	0.843	0.917	0.849	0.920
870	0.829	0.697	0.830	0.694
880	0.800	0.597	0.795	0.591
890	0.765	0.278	0.757	0.273
900	0.726	0.009	0.719	0.009
910	0.681	0.000	0.681	0.000
920	0.633	0.000	0.642	0.000
930	0.581	0.000	0.601	0.000
940	0.529	0.000	0.556	0.000
950	0.476	0.000	0.505	0.000
960	0.426	0.000	0.447	0.000
970	0.377	0.000	0.385	0.000
980	0.330	0.000	0.323	0.000
990	0.284	0.000	0.263	0.000
1000	0.239	0.000	0.208	0.000
1010	0.195	0.000	0.161	0.000
1020	0.154	0.000	0.122	0.000
1030	0.117	0.000	0.091	0.000
1040	0.085	0.000	0.066	0.000
1050	0.059	0.000	0.046	0.000
1060	0.040	0.000	0.032	0.000
1070	0.026	0.000	0.021	0.000
1080	0.016	0.000	0.014	0.000
1090	0.009	0.000	0.008	0.000
1100	0.004	0.000	0.004	0.000
1110	0.000	0.000	0.000	0.000

Table 49. SN Ia and Host Basic Data

SN Ia	Host galaxy	cz_{helio} km s ⁻¹	Morphology	SN Offsets		$E(B-V)_{\text{Galactic}}$ mag
				"N	"E	
1997E	NGC 2258	4001	S0	+57	-32	0.124
1997Y	NGC 4675	4806	Sb	+2	-8	0.017
1997bp	NGC 4680	2492	Sd/Irr	-20	-15	0.044
1997bq	NGC 3147	2780	Sbc	-60	+50	0.024
1997br	ESO 576-40	2085	Sd/Irr	+52	-21	0.113
1997cn	NGC 5490	4855	E	-12	+7	0.027
1997ew	NGC 105	5133	Sab	+4	+8	0.073
1997dg	anonymous	9238	...	0	+2	0.078
1997do	UGC 3845	3034	Sbc	-4	-3	0.063
1997dt	NGC 7448	2194	Sbc	+1	-9	0.057
1998D	NGC 5440	3765	Sa	-7	-26	0.015
1998V	NGC 6627	5268	Sb	+21	-21	0.196
1998ab	NGC 4704	8134	Sc	+12	+2	0.017
1998bp	NGC 6495	3127	E	+13	-1	0.076
1998co	NGC 7131	5418	S0	+5	+2	0.043
1998de	NGC 252	4990	S0	+3	+72	0.057
1998dh	NGC 7541	2678	Sbc	+10	-54	0.068
1998dk	UGC 139	3963	Sc	+3	+5	0.044
1998dm	MCG-01-4-44	1968	Sc	-37	-14	0.044
1998dx	UGC 11149	16197	Sb	-12	+21	0.041
1998ec	UGC 3576	5966	Sb	-20	-9	0.085
1998ef	UGC 646	5319	Sa	-2	+6	0.073
1998eg	UGC 12133	7423	Sc	-25	-26	0.123
1998es	NGC 632	3168	S0	+11	0	0.032
1999X	CGCG 180-22	7503	...	+6	+4	0.032
1999aa	NGC 2595	4330	Sc	+28	+1	0.040
1999ac	NGC 6063	2848	Scd	-30	+24	0.046
1999cc	NGC 6038	9392	Sc	+2	+17	0.023
1999cl	NGC 4501 (M88)	2281	Sb	+23	-46	0.038
1999cw	MCG-01-02-001	3725	Sab	-2	+21	0.036
1999dq	NGC 976	4295	Sc	-6	-4	0.110
1999ef	UGC 607	11733	Scd	-10	+20	0.087
1999ej	NGC 495	4114	S0/Sa	-20	+18	0.071
1999ek	UGC 3329	5253	Sbc	-12	-12	0.561
1999gd	NGC 2623	5535	...	+17	+7	0.041
1999gh	NGC 2986	2302	E	+16	+52	0.058
1999gp	UGC 1993	8018	Sb	+10	-11	0.056
2000B	NGC 2320	5901	E	+19	-14	0.068
2000ce	UGC 4195	4888	Sb	+17	+15	0.057
2000cf	MCG+11-19-25	10920	...	+4	+3	0.032
2000en	UGC 11064	7043	Scd	-7	-7	0.057
2000cx	NGC 524	2379	S0	-109	-23	0.082
2000dk	NGC 382	5228	E	+9	-5	0.070
2000fa	UGC 3770	6378	Sd/Irr	+4	+7	0.069

Table 50. Light Curve Data and $\Delta m_{15}(B)$ Template Fits

SN Ia	HJD _{Bmax}	First Obs.	$\Delta m_{15}(B)$ fits			
			$\Delta m_{15}(B)$	B_{Bmax}	V_{Bmax}	I_{Bmax}
1997E	2450468.0	−3.1	1.39(06)	15.59	15.47	15.50
1997Y	2450487.5	1.4	1.25(10)	15.28	15.31	15.39
1997bp	2450550.3	−3.5	1.00(05)	14.15	13.89	14.10
1997bq	2450558.5	−10.8	1.01(05)	14.57	14.27	14.38
1997br	2450559.7	−7.8	1.02(06)	14.02	13.61	13.45
1997cn	2450583.9	13.6	1.90(05)	16.93	16.44	16.24
1997cw	2450627.1	15.6	1.02(10)	16.00	15.52	15.34
1997dg	2450722.6	−1.6	1.13(09)	17.20	17.11	17.16
1997do	2450767.0	−7.0	0.99(10)	14.56	14.46	14.60
1997dt	2450786.6	−8.9	1.04(15)	15.64	15.08	14.55
1998D	2450841.2	32.4
1998V	2450891.1	2.9	1.06(05)	15.88	15.71	15.63
1998ab	2450915.2	−8.2	0.88(17)	15.94	15.93	15.99
1998bp	2450936.4	−1.5	1.83(06)	15.73	15.29	15.09
1998co	2450987.2	3.7
1998de	2451026.2	−4.2	1.93(05)	17.55	16.83	16.58
1998dh	2451030.0	−8.0	1.23(17)	14.24	13.99	14.07
1998dk	2451056.8	18.7	1.05(10)	14.93	14.74	14.82
1998dm	2451061.2	10.5	1.07(06)	14.70	14.48	14.29
1998dx	2451072.6	0.0	1.55(09)	17.71	17.76	17.90
1998ec	2451088.6	13.1	1.08(09)	16.44	16.21	16.23
1998ef	2451114.5	−7.7	0.97(10)	15.21	15.18	15.29
1998eg	2451111.4	−0.7	1.15(09)	16.62	16.50	16.51
1998es	2451143.4	−9.4	0.87(08)	13.99	13.87	14.12
1999X	2451206.0	11.5	1.11(08)	16.45	16.29	16.32
1999aa	2451233.0	−9.9	0.85(08)	14.91	14.91	15.25
1999ac	2451251.2	−4.2	1.00(08)	14.34	14.28	14.33
1999cc	2451315.5	−2.5	1.46(05)	16.85	16.85	17.08
1999cl	2451342.2	−6.5	1.19(19)	15.11	13.90	13.10
1999cw	2451355.9	20.8
1999dq	2451436.7	−9.5	0.88(08)	14.88	14.68	14.77
1999ef	2451457.7	6.9	1.06(05)	17.52	17.39	17.70
1999ej	2451483.7	4.0	1.41(05)	15.65	15.63	15.71
1999ek	2451481.6	6.2	1.13(09)	17.97	17.19	16.56
1999gd	2451518.5	3.4	1.16(06)	17.02	16.61	16.29
1999gh	2451510.4	10.4	1.69(05)	14.46	14.27	14.27
1999gp	2451551.1	−5.1	0.87(08)	16.25	16.12	16.44
2000B	2451564.8	13.8	1.46(05)	15.94	15.80	15.99
2000ce	2451667.6	6.9	1.06(10)	17.39	16.71	16.23
2000cf	2451674.4	2.4	1.27(12)	17.15	17.12	17.34
2000cn	2451707.5	−7.5	1.58(12)	16.82	16.64	16.71
2000cx	2451752.2	−0.2
2000dk	2451812.5	−4.5	1.57(09)	15.63	15.57	15.77
2000fa	2451892.7	−10.5	1.00(10)	15.99	15.95	16.13

Table 51. *UBV* Stretch Template Fits

SN Ia	U_{Bmax}	B_{Bmax}	V_{Bmax}	s_U	s_B	s_V	$t_U - t_B$	$t_V - t_B$	χ^2/dof
1997E	15.40(05)	15.62(02)	15.47(02)	0.79(04)	0.83(02)	0.87(03)	-1.8(0.8)	0.7(0.3)	2.3
1997Y	14.90(07)	15.35(08)	15.39(02)	0.96(08)	0.93(03)	0.91(04)	-1.9(1.3)	1.6(0.7)	0.2
1997bp	14.05(05)	14.10(02)	13.91(02)	1.12(03)	0.97(03)	1.07(03)	-3.1(1.0)	2.1(0.4)	2.3
1997bq	14.23(04)	14.53(02)	14.44(02)	0.89(02)	0.92(02)	1.02(02)	-2.1(0.2)	1.6(0.1)	0.7
1997br	13.29(12)	13.88(05)	13.62(02)	0.81(05)	0.91(03)	1.04(03)	-2.6(0.4)	1.1(0.2)	2.1
1998V	15.62(07)	15.91(04)	15.73(03)	0.89(07)	0.99(05)	0.96(04)	-1.8(1.8)	0.7(0.9)	4.0
1998ab	15.51(06)	16.08(03)	16.10(02)	0.83(03)	0.92(02)	1.02(02)	-2.0(0.2)	0.5(0.2)	1.1
1998bp	15.56(07)	15.63(02)	15.31(02)	0.71(04)	0.65(02)	0.66(02)	-3.1(1.2)	2.1(0.4)	2.7
1998dh	13.91(06)	14.15(02)	14.04(02)	0.90(03)	0.91(02)	0.98(02)	-1.9(0.3)	1.1(0.2)	0.7
1998dx	17.02(13)	17.69(05)	17.74(03)	0.70(06)	0.85(04)	0.81(04)	-2.0(1.3)	1.2(0.7)	1.4
1998eg	16.20(06)	16.61(02)	16.50(02)	0.88(06)	0.96(04)	0.98(04)	-2.3(0.9)	1.3(0.6)	0.6
1998es	13.45(04)	13.97(02)	13.87(01)	0.98(03)	1.13(02)	1.10(02)	-1.6(0.3)	0.4(0.2)	1.0
1999aa	14.37(04)	14.89(03)	14.94(02)	1.05(02)	1.11(03)	1.13(02)	-2.2(0.3)	0.0(0.2)	2.9
1999ac	14.03(06)	14.28(03)	14.22(02)	1.04(04)	0.93(05)	0.99(02)	-2.7(0.9)	2.0(0.4)	4.0
1999cc	16.60(06)	16.88(03)	16.89(02)	0.86(05)	0.81(03)	0.87(03)	-2.0(0.9)	0.3(0.5)	1.8
1999cl	15.76(05)	15.07(03)	13.88(02)	0.82(04)	0.97(04)	1.02(03)	-1.9(0.6)	1.7(0.4)	0.5
1999dq	14.43(04)	14.86(02)	14.69(02)	0.98(02)	1.08(02)	1.13(02)	-2.3(0.2)	0.3(0.2)	1.5
1999gp	15.67(07)	16.26(03)	16.19(02)	1.04(07)	1.17(06)	1.20(04)	-2.0(1.2)	0.8(0.6)	6.2
2000cf	16.84(11)	17.18(04)	17.21(02)	0.83(06)	0.87(02)	0.92(03)	-2.2(1.3)	1.4(0.7)	0.6
2000cn	16.76(07)	16.81(03)	16.59(02)	0.76(06)	0.77(03)	0.82(02)	-1.7(0.3)	1.2(0.2)	2.3
2000dk	15.36(05)	15.63(02)	15.57(02)	0.73(04)	0.74(02)	0.81(03)	-2.5(0.5)	1.1(0.2)	2.7
2000fa	15.82(08)	16.13(04)	16.04(03)	1.01(03)	1.04(03)	0.97(03)	-2.3(1.0)	1.4(0.8)	1.2